MERCURY TRANSFORMATION BY ANAEROBIC MICROORGANISMS

By

YUWEI WANG

A dissertation submitted to the

School of Graduate Studies

Rutgers, The State University of New Jersey

In partial fulfillment of the requirements

For the degree of

Doctor of Philosophy

Graduate Program in Environmental Sciences

Written under the direction of

Nathan Yee

And approved by

_____

_____

_____

_____

New Brunswick, New Jersey

[October 2019]

ABSTRACT OF THE DISSERTATION

Mercury transformation by anaerobic microorganisms

By YUWEI WANG

Dissertation Director

Nathan Yee

Mercury is a global pollutant that cycles in the environment. Anaerobic bacteria mediate the transformation of mercury which influences its toxicity and distribution. Methylmercury (MeHg) is a form of mercury that is of great concern because it is neurotoxic and bioaccumulates in the food chain. Previous studies focused on understanding the methylation of divalent mercury [Hg(II)], however, little work has been done to study the steps before and after MeHg production. Steps such as the transformation of mercury by pure cultures and microbial communities when elemental mercury [Hg(0)] is the sole or dominant source, the uptake of Hg(II) prior to methylation, the adsorption of MeHg after being released into the environment were still poorly understood. The objective of this study was to understand how anaerobic microorganisms control the formation and transport of MeHg.

Oxidation of Hg(0) is a key step for MeHg production. In Chapter 2, the mechanism of Hg(0) oxidation mediated by the sulfate-reducing bacterium *Desulfovibrio desulfuricans* ND132 is described. When Hg(0) was provided as the sole mercury source, it diffused into the bacterial cells and was oxidized by cellular thiol functional groups. X-ray absorption spectroscopy results confirmed the formation of oxidized mercury and showed that oxidized mercury was bound to intracellular thiol groups. This work demonstrated an important step of Hg(0) transformation inside the cells that provides substrate for methylation.

The results presented in Chapter 3 demonstrate the importance of MeHg adsorption, which can influence the fate of MeHg in the environment. *Geobacter bemidjiensis* Bem, a strain of iron-reducing bacteria that was reported to both produce and degrade MeHg was used as a model organism to study MeHg adsorption. X-ray absorption spectroscopy results show that MeHg was bound to the thiol functional groups on the cell membrane. By modeling the adsorption isotherm and the concentration of thiol sites on the cell membrane, the binding constant of MeHg to bacterial cells was estimated. This study highlighted the influence of MeHg adsorption on net MeHg production and provided a parameter that can be used in modeling mercury in the environment.

In Chapter 4, the uptake of inorganic Hg(II) in the mercury methylator *Geobacter sulfurreducens* PCA and a mutant strain of this species lacking the ability to methylate mercury was studied using mercury stable isotopes. The isotopic composition of Hg(II) was analyzed in different compartments of the bacterial cells. The offset in isotopic composition between Hg(II) in the dissolved phase and Hg(II) inside the cells

demonstrates isotope fractionation during Hg(II) uptake. The results of this study provide preliminary data on bioavailable Hg(II) pools utilized by bacteria for MeHg production.

In Chapter 5, results of experimental studies were extended to the real world. The methylation of mercury by microbial communities in estuarine sediments when Hg(0) was provided as the dominant mercury source was studied. By inhibiting the activities of certain families of microorganisms and conducting mercury methylation experiments, methanogens were found to play an important role in producing MeHg. These results reveal that methanogens are an overlooked groups of mercury methylators in estuarine sediments, especially when exposed to Hg(0).

ACKNOWLEDGMENTS

I want to first express my deepest gratitude to my advisor, Dr. Nathan Yee for his tremendous patience and support. Looking back at the first-draft presentation and manuscript I prepared, I came to realize how much I have grown as a scientist. Without his guidance hours after hours, I would not be able to make such tremendous progress in my research. This dissertation would not have been possible without him allowing me to learn from my mistakes, giving me timely supervision and providing me opportunities to learn from different institutes. His insight into both science and life inspires me to face these challenges head-on in order to be a strong researcher. I would like to thank Dr. Jeffra Schaefer who led me through the door of microbiology and made microbiology interesting in the process. Without the expert advice and the support she has given me to move my projects forward, I could not have recovered from the frustrations when my projects were not yielding results. I must also acknowledge Dr. John Reinfelder who has always been encouraging and treated me as a member of his lab. His insightful advice and generous support greatly facilitated my ability to perform experiments and move forward with my study. I would also like to thank the other members of my dissertation committee Dr. Tamar Barkay and Dr. Evert Elzinga for their time and comments on this dissertation. I would like to give a special thanks to Tamar, who has given me warm encouragement when I encountered major adversity and continues to provide me great support towards my future endeavors.

I would not have completed any of my research projects without the help of my collaborators Dr. Bhoopesh Mishra for helping with XAS figures in Chapters 2 and 3; Dr. Jeremy Fein and Dr. Qiang Yu for teaching me titration experiments and modeling

procedures in Chapter 3; Dr. Yundang Wu for helping generating *hgcAB* mutant in Chapter 4; and Spenser Roth for helping with running PCR in Chapter 5. I need to thank Dr. Weilin Huang for recommending me to my advisor which made my journal at Rutgers possible. I need to give a special thank you to my dear friend, my outstanding former colleague, and my current collaborator Dr. Sarah Janssen for teaching me mercury isotope analysis and making my research life fun and more accomplished. I am thankful to Thomas Wang who trained me on new techniques and experimental set-ups when I started working in the lab. In addition, I want to thank my friends Zhiyi and Xiaoshuai, my labmates Jessica, Phil, and Jennifer, and my roommate Yanmei for their support.

I thank the Chinese Scholarship Council, the National Science Foundation, the Department of Energy, and the New Jersey Water Resources Research Institute for providing me with funding for my projects. Additionally, I need to thank the GeoSoilEnviroCARS at the Advanced Photon Source and the Upper Midwest Water Science Center of USGS for their assistance in running the analyses.

Finally, I would like to thank all my family members in China for their endless support. I thank my father who used to be the only one of the family letting me leave my country to pursue my goals. I could not be more grateful to my mother who has sacrificed so much to support my dream. Her unconditional love and tremendous spirit have given me the strength to overcome the obstacles and challenges which I have faced. I dedicate this work to my beloved parents, and I hope I made them proud.

TABLE OF CONTENTS

LIST OF FIGURES

LIST OF TABLES

Chapter 1 Introduction

1.1 Mercury in the environment

1.1.1 Mercury is a global pollutant

Mercury (Hg) is a toxic element that is emitted and transported worldwide. Hg is released to the environment as a result of both natural and anthropogenic sources (Nriagu, 1993). Hg exists in the continental crust (Wedepohl, 1995) and is naturally emitted from volcanic eruptions, geothermal emissions, and Hg-enriched minerals (Gustin et al., 2008; Witt et al., 2010). However, most Hg is released into the environment through anthropogenic processes (Mason and Sheu, 2002), with gold mining and coal combustion as the most significant Hg inputs (Pirrone et al., 2010). According to the latest United Nations Global Mercury Assessment, current atmospheric Hg concentrations generated by human activities have increased by about 450% above natural levels. This has driven the average Hg increase 300%, 230% and 15% in deposition, surface marine waters and surface organic soils, respectively (Outridge et al., 2018). Hg is largely released into the atmosphere in the form of elemental mercury [Hg(0)] and stays as the most abundant form of mercury in the atmosphere (Pirrone and Mahaffey, 2005). The long atmospheric life-time and the circulation of Hg(0) due to its stability in the atmosphere make Hg a global pollutant and can be detected in remote areas of the earth (Fitzgerald et al., 1998; Lindberg et al., 2002; Mason et al., 1998). The oxidation of Hg(0) in the atmosphere produces divalent Hg [Hg(II)] which deposits into terrestrial and aquatic systems. The transformation of inorganic Hg to methylmercury (MeHg), a more toxic form of mercury, leads to the bioaccumulation of mercury in biota (Morel et al., 1998). The

biogeochemical cycle of Hg controls its fate and transport and affects the redistribution of Hg in the environment.

1.1.2 Local Hg(0) contamination

Historical deposits of Hg(0) from industrial areas across the United States has resulted in high levels of mercury contamination in the environment. The use of Hg(0) in the Y-12 National Security Complex in Oak Ridge caused Hg(0) spill in soil and could be a source of Hg source in groundwater where the water table is high (Miller et al., 2013). In the sediments of Clear Creek (CA), while a portion of Hg(0) introduced from the historical gold mining being transformed into other species, tiny Hg(0) globules were found persistently existing in the sediment (Slowey et al., 2005). There are also a number of mercury contaminated sites in New Jersey. For example, the Troy Chemical Company Site in Newark NJ, discharged approximately 300 pounds of mercury per day into the Newark Bay and severely contaminated Pierson's Creek (NJDEP, 2002). Mercury discharge from Ventron/Velsicol Site in the Hackensack Meadowlands also resulted in widespread mercury contamination in the surrounding area (Lipsky et al., 1980), including the notorious Berry's Creek which has been measured as having the highest mercury concentration of any freshwater sediment in the world (USNOAA and USFWS, 2014).

1.2 Biogeochemical cycling of mercury in aquatic systems

When Hg precipitate into aquatic systems, it undergoes both biotic and abiotic reactions. Hg(0) in the atmosphere is oxidized by photochemical reactions (Lindberg et al., 2002; Munthe, 1992; Siciliano et al., 2002; Thöming et al., 2000) and precipitated

into waters in the form of Hg(II). Hg(II) can be reduced abiotically by photo-reduction reactions (Amyot et al., 1997; Amyot et al., 1994; Bergquist and Blum, 2007), humic acids and iron minerals (Gu et al., 2011; Skogerboe and Wilson, 1981; Wiatrowski et al., 2009). Constitutive reduction of Hg(II) occurs under anoxic conditions at low Hg(II) concentrations by dissimilatory metal reducing bacteria (Ullrich et al., 2001; Wiatrowski et al., 2006). In oxic environments with high Hg(II) contamination, Hg(II) is reduced by mercury resistant bacteria with the *mer* operon induced by nanomolar level of Hg (Barkay et al., 2003). The produced Hg(0) becomes saturated in the surface water and fluxes back to the atmosphere (Morel et al., 1998). The coupled redox reactions lead to air-water exchange of mercury (Hg) and is a critical part of the global Hg cycle.

Direct discharge of Hg(0) to aquatic ecosystems is also subject to biogeochemical transformation processes (Bone et al., 2014; Bouffard and Amyot, 2009). Historical mercury discharge from industrial areas across the United States has resulted in high levels of Hg(0) contamination in surface and groundwater (Brooks and Southworth, 2011; Lechler et al., 1997; Miller et al., 2013; Slowey et al., 2005). Hg(0) oxidation occurs in waters by reacting with oxygen in the presence of chloride (Amyot et al., 1997; de Magalhães and Tubino, 1995), sulfhydryl compounds (Yamamoto, 1995; Zheng et al., 2013), ozone (Munthe, 1992), and radicals of Br and Cl (Ebinghaus et al., 2002; Lalonde et al., 2001; Lindberg et al., 2002) as well as microbial mediated processes (Colombo et al., 2013, 2014; Hu et al., 2013; Wang et al., 2016). In anoxic environments, both Hg(0) and its oxidized form Hg(II) are the substrates bioavailable for methylation (Barkay et al., 2003; Colombo et al., 2013; Hu et al., 2013; Mason et al., 1995; Smith et al., 1998).

Methylation of inorganic Hg in waters and sediments has great impact on aquatic environments and is of great environmental concern because MeHg bioaccumulates and biomagnifies in biota and food webs (Lavoie et al., 2013). MeHg is neurotoxic and can cause permanent damage to nerve systems (Aschner and Syversen, 2005). MeHg also causes other health issues such as change in hormones, disturbances in sensations and responses, emotional changes and neuromuscular changes (EPA, Health Effects of Exposures to Mercury). Human exposure to Hg is mainly due to seafood consumption. The Minamata disease was caused by methylmercury poisoning by ingesting MeHg contaminated fish and shellfish (Harada, 1995). MeHg was reported to be produced abiotically by nonenzymatic transfer of the methyl group to the mercuric ion (Ullrich et al., 2001). However, the production of MeHg is dominantly mediated by anaerobic microorganisms containing *hgcA* and *hgcB* genes (Parks et al., 2013). Sulfate-reducing (SRB) and iron-reducing bacteria (IRB) have been demonstrated as Hg methylators (Benoit et al., 2001; Benoit et al., 1999; Compeau and Bartha, 1985; Fleming et al., 2006; Kerin et al., 2006; King et al., 2000). Recently, methanogenic archaea and firmicutes were also found having the ability to methylate Hg (Gilmour et al., 2013; Parks et al., 2013; Yu et al., 2013). Syntrophic processes have also been demonstrated to contribute to MeHg production (Yu et al., 2018). MeHg can be degraded by photochemical reactions (Suda et al., 1993). In dark environment, microbial mercury demethylation dominates (Oremland et al., 1991; Schaefer et al., 2004). There are two microbial MeHg degradation pathways: reductive pathway and oxidative pathway. In the reductive pathway, MeHg was broken apart into CH_4 and Hg(II) by the organomercury lyase *MerB* followed by Hg(II) being reduced to Hg(0) by mercuric reductase *MerA* (Pitts and Summers, 2002).

Oxidative demethylation produces CO_2, small amount of CH_4 and Hg(II) (Marvin-DiPasquale et al., 2000; Oremland et al., 1991). The net accumulation of MeHg in aquatic systems governed by methylation and demethylation processes affects the bioaccumulation and biomagnification of MeHg in biota (Bloom, 1992).

1.3 Mercury transformation by microorganisms

Microorganisms play an important role in mercury transformation. Both aerobic and anaerobic microorganisms mediate redox reactions. However, microbes in responsible for MeHg production predominantly exist in anoxic environments.

1.3.1 Hg(II) reduction

In highly Hg(II) contaminated environments, aerobic bacteria with mercuric reductase (*merA*) catalyze Hg(II) reduction (Barkay et al., 2003). Under anoxic condition, however, Hg(II) is reduced by *Shewanella oneidensis* MR-1, *G. metallireducens* GS-15 and *G. sulfurreducens* PCA (grown with ferric citrate) via *mer* independent mechanisms (Wiatrowski et al., 2006). Although Hg(II) reduction by some anaerobes is likely through the activity of respiratory electron transport chains, the mechanism is not fully understood.

1.3.2 Hg(0) oxidation

The neutral Hg(0) can diffuse rapidly through lipid membranes (Morel et al., 1998) and react with diverse bacteria. Smith et al. found that aerobic *Escherichia coli* could contribute to the oxidation of Hg(0) (Smith et al., 1998). Anaerobic bacteria *Desulfovibrio desulfuricans* ND132 had been demonstrated to rapidly oxidize gaseous mercury into Hg(II) by cellular thiol functional groups (Wang et al., 2016). *S. oneidensis*

MR-1, *Cupriavidus metallidurans* AE104, and *Geothrix. fermentans* H5 were also found having the ability to oxidize Hg(0) (Colombo et al., 2014). Hu et al. found that *Desulfovibrio alaskensis* G20 can oxidize Hg(0), but *G. sulfurreducens* PCA shows negligible Hg(0) oxidation under given conditions unless thiol compounds such as cysteine is supplied (Hu et al., 2013). When Hg(0) was provided as the sole source of Hg, MeHg was produced by the pure culture *D. desulfuricans* ND132 (Colombo et al., 2013). However, the transformation of Hg(0) by microorganisms in aquatic systems is poorly explored and understood.

1.3.3 Hg methylation

In anoxic environments, sulfate-reducing bacteria and iron-reducing bacteria are known as the major mercury methylators. About 30 species of sulfate/iron-reducing bacteria were able to methylate Hg(II) (Gilmour et al., 2013). *D. desulfuricans* ND132 and *G. sulfurreducens* PCA were used as two model strains for studying Hg(II) methylation (Gilmour et al., 2013; Janssen et al., 2016; Schaefer et al., 2011). Recently, Parks et al found that a two-gene cluster *hgcAB* is required for mercury methylation. By analyzing phylogenetic distribution of *hgcAB* and conducting pure culture experiments, other species of microorganism including methanogens, and syntrophic, acetogenic, and fermentative firmicutes were confirmed as mercury methylators (Gilmour et al., 2018; Gilmour et al., 2013; Yu et al., 2013, 2018). The discovery of novel Hg-methylating organisms expanded the diversity of environmental niches where MeHg production may occur.

1.4 Environmental factors that affect fate and transport of Hg

Environmental factors control the distribution and transformation of mercury in aquatic systems. Organic matter and sulfide govern the speciation of mercury and inflects the partition of mercury between water and sediments (Hammerschmidt et al., 2008). Under anoxic conditions, the chemistry of mercury is dominantly controlled by sulfide while under oxic conditions, mercury is more likely complexed with organic matter (Ullrich et al., 2001). Concentrations of sulfur compounds affect the activity of microbes and thus influences the net production of MeHg (Gilmour et al., 1992; Schartup et al., 2014). For example, the existence of sulfide can both decrease the microbial activity (Gilmour et al., 1992) and reduce the bioavailability of Hg(II) by forming HgS (Drott et al., 2007; Skyllberg, 2008), resulting in low MeHg production. The addition of iron also decreases net MeHg production by decreasing the concentration of dissolved sulfide (Mehrotra and Sedlak, 2005). Notably, thiol compounds play an important role in interacting with mercury in the environment.

Thiols mediate Hg reactions and influence the bioavailability of Hg. Thiols are ubiquitous in aquatic systems. Previous studies showed that thiol concentration ranges from 5 nM to 12 uM in anoxic fresh water (Hu et al., 2006; Shea and MacCrehan, 1988), 0.2 nM to 30 uM in marine and estuary waters (Dyrssen et al., 1985; Tang et al., 2000), and 0.1 μM to 2.4 mM in sediments (Mopper and Taylor, 1986; Shea and MacCrehan, 1988). High thiol site concentrations were also detected on bacterial cells (Joe-Wong et al., 2012; Yu et al., 2014) and algea (Bouchet et al., 2018; Leclerc et al., 2015) that exist in water and sediments. Thiol compounds are important reactants for dissolved Hg(0) oxidation (Zheng et al., 2013; Wang et al., 2016). Because of the high affinity of Hg(II) to thiols (Skyllberg, 2008), the rate and extent of Hg(II) reduction (Gu et al., 2011) and

methylation (Gilmour et al., 2018; Schaefer and Morel, 2009) varies with the Hg(II)/thiol ratios that changes Hg(II) speciation. MeHg-thiols bonds were also demonstrated dominant in sediment–water interface (Zhang et al., 2004), fish (Harris et al., 2003) and bacterial cells (Wang et al., 2018) compared to other forms of MeHg complexes. The existence of thiol compounds affects the production and degradation of MeHg in aquatic systems (Bouchet et al., 2018; Wang et al., 2018).

1.5 Sulfate-reducing bacteria and iron-reducing bacteria

Sulfate-reducing bacteria are a ubiquitous group that can couple the oxidation of a variety of electron donors such as hydrocarbons, dicarboxylic acids, sugars and aromatic compounds with the reduction of sulfate (Hansen, 1993). Some organisms can grow with pyruvate in the absence of sulfate (Singleton, 1993). Some organisms transfer electrons from lactate or pyruvate oxidation to fumarate and generate succinate (Barton et al., 1970). Cytoplasmic enzymes are involved in respiratory sulfate reduction. For example, in members of genus *Desulfovibrio*, there are water-soluble cytochromes c and periplasmic hydrogenase undergoing redox reactions (Fauque et al., 1988). Sulfate reducers play an important role in the mobilization and toxicity of heavy metals in sewers, lakes, and streams (Odom, 1993). In recent years, transformation of mercury by sulfate reducing bacteria *D. desulfuricans* was found under sulfate limiting environment (Compeau and Bartha, 1985). By performing inhibition experiments, sulfate reducers were also demonstrated as the principal mercury methylators in anaerobic sediments (Compeau and Bartha, 1985; Oremland et al., 1991).

Iron-reducing bacteria are anaerobes that reduce ferric ions to ferrous ions. The membrane-bound terminal ferric reductase enzymes in iron-reducing bacteria make it

possible for the ferric minerals to be taken up into the cytoplasm (Lovley, 1993). Some species such as *Shewanella* secretes soluble electron shuttles to reduce ferric oxide without physical contact. Among the iron-reducing bacteria, *Geobacter* species are relatively well-studied. *Geobacter* couples the oxidation of organic compounds with the reduction of insoluble Fe(III) and Mn(IV) oxides in soils and sediments (Lovley et al., 2011). Some *Geobacter* species are able to oxide aromatic hydrocarbons and precipitate contaminants such as uranium, making it possible to utilize *Geobacter* for bioremediation in contaminated environments (Lovley et al., 2011). Iron-reducing bacteria were distinguished as either acetate oxidizing (*Geobacter*) or hydrogen oxidizing (*Shewanella*) species (Lovley, 1993) until the discovery of *G. sulfurreducens* PCA which couples acetate or hydrogen oxidation with the reduction of Fe(III) (Caccavo et al., 1994). Strain PCA was isolated from sediments of a hydrocarbon-contaminated ditch in Oklahoma that can grow in high salinity (Caccavo et al., 1994). However, strain PCA cannot reduce Fe(III) using aromatic compounds as electron donors (Caccavo et al., 1994). *Geobacter* species were also found to methylate mercury in sediments at environmentally significant rates (Fleming et al., 2006). Recent research found that comparing to sulfate-reducing bacteria, iron-reducing bacteria may contribute more to methylmercury formation in some sediments (Bravo et al., 2018).

1.6 Tools utilized to study microbe-mercury interaction

1.6.1 X-ray absorption spectroscopy

X-ray absorption spectroscopy (XAS) is widely used to determine mercury complexation. Analyzing the chemical complexation of mercury is essential to understand its mobility, solubility, bioavailability and toxicity that affects the fate and

transport of mercury in the environment. Using XAS, Skyllberg et al found that in soil humic substances, Hg(II) complexed with two reduced organic sulfur groups or an oxygen-oxygen/oxygen-nitrogen group when all high affinity sulfur sites were saturated (Skyllberg et al., 2006). The results provided important information to estimate the complexation constants for Hg-natural organic matter associations (Song et al., 2018) that can be used in biogeochemical models. Mishra et al demonstrated that the stoichiometry of mercury binding to bacterial cells alters with the metal to biomass ratio and the characteristics of cell envelopes (Mishra et al., 2017) which may influence the uptake and transformation of Hg(II). XAS also help understanding the redistribution of Hg(II) on bacterial cells by environmental factors such as pH and chloride concentrations (Dunham-Cheatham et al., 2014).

There are two regimes of x-ray absorption spectrum: x-ray absorption near-edge spectroscopy (XANES) and x-ray absorption fine-structure spectroscopy (XAFS) (Newville, 2014). The binding energy of a core electron is called an edge. XANES examines the X-ray absorption spectra generated when an electron is excited to an empty state from a core state by absorbing a photon (Henderson et al., 2014) and is utilized to determine the oxidation state and coordination chemistry of the absorbing atom (Newville, 2014). XAFS tells the absorption of x-rays by an atom at energies near and above its core-level binding energies. The absorption coefficient is altered by the photo-electron scattered back from the electrons of a neighboring atom to the absorbing atom (Newville, 2014). Thus, XAFS can be used to determine the species coordinating with the absorbing atom, the coordination number and the distance between the absorbing atom and its neighbors (Newville, 2014).

1.6.2 Mercury stable isotopes

Mercury stable isotopes is a useful tool to trace Hg source in the environment and monitor Hg transformation processes (Blum et al., 2014). There are seven Hg stable isotopes (^{196}Hg, ^{198}Hg, ^{199}Hg, ^{200}Hg, ^{201}Hg, ^{202}Hg, ^{204}Hg) and the maximum relative mass difference is 4%. The mass difference allows the isotope measurement using multi-collector inductively coupled plasma mass spectrometry (MC-ICP-MS) techniques. Hg stable isotopes are reported using delta notation in the unit of per mil (‰):

$$\delta^{xxx}\mathrm{Hg} = \left[\frac{\left(\frac{xxx_{Hg}}{198_{Hg}}\right)sample}{\left(\frac{xxx_{Hg}}{198_{Hg}}\right)standard} - 1\right] \times 1000$$

Since ^{202}Hg is the most abundant isotope, it is generally used as denominator (Blum and Bergquist, 2007). A positive delta value indicates the sample is isotopically enriched in heavier isotope, while a negative value indicates the samples is depleted in the heavier isotope.

The biogeochemical reactions of Hg undergo isotope fractionation that indicates the relative partitioning of heavier and lighter isotopes between two phases. Isotope fractionation between molecules indicates the differences in their zero point energies. There are mass dependent fractionation (MDF) and mass independent fractionation (MIF). MDF occurs when the difference of chemical and physical properties is caused by the mass difference of various isotopes of an element (Kendall and Caldwell, 1998). The bonds of the lighter molecules break faster and thus preferentially accumulate in the product, while the heavier isotopes enrich in the reactant. MIF depends on the nuclear interactions (Kendall and Caldwell, 1998) and occurs in the reactions that separate

isotopes by the rates of magnetic and non-magnetic isotopes during spin reactions and is usually caused by photolysis (Bergquist and Blum, 2009). MIF was barely observed in Hg microbial transformation dark reactions. The extent of fractionation during any process can be quantified using fractionation factors. The calculation of fractionation factors are shown in the equations below:

$$Ln(R_{ri}/R_{r0}) = ((1/\alpha)-1)lnf$$

$$Ln(R_{pi}/R_{r0}) = ((1/\alpha)-1)ln(f) + ln(1/\alpha)$$

where R represents the relative isotope ratio $(^{202}Hg/^{198}Hg)_{sample}$/ $(^{202}Hg/^{198}Hg)_{NIST\ 3133}$; p equals to product (0 = time 0; i = time i); r is reactant; α is $(^{202}Hg/^{198}Hg)_{reactant}/(^{202}Hg/^{198}Hg)_{product}$; f = fraction of added Hg(II) remaining.

Hg stable isotopes can be applied to study microbial transformation processes. Microbes play a vital role in mercury biogeochemical cycling, and the transformation of mercury leads to isotope fractionation. Therefore, studying the change in isotope ratios during microbial processes is useful to understand the mechanisms of the transformation processes. Isotope fractionation during Hg transformation has been demonstrated in previous studies. Reduction of Hg(II) to Hg(0) via different pathways and the degradation of MeHg to Hg(0) have been demonstrated to cause isotope fractionation, where light isotope was enriched in the product Hg(0), leaving the reactant Hg(II) or MeHg pool isotopically heavier (Kritee et al., 2009; Kritee et al., 2008; Kritee et al., 2007). Interestingly, during the Hg(II) methylation processes mediated by *G. sulfurreducens* PCA and *D. desulfuricans* ND132, a heavier Hg(II) pool was utilized to produce MeHg (Janssen et al., 2016).

1.7 Purpose of study

Although the transformation of Hg have been largely studied, very few studies have investigated the oxidation and methylation of mercury by anaerobic bacteria when Hg(0) was provided as the sole mercury source. The processes before and after the production of MeHg by microorganisms have also been partially understood. Therefore, several steps that influence the biogeochemical reactions of Hg are still missing. The goal of this study was to better understand the oxidation and methylation of Hg and the fate of MeHg products. The specific objectives of each chapter were to:

Chapter 2: Understand the mechanism of Hg(0) oxidation by *D. desulfuricans* ND132 and the speciation of oxidized Hg.

Chapter 3: Investigate the adsorption of MeHg by a mercury methylator and demethylator *Geobacter bemidjiensis* Bem.

Chapter 4: Study isotopic fractionation of Hg during the uptake of Hg(II) in iron-reducing bacteria pure cultures.

Chapter 5: Examine the transformation of Hg(0) by microbial communities in the sediments and the possible microbes responsible for Hg(II) and MeHg formation.

References:

Amyot, M., Gill, G.A. and Morel, F.M. (1997) Production and loss of dissolved gaseous mercury in coastal seawater. Environmental Science & Technology 31, 3606-3611.

Amyot, M., McQueen, D.J., Mierle, G. and Lean, D.R.S. (1994) Sunlight-Induced Formation of Dissolved Gaseous Mercury in Lake Waters. Environmental Science & Technology 28, 2366-2371.

Aschner, M. and Syversen, T. (2005) Methylmercury: recent advances in the understanding of its neurotoxicity. Therapeutic drug monitoring 27, 278-283.

Barkay, T., Miller, S.M. and Summers, A.O. (2003) Bacterial mercury resistance from atoms to ecosystems. FEMS Microbiology Reviews 27, 355-384.

Barton, L.L., Gall, J.L. and Peck, H.D. (1970) Phosphorylation coupled to oxidation of hydrogen with fumarate in extracts of the sulfate reducing bacterium, *Desulfovibrio gigas*. Biochemical and Biophysical Research Communications 41, 1036-1042.

Benoit, J.M., Gilmour, C.C. and Mason, R.P. (2001) The Influence of Sulfide on Solid-Phase Mercury Bioavailability for Methylation by Pure Cultures of *Desulfobulbus propionicus* (1pr3). Environmental Science & Technology 35, 127-132.

Benoit, J.M., Gilmour, C.C., Mason, R.P. and Heyes, A. (1999) Sulfide controls on mercury speciation and bioavailability to methylating bacteria in sediment pore waters. Environmental Science & Technology 33, 951-957.

Bergquist, B.A. and Blum, J.D. (2007) Mass-Dependent and -Independent Fractionation of Hg Isotopes by Photoreduction in Aquatic Systems. Science 318, 417.

Bergquist, B.A. and Blum, J.D. (2009) The odds and evens of mercury isotopes: applications of mass-dependent and mass-independent isotope fractionation. Elements 5, 353-357.

Bloom, N.S. (1992) On the Chemical Form of Mercury in Edible Fish and Marine Invertebrate Tissue. Canadian Journal of Fisheries and Aquatic Sciences, Canadian Journal of Fisheries and Aquatic Sciences.

Blum, J.D. and Bergquist, B.A. (2007) Reporting of variations in the natural isotopic composition of mercury. Analytical and Bioanalytical Chemistry 388, 353-359.

Blum, J.D., Sherman, L.S. and Johnson, M.W. (2014) Mercury isotopes in earth and environmental sciences. Annual Review of Earth and Planetary Sciences 42, 249-269.

Bone, S.E., Bargar, J.R. and Sposito, G. (2014) Mackinawite (FeS) Reduces Mercury(II) under Sulfidic Conditions. Environmental Science & Technology 48, 10681-10689.

Bouchet, S., Goñi-Urriza, M., Monperrus, M., Guyoneaud, R., Fernandez, P., Heredia, C., Tessier, E., Gassie, C., Point, D., Guédron, S., Achá, D. and Amouroux, D. (2018) Linking Microbial Activities and Low-Molecular-Weight Thiols to Hg Methylation in Biofilms and Periphyton from High-Altitude Tropical Lakes in the Bolivian Altiplano. Environmental Science & Technology 52, 9758-9767.

Bouffard, A. and Amyot, M. (2009) Importance of elemental mercury in lake sediments. Chemosphere 74, 1098-1103.

Bravo, A.G., Peura, S., Buck, M., Ahmed, O., Mateos-Rivera, A., Ortega, S.H., Schaefer, J.K., Bouchet, S., Tolu, J. and Björn, E. (2018) Methanogens and iron-reducing bacteria: the overlooked members of mercury-methylating microbial communities in boreal lakes. Appl. Environ. Microbiol. 84, e01774-01718.

Brooks, S.C. and Southworth, G.R. (2011) History of mercury use and environmental contamination at the Oak Ridge Y-12 Plant. Environmental Pollution 159, 219-228.

Caccavo, F., Lonergan, D.J., Lovley, D.R., Davis, M., Stolz, J.F. and McInerney, M.J. (1994) *Geobacter sulfurreducens* sp. nov., a hydrogen- and acetate-oxidizing dissimilatory metal-reducing microorganism. Applied and Environmental Microbiology 60, 3752.

Colombo, M.J., Ha, J., Reinfelder, J.R., Barkay, T. and Yee, N. (2013) Anaerobic oxidation of Hg(0) and methylmercury formation by *Desulfovibrio desulfuricans* ND132. Geochimica et Cosmochimica Acta 112, 166-177.

Colombo, M.J., Ha, J., Reinfelder, J.R., Barkay, T. and Yee, N. (2014) Oxidation of Hg(0) to Hg(II) by diverse anaerobic bacteria. Chemical Geology 363, 334-340.

Compeau, G.C. and Bartha, R. (1985) Sulfate-Reducing Bacteria: Principal Methylators of Mercury in Anoxic Estuarine Sediment. Applied and Environmental Microbiology 50, 498.

de Magalhães, M.E.A. and Tubino, M. (1995) A possible path for mercury in biological systems: the oxidation of metallic mercury by molecular oxygen in aqueous solutions. Science of the total environment 170, 229-239.

Drott, A., Lambertsson, L., Björn, E. and Skyllberg, U. (2007) Importance of Dissolved Neutral Mercury Sulfides for Methyl Mercury Production in Contaminated Sediments. Environmental Science & Technology 41, 2270-2276.

Dunham-Cheatham, S., Farrell, B., Mishra, B., Myneni, S. and Fein, J.B. (2014) The effect of chloride on the adsorption of Hg onto three bacterial species. Chemical Geology 373, 106-114.
Dyrssen, D., Haraldsson, C., Westerlund, S. and Årén, K. (1985) Indication of thiols in black sea deep water. Marine Chemistry 17, 323-327.

Ebinghaus, R., Kock, H.H., Temme, C., Einax, J.W., Löwe, A.G., Richter, A., Burrows, J.P. and Schroeder, W.H. (2002) Antarctic Springtime Depletion of Atmospheric Mercury. Environmental Science & Technology 36, 1238-1244.

Fauque, G., Peck, H.D., Jr., Moura, J.J.G., Huynh, B.H., Berlier, Y., DerVartanian, D.V., Teixeira, M., Przybyla, A.E., Lespinat, P.A., Moura, I. and LeGall, J. (1988) The three classes of hydrogenases from sulfate-reducing bacteria of the genus Desulfovibrio. FEMS Microbiology Reviews 4, 299-344.

Fitzgerald, W.F., Engstrom, D.R., Mason, R.P. and Nater, E.A. (1998) The case for atmospheric mercury contamination in remote areas. Environmental science & technology 32, 1-7.

Fleming, E.J., Mack, E.E., Green, P.G. and Nelson, D.C. (2006) Mercury Methylation from Unexpected Sources: Molybdate-Inhibited Freshwater Sediments and an Iron-Reducing Bacterium. Applied and Environmental Microbiology 72, 457.

Gilmour, C.C., Bullock, A.L., McBurney, A., Podar, M. and Elias, D.A. (2018) Robust Mercury Methylation across Diverse Methanogenic Archaea. mBio 9, e02403-02417.

Gilmour, C.C., Henry, E.A. and Mitchell, R. (1992) Sulfate stimulation of mercury methylation in freshwater sediments. Environmental Science & Technology 26, 2281-2287.

Gilmour, C.C., Podar, M., Bullock, A.L., Graham, A.M., Brown, S.D., Somenahally, A.C., Johs, A., Hurt, R.A., Bailey, K.L. and Elias, D.A. (2013) Mercury Methylation by Novel Microorganisms from New Environments. Environmental Science & Technology 47, 11810-11820.

Gu, B., Bian, Y., Miller, C.L., Dong, W., Jiang, X. and Liang, L. (2011) Mercury reduction and complexation by natural organic matter in anoxic environments. Proceedings of the National Academy of Sciences 108, 1479.

Gustin, M.S., Lindberg, S.E. and Weisberg, P.J. (2008) An update on the natural sources and sinks of atmospheric mercury. Applied Geochemistry 23, 482-493.

Hammerschmidt, C.R., Fitzgerald, W.F., Balcom, P.H. and Visscher, P.T. (2008) Organic matter and sulfide inhibit methylmercury production in sediments of New York/New Jersey Harbor. Marine Chemistry 109, 165-182.

Hansen, T.A. (1993) Carbon Metabolism of Sulfate-Reducing Bacteria. Brock/Springer Series in Contemporary Bioscience. Springer, New York, NY, The Sulfate-Reducing Bacteria: Contemporary Perspectives.

Harada, M. (1995) Minamata disease: methylmercury poisoning in Japan caused by environmental pollution. Critical reviews in toxicology 25, 1-24.

Harris, H.H., Pickering, I.J. and George, G.N. (2003) The Chemical Form of Mercury in Fish. Science 301, 1203.

Henderson, G.S., De Groot, F.M. and Moulton, B.J. (2014) X-ray absorption near-edge structure (XANES) spectroscopy. Reviews in Mineralogy and Geochemistry 78, 75-138.

Hu, H., Lin, H., Zheng, W., Tomanicek, S.J., Johs, A., Feng, X., Elias, D.A., Liang, L. and Gu, B. (2013) Oxidation and methylation of dissolved elemental mercury by anaerobic bacteria. Nature Geoscience 6, 751.

Hu, H., Mylon, S.E. and Benoit, G. (2006) Distribution of the thiols glutathione and 3-mercaptopropionic acid in Connecticut lakes. Limnology and Oceanography 51, 2763-2774.

Impact of mercury on NJ's ecosystems (2002): https://www.nj.gov/dep/dsr/mercury/Mercury%20Task%20Force_Volume%20Two.pdf

Janssen, S.E., Schaefer, J.K., Barkay, T. and Reinfelder, J.R. (2016) Fractionation of mercury stable isotopes during microbial methylmercury production by iron-and sulfate-reducing bacteria. Environmental science & technology 50, 8077-8083.

Joe-Wong, C., Shoenfelt, E., Hauser, E.J., Crompton, N. and Myneni, S.C.B. (2012) Estimation of Reactive Thiol Concentrations in Dissolved Organic Matter and Bacterial Cell Membranes in Aquatic Systems. Environmental Science & Technology 46, 9854-9861.

Kendall, C. and Caldwell, E.A. (1998) Fundamentals of isotope geochemistry, Isotope tracers in catchment hydrology. Elsevier, pp. 51-86.

Kerin, E.J., Gilmour, C.C., Roden, E., Suzuki, M.T., Coates, J.D. and Mason, R.P. (2006) Mercury Methylation by Dissimilatory Iron-Reducing Bacteria. Applied and Environmental Microbiology 72, 7919.

King, J.K., Kostka, J.E., Frischer, M.E. and Saunders, F.M. (2000) Sulfate-Reducing Bacteria Methylate Mercury at Variable Rates in Pure Culture and in Marine Sediments. Applied and Environmental Microbiology 66, 2430.

Kritee, K., Barkay, T. and Blum, J.D. (2009) Mass dependent stable isotope fractionation of mercury during mer mediated microbial degradation of monomethylmercury. Geochimica et Cosmochimica Acta 73, 1285-1296.

Kritee, K., Blum, J.D. and Barkay, T. (2008) Mercury stable isotope fractionation during reduction of Hg (II) by different microbial pathways. Environmental science & technology 42, 9171-9177.

Kritee, K., Blum, J.D., Johnson, M.W., Bergquist, B.A. and Barkay, T. (2007) Mercury stable isotope fractionation during reduction of Hg (II) to Hg (0) by mercury resistant microorganisms. Environmental science & technology 41, 1889-1895.

Lalonde, J.D., Amyot, M., Kraepiel, A.M.L. and Morel, F.M.M. (2001) Photooxidation of Hg(0) in Artificial and Natural Waters. Environmental Science & Technology 35, 1367-1372.

Lavoie, R.A., Jardine, T.D., Chumchal, M.M., Kidd, K.A. and Campbell, L.M. (2013) Biomagnification of mercury in aquatic food webs: a worldwide meta-analysis. Environmental science & technology 47, 13385-13394.

Lechler, P.J., Miller, J.R., Hsu, L.-C. and Desilets, M.O. (1997) Mercury mobility at the Carson River Superfund Site, west-central Nevada, USA: Interpretation of mercury speciation data in mill tailings, soils, and sediments. Journal of Geochemical Exploration 58, 259-267.

Leclerc, M., Planas, D. and Amyot, M. (2015) Relationship between Extracellular Low-Molecular-Weight Thiols and Mercury Species in Natural Lake Periphytic Biofilms. Environmental Science & Technology 49, 7709-7716.

Lindberg, S.E., Brooks, S., Lin, C.-J., Scott, K.J., Landis, M.S., Stevens, R.K., Goodsite, M. and Richter, A. (2002) Dynamic oxidation of gaseous mercury in the Arctic troposphere at polar sunrise. Environmental science & technology 36, 1245-1256.

Lipsky, D., R.J. Reed, and R. Harkov (1980) Mercury Levels in Berry's Creek. Office of Cancer and Toxic Substances Research. NJDEP. 76 pp

Lovley, D.R. (1993) DISSIMILATORY METAL REDUCTION. Annual Review of Microbiology 47, 263-290.

Lovley, D.R., Ueki, T., Zhang, T., Malvankar, N.S., Shrestha, P.M., Flanagan, K.A., Aklujkar, M., Butler, J.E., Giloteaux, L., Rotaru, A.-E., Holmes, D.E., Franks, A.E., Orellana, R., Risso, C. and Nevin, K.P. (2011) *Geobacter*: The Microbe Electric's Physiology, Ecology, and Practical Applications, in: Poole, R.K. (Ed.), Advances in Microbial Physiology. Academic Press, pp. 1-100.

Marvin-DiPasquale, M., Agee, J., McGowan, C., Oremland, R.S., Thomas, M., Krabbenhoft, D. and Gilmour, C.C. (2000) Methyl-Mercury Degradation Pathways: A Comparison among Three Mercury-Impacted Ecosystems. Environmental Science & Technology 34, 4908-4916.

Mason, R., Rolfhus, K.a. and Fitzgerald, W. (1998) Mercury in the north Atlantic. Marine Chemistry 61, 37-53.

Mason, R.P., Morel, F.M.M. and Hemond, H.F. (1995) The role of microorganisms in elemental mercury formation in natural waters. Water Air Soil Pollut Water Air Soil Pollut

Mason, R.P. and Sheu, G.R. (2002) Role of the ocean in the global mercury cycle. Global biogeochemical cycles 16, 40-41-40-14.

Mehrotra, A.S. and Sedlak, D.L. (2005) Decrease in Net Mercury Methylation Rates Following Iron Amendment to Anoxic Wetland Sediment Slurries. Environmental Science & Technology 39, 2564-2570.

Miller, C.L., Watson, D.B., Lester, B.P., Lowe, K.A., Pierce, E.M. and Liang, L. (2013) Characterization of soils from an industrial complex contaminated with elemental mercury. Environmental Research 125, 20-29.

Mishra, B., Shoenfelt, E., Yu, Q., Yee, N., Fein, J.B. and Myneni, S.C. (2017) Stoichiometry of mercury-thiol complexes on bacterial cell envelopes. Chemical Geology 464, 137-146.

Mopper, K. and Taylor, B.F. (1986) Biogeochemical Cycling of Sulfur, Organic Marine Geochemistry. American Chemical Society, pp. 324-339.

Morel, F.M., Kraepiel, A.M. and Amyot, M. (1998) The chemical cycle and bioaccumulation of mercury. Annual review of ecology and systematics 29, 543-566.

Munthe, J. (1992) The aqueous oxidation of elemental mercury by ozone. Atmospheric Environment. Part A. General Topics 26, 1461-1468.

Newville, M. (2014) Fundamentals of XAFS. Reviews in Mineralogy and Geochemistry 78, 33-74.

Nriagu, J.O. (1993) Legacy of mercury pollution. Nature 363, 589-589.

Odom, J.M. (1993) Industrial and Environmental Activities of Sulfate-Reducing Bacteria. . Brock/Springer Series in Contemporary Bioscience. Springer, New York, NY, The Sulfate-Reducing Bacteria: Contemporary Perspectives.

Oremland, R.S., Culbertson, C.W. and Winfrey, M.R. (1991) Methylmercury Decomposition in Sediments and Bacterial Cultures: Involvement of Methanogens and Sulfate Reducers in Oxidative Demethylation. Applied and Environmental Microbiology 57, 130.

Outridge, P.M., Mason, R.P., Wang, F., Guerrero, S. and Heimbürger-Boavida, L.E. (2018) Updated Global and Oceanic Mercury Budgets for the United Nations Global Mercury Assessment 2018. Environmental Science & Technology 52, 11466-11477.

Parks, J.M., Johs, A., Podar, M., Bridou, R., Hurt, R.A., Smith, S.D., Tomanicek, S.J., Qian, Y., Brown, S.D., Brandt, C.C., Palumbo, A.V., Smith, J.C., Wall, J.D., Elias, D.A. and Liang, L. (2013) The Genetic Basis for Bacterial Mercury Methylation. Science 339, 1332.

Pirrone, N., Cinnirella, S., Feng, X., Finkelman, R.B., Friedli, H.R., Leaner, J., Mason, R., Mukherjee, A.B., Stracher, G.B. and Streets, D. (2010) Global mercury emissions to the atmosphere from anthropogenic and natural sources. Atmospheric Chemistry and Physics 10, 5951-5964.

Pirrone, N. and Mahaffey, K.R. (2005) Dynamics of mercury pollution on regional and global scales: atmospheric processes and human exposures around the world. Springer Science & Business Media.

Pitts, K.E. and Summers, A.O. (2002) The Roles of Thiols in the Bacterial Organomercurial Lyase (MerB). Biochemistry 41, 10287-10296.

Schaefer, J.K. and Morel, F.M.M. (2009) High methylation rates of mercury bound to cysteine by *Geobacter sulfurreducens*. Nature Geoscience 2, 123.

Schaefer, J.K., Rocks, S.S., Zheng, W., Liang, L., Gu, B. and Morel, F.M. (2011) Active transport, substrate specificity, and methylation of Hg (II) in anaerobic bacteria. Proceedings of the National Academy of Sciences 108, 8714-8719.

Schaefer, J.K., Yagi, J., Reinfelder, J.R., Cardona, T., Ellickson, K.M., Tel-Or, S. and Barkay, T. (2004) Role of the Bacterial Organomercury Lyase (MerB) in Controlling Methylmercury Accumulation in Mercury-Contaminated Natural Waters. Environmental Science & Technology 38, 4304-4311.

Schartup, A.T., Balcom, P.H. and Mason, R.P. (2014) Sediment-Porewater Partitioning, Total Sulfur, and Methylmercury Production in Estuaries. Environmental Science & Technology 48, 954-960.

Shea, D. and MacCrehan, W.A. (1988) Determination of hydrophilic thiols in sediment porewater using ion-pair liquid chromatography coupled to electrochemical detection. Analytical Chemistry 60, 1449-1454.

Siciliano, S.D., O'Driscoll, N.J. and Lean, D. (2002) Microbial reduction and oxidation of mercury in freshwater lakes. Environmental science & technology 36, 3064-3068.

Singleton, R. (1993) The Sulfate-Reducing Bacteria: An Overview. Brock/Springer Series in Contemporary Bioscience. Springer, New York, NY, The Sulfate-Reducing Bacteria: Contemporary Perspectives.

Skogerboe, R.K. and Wilson, S.A. (1981) Reduction of ionic species by fulvic acid. Analytical Chemistry 53, 228-232.

Skyllberg, U. (2008) Competition among thiols and inorganic sulfides and polysulfides for Hg and MeHg in wetland soils and sediments under suboxic conditions: Illumination of controversies and implications for MeHg net production. Journal of Geophysical Research: Biogeosciences 113.

Skyllberg, U., Bloom, P.R., Qian, J., Lin, C.-M. and Bleam, W.F. (2006) Complexation of mercury (II) in soil organic matter: EXAFS evidence for linear two-coordination with reduced sulfur groups. Environmental science & technology 40, 4174-4180.

Slowey, A.J., Rytuba, J.J. and Brown, G.E. (2005) Speciation of Mercury and Mode of Transport from Placer Gold Mine Tailings. Environmental Science & Technology 39, 1547-1554.

Smith, T., Pitts, K., McGarvey, J.A. and Summers, A.O. (1998) Bacterial Oxidation of Mercury Metal Vapor, Hg(0). Applied and Environmental Microbiology 64, 1328.

Song, Y., Jiang, T., Liem-Nguyen, V., Sparrman, T., Björn, E. and Skyllberg, U. (2018) Thermodynamics of hg (II) bonding to thiol groups in Suwannee River natural organic matter resolved by competitive ligand exchange, hg LIII-edge EXAFS and 1H NMR spectroscopy. Environmental science & technology 52, 8292-8301.

Suda, I., Suda, M. and Hirayama, K. (1993) Degradation of methyl and ethyl mercury by singlet oxygen generated from sea water exposed to sunlight or ultraviolet light. Arch Toxicol, Arch Toxicol.

Tang, D., Hung, C.-C., Warnken, K.W. and Santschi, P.H. (2000) The distribution of biogenic thiols in surface waters of Galveston Bay. Limnology and Oceanography 45, 1289-1297.

Thöming, J., Kliem, B.K. and Ottosen, L.M. (2000) Electrochemically enhanced oxidation reactions in sandy soil polluted with mercury. Science of the total environment 261, 137-147.

Ullrich, S.M., Tanton, T.W. and Abdrashitova, S.A. (2001) Mercury in the Aquatic Environment: A Review of Factors Affecting Methylation. Critical Reviews in Environmental Science and Technology 31, 241-293.

U.S.N.O.A.A. and U.S.F.W.S. (2014) Preassessment Screen Determination for the Berry's Creek Watershed: https://www.fws.gov/northeast/njfieldoffice/pdf/BCSA_PAS.pdf

Wang, Y., Schaefer, J.K., Mishra, B. and Yee, N. (2016) Intracellular Hg(0) Oxidation in *Desulfovibrio desulfuricans* ND132. Environmental Science & Technology 50, 11049-11056.

Wang, Y., Yu, Q., Mishra, B., Schaefer, J.K., Fein, J.B. and Yee, N. (2018) Adsorption of Methylmercury onto *Geobacter bemidjiensis* Bem. Environmental Science & Technology 52, 11564-11572.

Wedepohl, K.H. (1995) The composition of the continental crust. Geochimica et cosmochimica Acta 59, 1217-1232.

Wiatrowski, H.A., Das, S., Kukkadapu, R., Ilton, E.S., Barkay, T. and Yee, N. (2009) Reduction of Hg(II) to Hg(0) by Magnetite. Environmental Science & Technology 43, 5307-5313.

Wiatrowski, H.A., Ward, P.M. and Barkay, T. (2006) Novel Reduction of Mercury(II) by Mercury-Sensitive Dissimilatory Metal Reducing Bacteria. Environmental Science & Technology 40, 6690-6696.

Witt, M.L., Pyle, D., Mather, T., Aiuppa, A., Bagnato, E. and Martin, R. (2010) The importance of volcanoes and geothermal sources of mercury to the atmosphere.

Yamamoto, M. (1995) Possible mechanism of elemental mercury oxidation in the presence of SH compounds in aqueous solution. Chemosphere 31, 2791-2798.

Yu, Q., Szymanowski, J., Myneni, S.C.B. and Fein, J.B. (2014) Characterization of sulfhydryl sites within bacterial cell envelopes using selective site-blocking and potentiometric titrations. Chemical Geology 373, 50-58.

Yu, R.-Q., Reinfelder, J.R., Hines, M.E. and Barkay, T. (2013) Mercury Methylation by the Methanogen *Methanospirillum hungatei*. Applied and Environmental Microbiology 79, 6325.

Yu, R.-Q., Reinfelder, J.R., Hines, M.E. and Barkay, T. (2018) Syntrophic pathways for microbial mercury methylation. The ISME Journal 12, 1826-1835.

Zhang, J., Wang, F., House, J.D. and Page, B. (2004) Thiols in wetland interstitial waters and their role in mercury and methylmercury speciation. Limnology and Oceanography 49, 2276-2286.

Zheng, W., Lin, H., Mann, B.F., Liang, L. and Gu, B. (2013) Oxidation of Dissolved Elemental Mercury by Thiol Compounds under Anoxic Conditions. Environmental Science & Technology 47, 12827-12834.

Chapter 2 Intracellular Hg(0) Oxidation in *Desulfovibrio desulfuricans* ND132

Published in ES&T, 50(20), 11049-11056.

Abstract:

The disposal of elemental mercury [Hg(0)] wastes in mining and manufacturing areas has caused serious soil and groundwater contamination issues. Under anoxic conditions, certain anaerobic bacteria can oxidize dissolved elemental mercury and convert the oxidized Hg to neurotoxic methylmercury. In this study, we conducted experiments with the Hg-methylating bacterium *Desulfovibrio desulfuricans* ND132 to elucidate the role of cellular thiols in anaerobic Hg(0) oxidation. The concentrations of cell-surface and intracellular thiols were measured, and specific fractions of *D. desulfuricans* ND132 were examined for Hg(0) oxidation activity and analyzed with extended X-ray absorption fine structure (EXAFS) spectroscopy. The experimental data indicate that intracellular thiol concentrations are approximately six times higher than those of the cell wall. Cells reacted with a thiol-blocking reagent were severely impaired in Hg(0) oxidation activity. Spheroplasts lacking cell walls rapidly oxidized Hg(0) to Hg(II), while cell wall fragments exhibited low reactivity toward Hg(0). EXAFS analysis of spheroplast samples revealed that multiple different forms of Hg-thiols are produced by the Hg(0) oxidation reaction and that the local coordination environment of the oxidized Hg changes with reaction time. The results of this study indicate that Hg(0) oxidation in *D. desulfuricans* ND132 is an intracellular process that occurs by reaction with thiol containing molecules.

Introduction:

The fate and transport of mercury (Hg) in contaminated groundwater is strongly affected by redox transformations (Barringer et al., 2013; Lamborg et al., 2013; Richard et al., 2016). Whereas oxidized ionic mercury [Hg(II)] binds strongly to natural organic matter via complexation with thiol functional groups (Ravichandran, 2004; Xia et al., 1999), elemental mercury [Hg(0)] is mobile in groundwater and can migrate horizontally over long distances through the unsaturated zone as a volatile gas (Bollen et al., 2008; Walvoord et al., 2008). The conversion of Hg(0) to Hg(II) also affects the bioavailability of mercury for bacterial uptake, the production of neurotoxic methylmercury [MeHg], and subsequent bioaccumulation of MeHg in aquatic food webs (Hsu-Kim et al., 2013; Lin et al., 2012; Morel et al., 1998). Understanding the biogeochemical processes that control Hg(0) oxidation is particularly important for predicting the formation of MeHg in industrial areas contaminated with large amount elemental mercury, such as historic mining sites and nuclear weapon production facilities (Brooks and Southworth, 2011; Lechler et al., 1997; Miller et al., 2013; Slowey et al., 2005).

Certain anaerobic bacteria have been shown to produce MeHg from Hg(0) as the sole mercury source (Colombo et al., 2013; Hu et al., 2013b). A key step in the microbial conversion of dissolved elemental mercury to methylmercury is the cellular oxidation of Hg(0) to Hg(II) (Lin et al., 2014a). The Hg-methylating bacterium *Desulfovibrio desulfuricans* ND132 oxidizes dissolved elemental mercury to Hg(II) and the oxidized Hg(II) covalently bonds to cellular functional groups (Colombo et al., 2013). *Geobacter sulfurreducens* PCA can also convert Hg(0) to Hg(II) but requires either high cell concentrations or the addition of thiol compounds in its growth medium (Hu et al.,

2013b; Lin et al., 2014b). Because thiol functional groups in natural organic matter have been shown to oxidize Hg(0) via oxidative complexation (Gu et al., 2011; Zheng et al., 2012), thiol-containing molecules associated with bacterial cells may also be important for microbial Hg(0) oxidation. Currently the role of cellular thiols, the location of Hg(0) oxidation, and the chemical forms of oxidized mercury in Hg-methylating bacteria are poorly understood.

In this study, we conducted laboratory experiments to investigate thiol-mediated Hg(0) oxidation in *D. desulfuricans* ND132. Cells were separated into spheroplasts (cells without cell walls) and cell wall fragments, and experiments were conducted with the two fractions to better understand cell-surface versus intracellular Hg(0) oxidation activity. The objectives of this study were: (1) to quantify the concentration and distribution of thiol functional groups in *D. desulfuricans* ND132; (2) to determine the cellular location of Hg(0) oxidation; and (3) to characterize the chemical forms of oxidized mercury by EXAFS spectroscopy. The results of this study provide new insights into Hg(0) uptake and complexation of Hg(II) in anaerobic Hg-methylating bacteria.

Materials and Methods:

Bacterial growth conditions. *D. desulfuricans* ND132 was grown anaerobically (N_2 headspace) in a low sulfate medium modified from Gilmour et al. (Gilmour et al., 2011) containing 25 mM pyruvate, 40 mM fumarate, 0.17 M NaCl, 6.4 mM NH_4Cl, 10 mM MOPS, 1.5 mM KH_2PO_4, 3.62 µM $FeCl_2$, 6.7 mM KCl, 3.15 mM $MgCl_2 \cdot 6H_2O$, 1.36 mM $CaCl_2 \cdot 2H_2O$, 1 mL/L sulfate-free SL-7 trace metals (Widdel and Pfennig, 1981), 0.5g/L yeast extract, and NaOH to adjust the pH to 7.2. Growth medium and buffer

solutions were rendered anoxic by boiling and bubbling with O_2-free N_2 gas. Cultures were incubated statically at 30℃, harvested during mid-exponential phase (OD_{600} ~ 0.25), and washed twice with 0.5 mM MOPS buffer in an anaerobic glove box (Coy; 5:95 H_2:N_2 headspace), before experimentation.

Preparation of cell fractions. *D. desulfuricans* ND132 cell walls were removed by a procedure modified from a spheroplasts preparation method for *Geobacter sulfurreducens* (Coppi et al., 2007). Briefly, cells harvested at exponential phase were washed twice with a wash medium containing 3.09 mM KH_2PO_4, 1.26 mM K_2HPO_4, 5.10mM KCl, 0.08M NaCl, 0.01 M MOPS, 350 mM sucrose at pH 6.8. The cells were then resuspended in 4 mL of 250 mM Tris buffer (pH 7.5) and 0.4 mL of 500 mM EDTA was added to chelate structural ions in the peptidoglycan layer. After 1 min reaction with EDTA, 700 mM sucrose (4 mL) was added into the cell suspension for a 1.5 min reaction followed by the addition of lysozyme (75 mg). The cells were then incubated at 30 ℃ for 6 hours, at which point 8 mL of ultrapure water was added to induce osmotic shock. The resulting spheroplasts were immediately harvested by centrifugation at 20,000 *g* for 10 min. The cell wall fragments in the supernatant were collected by ultracentrifugation at 177,500 g for 2 hours. Spheroplast formation was verified by fluorescence microscopy in acridine orange-stained cells and quantified by direct counting method. The remaining whole cells contributed less than 10% of the total bacterial population (Hobbie et al., 1977). Finally, spheroplast lysate was produced by resuspending the spheroplasts in a hypotonic 0.5 mM MOPS buffer solution. All cell preparations were done before being exposed to Hg(0). Protein concentrations of intact cells, spheroplasts and cell walls were

measured by Bio-Rad protein assay. Spheroplasts were washed twice with wash medium to remove lysozyme before lysed for protein measurement.

Determination of thiol functional groups. The abundance of thiol functional groups was determined by a florescence-labeling method using Thiol Fluorescent Probe 4 (TFP-4) [3-(7-Hydroxy-2-oxo-2H-chromen-3-ylcarbamoyl) acrylic acid methyl ester] (EMD Millipore Corporation). TFP-4 is a cell-permeable fluorogenic probe that exhibits fluorescence when reacted with R-SH compounds via a 1:1 Michael adduct formation (Campuzano et al., 2015; Yi et al., 2009). A 1 mM stock solution was prepared by dissolving TFP-4 in dimethyl sulfoxide and diluting with acetonitrile. Experiments were conducted with spheroplasts and cell wall fragments isolated from 7.4×10^8 cells/mL cell suspensions and re-suspended in 0.5 mM MOPS buffer. Whole cells experiments were conducted at a cell density of 7.7×10^8 cells/mL. TFP-4 titrations were performed by adding a known amount of the TFP-4 stock solution to a set of sample and allowing the suspensions to react at room temperature for 2 h. Fluorescence measurements were then made in 1 mL quartz cuvettes at an excitation wavelength of 400 nm and peak emission intensity at 465 nm by Molecular Devices Plate Reader. For each set of samples, the TFP-4 titration resulted in a distinct inflection in the emission intensity precisely at the point corresponding to the thiol concentration of the sample. The thiol content per cell was determined by Avogadro's constant and normalizing the thiol concentration to cell density.

Hg(0) oxidation experiments. The oxidation of Hg(0) by *D. desulfuricans* ND132 was examined by exposing washed cell suspensions to a continuous source of Hg(0) gas. A drop of liquid Hg(0) bead was placed in an uncapped HPLC vial inside of a

30 mL serum bottle wrapped in aluminum foil and capped with a Teflon stopper. After purging the headspace of the bottle with ultra-high purity N_2 for 25 min, the liquid Hg(0) bead was allowed to evaporate and equilibrate with gas phase for 24 h. The Hg(0) oxidation reaction was initiated by injecting 5 mL of cell suspension into the serum bottle around the HPLC vial. The reactors were shaken gently at 30 ℃ and sampled periodically for formation of non-purgeable Hg(II). Triplicate bottles were used for each experiment. Cell suspension was removed from the reactor to an acid-cleaned I-Chem$^{@}$ vial at periodic intervals using needle and syringe and the subsample was purged immediately with ultra-high purity N_2 for 2 min to remove unreacted Hg(0) gas. All subsamples were digested with 4 M nitric acid and 0.2 M BrCl. Total Hg contents remaining in the samples were analyzed by cold vapor atomic fluorescence spectrometry using a BrooksRand$^{@}$ MERX Total Mercury Analytical System (EPA Method 1631) or cold vapor atomic absorption using a Leeman Labs Hydra AA Mercury Analyzer (EPA Method 245.1). Hg(0) oxidation experiments were repeated for TFP-4 treated cells, spheroplasts, and cell wall fragments. TFP-4 treatment was carried out by suspending washed cells in deoxygenated 0.5 mM MOPS buffer and reacting the cells with 233 μM TFP-4 to block cellular thiols. After 2 hours of reaction with TFP-4, cells were washed and resuspended with MOPS buffer, and then injected into reactors for the Hg(0) oxidation experiment. Experiments with spheroplasts and cell wall fragments were performed with cell suspensions at concentration of 8×10^{8} cells/mL, where the spheroplasts and cell wall fragments were separated by the protocol described above. The spheroplasts were suspended in a sucrose (350 mM) buffer to maintain isotonic conditions throughout the

experiment. Hg(0) oxidation experiments with cell wall fragments were also conducted in the sucrose buffer to allow for direct comparison with the spheroplast data.

X-ray absorption spectroscopy. Hg(0)-reacted *D. desulfuricans* ND132 spheroplasts were analyzed using X-ray Absorption spectroscopy. Spheroplasts reacted with Hg(0) were collected from the reaction bottles and purged by ultra-high purity N_2 for 25 min and centrifuged at 12,000 *g* for 15 min. The pellets were then transferred to Teflon sample holder and sealed with Kapton tape in an anaerobic chamber. The samples were placed in deoxygenated containers and shipped to the Advanced Photon Source at Argonne National Laboratory for XAS analysis. Hg L_{III}-edge EXAFS spectra were collected at beam line 13-ID-E, GeoSoilEnviroCARS, using Si (111) monochromatic crystal with a 13 element germanium detector. Although sector 13-ID-E is capable of focusing beam to 2 μm × 2 μm in vertical and horizontal directions, beam was defocused to 200 μm × 200 μm in vertical and horizontal directions and sample position was moved after every 2 scans to a fresh spot to mitigate beam induced chemistry. Spectra were collected under ambient temperature, pressure, and an N_2 atmosphere. Energy calibration was performed such that the first inflection points of Au foil and HgSn amalgam were assigned as 11919 and 12,284 eV respectively. At least 15 spectra were collected for each sample to improve the signal-to-noise ratio. Spectral features between scans were highly reproducible indicating minimal beam induced chemistry in samples during data collection.

The data were analyzed by using the methods described in the UWXAFS package (Stern et al., 1995). Data processing and fitting were done with the programs ATHENA and ARTEMIS (Ravel and Newville, 2005). The data range used for Fourier transformation

of the *k*-space data was 2.5–8.5 $Å^{-1}$. The Hanning window function was used with dk = 1.0 $Å^{-1}$. Fitting of each spectrum was performed in *r*-space, at 1.2-2.8 Å, with multiple *k*-weighting (k^1, k^2, k^3) unless otherwise stated. Lower χ_v^2 (reduced chi square) was used as the criterion for inclusion of an additional shell in the shell-by-shell EXAFS fitting procedure. Hg(0) and three Hg(II) standards [Hg-cysteine, Hg-$(cysteine)_3$, and Hg-acetate] were measured to fingerprint Hg species in this study. Details of the shell-by-shell simultaneous fitting approach used to model the EXAFS data are described elsewhere (Mishra et al., 2010).

Results:

Quantification of cellular thiols. To determine the concentration of the intracellular thiols, the cell wall of *D. desulfuricans* ND132 was removed and the spheroplast lysate was titrated with the thiol-specific fluorescent probe TFP-4, which reacts with free, reduced solvent exposed thiols that are most likely to be reactive with Hg(0). The fluorescence emission increased steeply and linearly until all the TFP-4 reactive thiols in the sample reacted with the fluorophore (Fig. 2.1A). After stoichiometric reaction with the R-SH moieties, a decrease in slope in the titration curve was observed. Best fit lines of the two linear regions of the titration curve showed an inflection point at 12 µM which corresponded to the thiol concentration in the spheroplasts lysate sample. To determine the concentration of thiol functional groups associated with the cell envelope, TFP-4 titrations were conducted with cell wall fragments. Similar to the spheroplast lysate experiment, the slope of the titration curve increased steeply and linearly followed by a marked decrease in fluorescence intensities

at high TFP-4 concentrations (Fig. 2.1B). The titration curve for the cell wall fragments showed an inflection point at 2 μM. Normalized to cell density, the thiol content of the spheroplast (9.5×10^6 thiols/cell) was approximately 6 times higher than that of the cell wall (1.7×10^6 thiols/cell). The combined thiols of the spheroplasts and cell walls was in close agreement to the total thiol concentration determined for *D. desulfuricans* ND132 whole cells, which exhibited an inflection point at 14 μM corresponding to a thiol number of 1.06×10^7 thiols/cell (Fig. 2.1C).

Oxidation of Hg(0) to Hg(II). We conducted experiments to determine the role of thiol-containing molecules in Hg(0) oxidation by blocking the cellular sulfhydryl groups with TFP-4 before reacting the cells with Hg(0). TFP-4 conjugation with cellular thiols resulted in severe impairment of Hg(0) oxidation activity (Fig. 2.2A). After 48 h, *D. desulfuricans* ND132 cells formed 464 ppb Hg(II), while the TFP-4 treated cells produced only 60 ppb Hg(II). Over 85% in Hg(0) oxidation activity was lost due to the blocking of cellular thiols with TFP-4.

To localize Hg(0) oxidation activity in the bacterial cells, experiments were conducted with specific cell fractions of *D. desulfuricans* ND132. Spheroplasts lacking cell walls rapidly oxidized Hg(0) with over 50 ppb of non-purgeable Hg formed in 6 h (Fig. 2.2B). Conversely, only 6 ppb was generated by cell wall fragments during this reaction time. The Hg(0) oxidized by spheroplasts was approximately 8 times more than Hg(0) oxidized by cell walls. In order to determine if intracellular components can account for the total Hg(0) oxidation activity observed in whole cells, Hg(0) oxidation experiments were performed on lysed spheroplasts. Both whole cells and spheroplast lysate exhibited similar Hg(0) oxidation capacity (Fig 2.2C). Heat-treated spheroplast

lysate retained Hg(0) oxidation activity (Figure S2.1). Whole cells and spheroplasts suspended in sucrose buffer showed similar Hg(0) oxidation activity, but slower reaction rates were observed in sucrose buffer compared to MOPS buffer likely due to Hg(0) diffusion and solubility effects in the concentrated sucrose solution (Figure S2.2). Interestingly, in MOPS buffer the whole cells oxidized Hg(0) at a faster initial rate (8 ppb/h) compared to the spheroplast lysate (6 ppb/h), suggesting that lysate conditions were suboptimal relative to those maintained natively by the cell (e.g., intact whole cells). This could be due to a number of factors including the dispersal and dilution of subcellular components and/or the oxidation of thiol functional groups upon exposure to the buffer. Despite this difference in initial oxidation rate, both spheroplast lysates and whole cells oxidized a similar total amount of Hg(0) and there is no statistical difference in the overall amount of nonpurgeable Hg formed at the end of the experiment.

Chemical Speciation of Oxidized Hg. X-ray absorption spectroscopy was performed to examine the oxidation state and local binding environment of the spheroplast-associated Hg. The Hg L_{III}-edge XANES spectra of the 1 h and 6 h samples were highly reproducible and showed similarities with Hg-cysteine and Hg-$(cysteine)_3$ standards (Figures 2.3A and S2.3). The normalized XANES spectra for spheroplast samples lack the pre-edge peak observed in the Hg-acetate standard, suggesting that cell-associated Hg was not complexed to carboxyl functional groups. First derivative of Hg XANES exhibited an energy separation (ΔE) between the first and second energy peak for the spheroplast samples of 7.5 eV. The ΔE value was similar to that of Hg-cysteine standard and significantly smaller than the ΔE value measured for the Hg-acetate standard (Fig. S2.3B).

These results indicate that the oxidized Hg is coordinated to sulfur (S) rather than oxygen (O) atoms.

While no significant differences in the XANES spectra were observed between the 1 h and 6 h hours samples, the k^2 weighted $\chi(k)$ spectra showed a clear phase shift in the k^2 weighted $\chi(k)$ EXAFS oscillations between the 1 h and 6 h samples (Fig. 2.3B and S2.4). For the 6 h sample, the phase of EXAFS oscillations shifted towards lower k values, which was manifested as longer bond distance of the nearest neighbor atoms in the Fourier Transformed (FT) EXAFS data (Fig. 2.3C). The Hg-S bond distance increased from 2.35 Å at 1 h to 2.43 Å at 6 h. The change in the Hg-S bond distance was also evident from the real part of the FT EXAFS spectra (Fig. 2.3D). The Hg-S bond distance for 1 h sample was slightly longer than the Hg-cysteine standard (2.30 Å) and the Hg-S bond distance for 6 h sample was slightly shorter than the Hg-$(cysteine)_3$ standard (2.48 Å), indicating there was a mixture of Hg-S species in both samples. A shell-by-shell simultaneous fitting approach was used to model the EXAFS data. Coordination numbers and bond distances for the EXAFS modeling results are consistent with approximately 80% Hg-S_1 and 20% Hg-S_3 in 1 hour sample and 20% Hg-S_1 and 80% Hg-S_3 in 6 hour sample. Best fit values for EXAFS results are shown in Table 2.1, and data and model fit are shown in Figure 2.4.

Discussion:

The experimental results presented in this study show that reduced thiols in *D. desulfuricans* ND132 mediate Hg(0) oxidation. Inhibition of Hg(0) oxidation activity by the blocking of sulfhydryl functional groups with the fluorophore TFP-4 indicates thiol functional groups in biomolecules produced by *D. desulfuricans* ND132 chemically

oxidize Hg(0) to Hg(II). The oxidative process involves complexation of the thiols with Hg(0) followed by electron transfer to an electron acceptor. This process is analogous to the redox reaction observed with liquid Hg(0) drops reacted in thiol solutions:

$RSH + Hg(0) \leftrightarrow RS\text{-}Hg + H^+ + e^-$ (1)

Open circuit potential measurements have demonstrated that the adsorption of thiol compounds onto hanging mercury drop electrodes leads to spontaneous Hg(0) oxidation (Cohen-Atiya and Mandler, 2003; Mandler and Kraus-Ophir, 2011; Muskal and Mandler, 1999). Protons have been suggested as the electron acceptor for this electrochemical process (Cohen-Atiya and Mandler, 2003), with hydrogen (H_2) as the reaction product. A similar mechanism has been proposed for Hg(0)(aq) oxidation by low-molecular-weight thiol compounds (Zheng et al., 2012; Zheng et al., 2013). This oxidative mechanism would also be expected to occur with biogenic thiol containing molecules produced by *D. desulfuricans* ND132 in both resting and metabolically active cells (Colombo et al., 2013; Hu et al., 2013b).

Hg(0) oxidation in *D. desulfuricans* ND132 is an intracellular process rather than a cell-surface mediated reaction as previously suggested (Hu et al., 2013b; Lin et al., 2014a). The experimental data implicate thiol-containing molecules in either the cytoplasm or inner membrane as the reactive agents responsible for Hg(0) oxidation (Figure 2.2A). Because the intracellular thiol concentrations in *D. desulfuricans* ND132 are approximately 6 times higher than the concentrations of thiols on the cell walls (Figure 2.1), Hg(0) oxidation within the cell is significantly more favorable than in the cell wall. Accordingly, our results showed that intracellular Hg(0) oxidation by spheroplasts was 8 times faster than cell surface Hg(0) oxidation (Figure 2.2B). The fact

that Hg(0) oxidation by spheroplasts can account for all the Hg(0) oxidation activity observed in whole cells (Figure 2.2C) further supports the hypothesis that the oxidation of Hg(0) to Hg(II) is mediated by intracellular reactions.

It is notable that the cell wall of *D. desulfuricans* ND132 exhibits very low reactivity toward Hg(0) (Figure 2.2B). Cell surface-associated thiols are reactive sites for Hg(II) adsorption in Gram-negative bacteria (Dunham-Cheatham et al., 2015; Hu et al., 2013a), and surface complexation reactions form thermodynamically stable Hg−S complexes in the bacterial cell wall (Mishra et al., 2011). Although surface-associated thiols have been proposed as the sites for Hg(0) oxidation in *G. sulfurreducens* PCA (Hu et al., 2013b; Lin et al., 2014b), our data indicate the cell surface thiols of *D. desulfuricans* ND132 do not play a central role in Hg(0) oxidation. It is generally thought that Hg(0) can diffuse across bacterial membranes without undergoing oxidation (Barkay et al., 2003). For example, during mercury detoxification by mercury resistant bacteria, Hg(II) is reduced to Hg(0) in the cytoplasm and dissolved gaseous mercury passively diffuses out of the cell. The data presented in this study suggest that the reverse process can also occur, whereby Hg(0) passively diffuses into the cell and undergoes oxidation to Hg(II) inside the cytoplasm.

Hg(0) oxidation by *D. desulfuricans* ND132 is faster and occurs to a greater extent compared to *G. sulfurreducens* PCA (Hu et al., 2013b), and the difference in reactivity toward Hg(0) may be the result of the relative cellular thiol concentration. Thiols are five hundred times more abundant in *D. desulfuricans* ND132 than in *G. sulfurreducens*, where 2.1×10^4 thiols/cell were measured using the maleimide-containing probe ThioGlo-1 (Rao et al., 2014). This large difference in the number of

reactive cellular thiols is expected to affect the kinetics and overall extent of Hg(0) oxidation. Furthermore, Hu et al. (Hu et al., 2013b) showed that at low cell concentrations *G. sulfurreducens* PCA oxidizes very little Hg(0) and requires the addition of exogenous cysteine to facilitate Hg(0) oxidation. These observations suggest that biosynthesis of thiol-containing molecules and the flux between oxidized and reduced thiol pools may be key controls on Hg(0) oxidation by anaerobic Hg methylating bacteria.

The thiol compounds in *D. desulfuricans* ND132 involved in Hg(0) oxidation have not yet been identified. The most likely sites of reaction are the sulfhydryl functional groups associated with cysteine residuals in solvent-exposed proteins or small biomolecules. Oxidized Hg has been shown to interact with thioredoxins (Wang et al., 2013) which are small cysteine-containing proteins produced by *D. desulfuricans* in response to oxidative stress (Fournier et al., 2006). Oxidative stress also induces the expression of several thiolspecific peroxidases in *Desulfovibrio* including thiol-peroxidase, bacterioferritin comigratory protein (BCP), and glutaredoxin (Fahey et al., 1978). Conversely glutathione, which occurs at high levels in aerobic bacteria, is not produced by *Desulfovibrio* (Fahey et al., 1978) and is unlikely to be involved in Hg(0) oxidation unless assimilated from external sources.

The EXAFS analysis revealed that multiple forms of Hg−thiol complexes are produced by intracellular Hg(0) oxidation in *D. desulfuricans* ND132. Linear combination fitting (LCF) of the k^2 weighted $\chi(k)$ data using Hg−cysteine and Hg−$(cysteine)_3$ standards as end members suggest a distribution of 70% Hg−S_1 and 30% Hg−S_3 in the 1-h spheroplast sample, and 15% Hg−S_1 and 85% Hg−S_3 in the 6-h sample.

These LCF estimates are in reasonably good agreement with the shell-by-shell fitting results shown in Figure 4 and Table 1. A mixture of Hg−S_1 and Hg−S_3 was also observed in the amplitude of the FT EXAFS data (Figure S2.5). Destructive interference of Hg−S_1 and Hg−S_3 signals, which are out of phase, resulted in much lower amplitude for the FT EXAFS data for 1-h sample compared with the Hg−cysteine standard. The chemical species Hg−S_2, which has a strong EXAFS signal, was not detected. On the other hand, the amplitude for the FT EXAFS data for 6-h sample is similar to that of Hg−$(cysteine)_3$ standard.

Notably, the EXAFS analysis showed that the bond distance of Hg−S complexes changes over time from 2.35 Å for the 1-h sample to 2.43 Å for the 6-h sample (Figure 2.3B−D). This increase in Hg−S bond distance is consistent with a modification of the Hg coordination environment from 1 S atom to 3 S atoms (Manceau and Nagy, 2008). The Hg−S bond distance for the 1-h sample is similar to Hg−thiol bonds distances found in natural organic matter (2.34 Å) where Hg coordinates to a single sulfur atom in a thiolated aromatic unit (Nagy et al., 2011). The 6-h sample is dominated by a Hg−S_3 complex which has been shown to form in aqueous solutions when the cysteine ligand concentration exceeds that of oxidized Hg by 2-fold (Cheesman et al., 1988). Hg−S_4 complexes, which form in highly alkaline solutions (Jalilehvand et al., 2006), are not likely to occur at physiological pH values of strain ND132. These findings indicate that, in the presence of thiol-containing biomolecules, there is an evolution of the local coordination environment of the intracellular oxidized Hg, with the stoichiometry of Hg−S bonding changing from a predominately Hg−S_1 coordination environment to a more stable Hg−S_3 configuration with increasing reaction time.

Environmental Implications. The experimental setup employed in our study resembles the mercury contaminant situation at many industrial areas where a significant amount of the elemental mercury waste persists in soils and sediments as liquid Hg beads (Liang et al., 2012). Constant evaporation and dissolution of the elemental mercury in our experiments mimic the continuous supply of Hg that is leached into groundwater and becomes available for microbial interaction as dissolved Hg(0). An example of this is the mercury contamination at Oak Ridge National Laboratory (ORNL), Tennessee (USA) where members of *Desulfovibrionaceae* have been found in groundwater monitoring wells at the Field Research Center of ORNL (Gihring et al., 2011; Hwang et al., 2009) adjacent to areas where large amounts of elemental mercury were released into the environment (Brooks and Southworth, 2011; Miller et al., 2013). The oxidation of Hg(0) by *Desulfovibrionaceae* may represent one of the pathways of mercury transformation at this site. Intracellular Hg(0) oxidation in *D. desulfuricans* ND132 has important implications for the production of methylmercury from dissolved elemental mercury. Because mercury methylation is a cytosolic process, intracellular oxidation of Hg(0) to Hg(II) bypasses uptake limitations for importing mercury into the cell and may provide a direct pathway for methylation. Conversely, oxidized mercury associated with the cell wall can undergo desorption in the presence of high-affinity aqueous ligands. Low molecular-weight thiol compounds that strongly bind Hg are common in anoxic aquatic systems (Xia et al., 1998), and the competitive binding of Hg(II) by fulvic acids has been shown to decrease the extent of mercury adsorption onto cell walls of *Bacillus subtilis*, *Shewanella oneidensis* MR-1, and *G. sulfurreducens* PCA bacterial species (Dunham-Cheatham et al., 2015). Furthermore, in sulfidic waters, cell-surface-associated Hg can

partition into mineral forms and precipitate as mercuric sulfide thus removing oxidized mercury from the cell. This is in contrast to intracellular oxidized mercury which is not subject to desorption/precipitation processes. What is not known is the reactivity of the intracellular oxidized mercury for methylation. An interesting question is whether or not the $Hg{-}S_1$ and $Hg{-}S_3$ forms of intracellular mercury detected in *D. desulfuricans* ND132 represent different bioavailable pools for methylation. Understanding the reactive forms of intracellular mercury and the molecular reactions that connect Hg(0) oxidation to MeHg production merit further investigation.

References:

Barkay, T., Miller, S.M. and Summers, A.O. (2003) Bacterial mercury resistance from atoms to ecosystems. FEMS Microbiology Reviews 27, 355-384.

Bollen, A., Wenke, A. and Biester, H. (2008) Mercury speciation analyses in $HgCl_2$-contaminated soils and groundwater—implications for risk assessment and remediation strategies. Water Research 42, 91-100.

Brooks, S.C. and Southworth, G.R. (2011) History of mercury use and environmental contamination at the Oak Ridge Y-12 Plant. Environmental pollution 159, 219-228.

Campuzano, I.D., San Miguel, T., Rowe, T., Onea, D., Cee, V.J., Arvedson, T. and McCarter, J.D. (2015) High-Throughput Mass Spectrometric Analysis of Covalent Protein-Inhibitor Adducts for the Discovery of Irreversible Inhibitors A Complete Workflow. Journal of biomolecular screening, 1087057115621288.

Cheesman, B.V., Arnold, A.P. and Rabenstein, D.L. (1988) Nuclear magnetic resonance studies of the solution chemistry of metal complexes. 25. Hg $(thiol)_3$ complexes and Hg (II)-thiol ligand exchange kinetics. Journal of the American Chemical Society 110, 6359-6364.

Cohen-Atiya, M. and Mandler, D. (2003) Studying thiol adsorption on Au, Ag and Hg surfaces by potentiometric measurements. Journal of Electroanalytical Chemistry 550-551, 267-276.

Colombo, M.J., Ha, J., Reinfelder, J.R., Barkay, T. and Yee, N. (2013) Anaerobic oxidation of Hg(0) and methylmercury formation by *Desulfovibrio desulfuricans* ND132. Geochimica et Cosmochimica Acta 112, 166-177.

Coppi, M.V., O'Neil R, A., Leang, C., Kaufmann, F., Methe, B.A., Nevin, K.P., Woodard, T.L., Liu, A. and Lovley, D.R. (2007) Involvement of *Geobacter sulfurreducens* SfrAB in acetate metabolism rather than intracellular, respiration-linked Fe(III) citrate reduction. Microbiology 153, 3572-3585.

Dunham-Cheatham, S., Mishra, B., Myneni, S. and Fein, J.B. (2015) The effect of natural organic matter on the adsorption of mercury to bacterial cells. Geochimica et Cosmochimica Acta 150, 1-10.

Fahey, R., Brown, W., Adams, W. and Worsham, M. (1978) Occurrence of glutathione in bacteria. Journal of Bacteriology 133, 1126-1129.

Fournier, M., Aubert, C., Dermoun, Z., Durand, M.-C., Moinier, D. and Dolla, A. (2006) Response of the anaerobe *Desulfovibrio vulgaris* Hildenborough to oxidative conditions: proteome and transcript analysis. Biochimie 88, 85-94.

Gihring, T.M., Zhang, G., Brandt, C.C., Brooks, S.C., Campbell, J.H., Carroll, S., Criddle, C.S., Green, S.J., Jardine, P., Kostka, J.E., Lowe, K., Mehlhorn, T.L., Overholt, W., Watson, D.B., Yang, Z., Wu, W.M. and Schadt, C.W. (2011) A limited microbial consortium is responsible for extended bioreduction of uranium in a contaminated aquifer. Appl Environ Microbiol 77, 5955-5965.

Gilmour, C.C., Elias, D.A., Kucken, A.M., Brown, S.D., Palumbo, A.V., Schadt, C.W. and Wall, J.D. (2011) Sulfate-reducing bacterium *Desulfovibrio desulfuricans* ND132 as a model for understanding bacterial mercury methylation. Appl Environ Microbiol 77, 3938-3951.

Gu, B., Bian, Y., Miller, C.L., Dong, W., Jiang, X. and Liang, L. (2011) Mercury reduction and complexation by natural organic matter in anoxic environments. Proc Natl Acad Sci U S A 108, 1479-1483.

Hobbie, J.E., Daley, R.J. and Jasper, S. (1977) Use of nuclepore filters for counting bacteria by fluorescence microscopy. Appl. Environ. Microbiol. 33, 1225-1228.

Hsu-Kim, H., Kucharzyk, K.H., Zhang, T. and Deshusses, M.A. (2013) Mechanisms regulating mercury bioavailability for methylating microorganisms in the aquatic environment: a critical review. Environmental science & technology 47, 2441-2456.

Hu, H., Lin, H., Zheng, W., Rao, B., Feng, X., Liang, L., Elias, D.A. and Gu, B. (2013a) Mercury reduction and cell-surface adsorption by *Geobacter sulfurreducens* PCA. Environ Sci Technol 47, 10922-10930.

Hu, H., Lin, H., Zheng, W., Tomanicek, S.J., Johs, A., Feng, X., Elias, D.A., Liang, L. and Gu, B. (2013b) Oxidation and methylation of dissolved elemental mercury by anaerobic bacteria. Nature Geoscience 6, 751-754.

Hwang, C., Wu, W., Gentry, T.J., Carley, J., Corbin, G.A., Carroll, S.L., Watson, D.B., Jardine, P.M., Zhou, J. and Criddle, C.S. (2009) Bacterial community succession during in situ uranium bioremediation: spatial similarities along controlled flow paths. The ISME journal 3, 47-64.

Jalilehvand, F., Leung, B.O., Izadifard, M. and Damian, E. (2006) Mercury (II) cysteine complexes in alkaline aqueous solution. Inorganic chemistry 45, 66-73.

Julia, B.L., Szabo, Z. and Pemela, R.A. (2013) Occurrence and Mobility of Mercury in Groundwater.

Lamborg, C.H., Kent, D.B., Swarr, G.J., Munson, K.M., Kading, T., O'Connor, A.E., Fairchild, G.M., LeBlanc, D.R. and Wiatrowski, H.A. (2013) Mercury speciation and mobilization in a wastewater-contaminated groundwater plume. Environmental science & technology 47, 13239-13249.

Lechler, P.J., Miller, J.R., Hsu, L.-C. and Desilets, M.O. (1997) Mercury mobility at the Carson River Superfund Site, west-central Nevada, USA: interpretation of mercury speciation data in mill tailings, soils, and sediments. Journal of Geochemical Exploration 58, 259-267.

Liang, L., Watson, D.B., Miller, C., Howe, J., He, F. and Pierce, E. (2012) The fate of mercury at a contaminated site.

Lin, C.C., Yee, N. and Barkay, T. (2012) Microbial transformations in the mercury cycle. Environmental Chemistry and Toxicology of Mercury, 155-191.

Lin, H., Hurt Jr, R.A., Johs, A., Parks, J.M., Morrell-Falvey, J.L., Liang, L., Elias, D.A. and Gu, B. (2014a) Unexpected Effects of Gene Deletion on Interactions of Mercury with the Methylation-Deficient Mutant *Δ hgcAB*. Environmental Science & Technology Letters 1, 271-276.

Lin, H., Morrell-Falvey, J.L., Rao, B., Liang, L. and Gu, B. (2014b) Coupled mercury-cell sorption, reduction, and oxidation on methylmercury production by *Geobacter Sulfurreducens* PCA. Environ Sci Technol 48, 11969-11976.

Manceau, A. and Nagy, K.L. (2008) Relationships between Hg(II)-S bond distance and Hg(II) coordination in thiolates. Dalton Trans, 1421-1425.

Mandler, D. and Kraus-Ophir, S. (2011) Self-assembled monolayers (SAMs) for electrochemical sensing. Journal of Solid State Electrochemistry 15, 1535-1558.

Miller, C.L., Watson, D.B., Lester, B.P., Lowe, K.A., Pierce, E.M. and Liang, L. (2013) Characterization of soils from an industrial complex contaminated with elemental mercury. Environmental research 125, 20-29.

Mishra, B., Boyanov, M., Bunker, B.A., Kelly, S.D., Kemner, K.M. and Fein, J.B. (2010) High- and low-affinity binding sites for Cd on the bacterial cell walls of *Bacillus subtilis* and *Shewanella oneidensis*. Geochimica et Cosmochimica Acta 74, 4219-4233.

Mishra, B., O'Loughlin, E.J., Boyanov, M.I. and Kemner, K.M. (2011) Binding of HgII to high-affinity sites on bacteria inhibits reduction to Hg0 by Mixed FeII/III phases. Environmental science & technology 45, 9597-9603.

Morel, F.M., Kraepiel, A.M. and Amyot, M. (1998) The chemical cycle and bioaccumulation of mercury. Annual review of ecology and systematics, 543-566.

Muskal, N. and Mandler, D. (1999) Thiol self-assembled monolayers on mercury surfaces: the adsorption and electrochemistry of ω-mercaptoalkanoic acids. Electrochimica acta 45, 537-548.

Nagy, K.L., Manceau, A., Gasper, J.D., Ryan, J.N. and Aiken, G.R. (2011) Metallothionein-like multinuclear clusters of mercury (II) and sulfur in peat. Environmental science & technology 45, 7298-7306.

Rao, B., Simpson, C., Lin, H., Liang, L. and Gu, B. (2014) Determination of thiol functional groups on bacteria and natural organic matter in environmental systems. Talanta 119, 240-247.

Ravel, B. and Newville, M. (2005) ATHENA and ARTEMIS: interactive graphical data analysis using IFEFFIT. Physica Scripta 2005, 1007.

Ravichandran, M. (2004) Interactions between mercury and dissolved organic matter--a review. Chemosphere 55, 319-331.

Richard, J.-H., Bischoff, C., Ahrens, C.G. and Biester, H. (2016) Mercury (II) reduction and co-precipitation of metallic mercury on hydrous ferric oxide in contaminated groundwater. Science of The Total Environment 539, 36-44.

Slowey, A.J., Rytuba, J.J. and Brown, G.E. (2005) Speciation of mercury and mode of transport from placer gold mine tailings. Environmental science & technology 39, 1547-1554.

Stern, E., Newville, M., Ravel, B. and Yacoby, Y. (1995) The UWXAFS analysis package: philosophy and details. Physica B: Condensed Matter, 117-120.

Walvoord, M.A., Andraski, B.J., Krabbenhoft, D.P. and Striegl, R.G. (2008) Transport of elemental mercury in the unsaturated zone from a waste disposal site in an arid region. Applied Geochemistry 23, 572-583.

Wang, Y., Robison, T. and Wiatrowski, H. (2013) The impact of ionic mercury on antioxidant defenses in two mercury-sensitive anaerobic bacteria. Biometals 26, 1023-1031.

Widdel, F. and Pfennig, N. (1981) Sporulation and further nutritional characteristics of Desulfotomaculum acetoxidans. Archives of Microbiology 129, 401-402.

Xia, K., Skyllberg, U., Bleam, W., Bloom, P., Nater, E. and Helmke, P. (1999) X-ray absorption spectroscopic evidence for the complexation of Hg (II) by reduced sulfur in soil humic substances. Environmental science & technology 33, 257-261.

Xia, K., Weesner, F., Bleam, W., Helmke, P., Bloom, P. and Skyllberg, U. (1998) XANES studies of oxidation states of sulfur in aquatic and soil humic substances. Soil Science Society of America Journal 62, 1240-1246.

Yi, L., Li, H., Sun, L., Liu, L., Zhang, C. and Xi, Z. (2009) A Highly Sensitive Fluorescence Probe for Fast Thiol-Quantification Assay of Glutathione Reductase. Angewandte Chemie International Edition 48, 4034-4037.

Zheng, W., Liang, L. and Gu, B. (2012) Mercury reduction and oxidation by reduced natural organic matter in anoxic environments. Environ Sci Technol 46, 292-299.

Zheng, W., Lin, H., Mann, B.F., Liang, L. and Gu, B. (2013) Oxidation of dissolved elemental mercury by thiol compounds under anoxic conditions. Environ Sci Technol 47, 12827-12834.

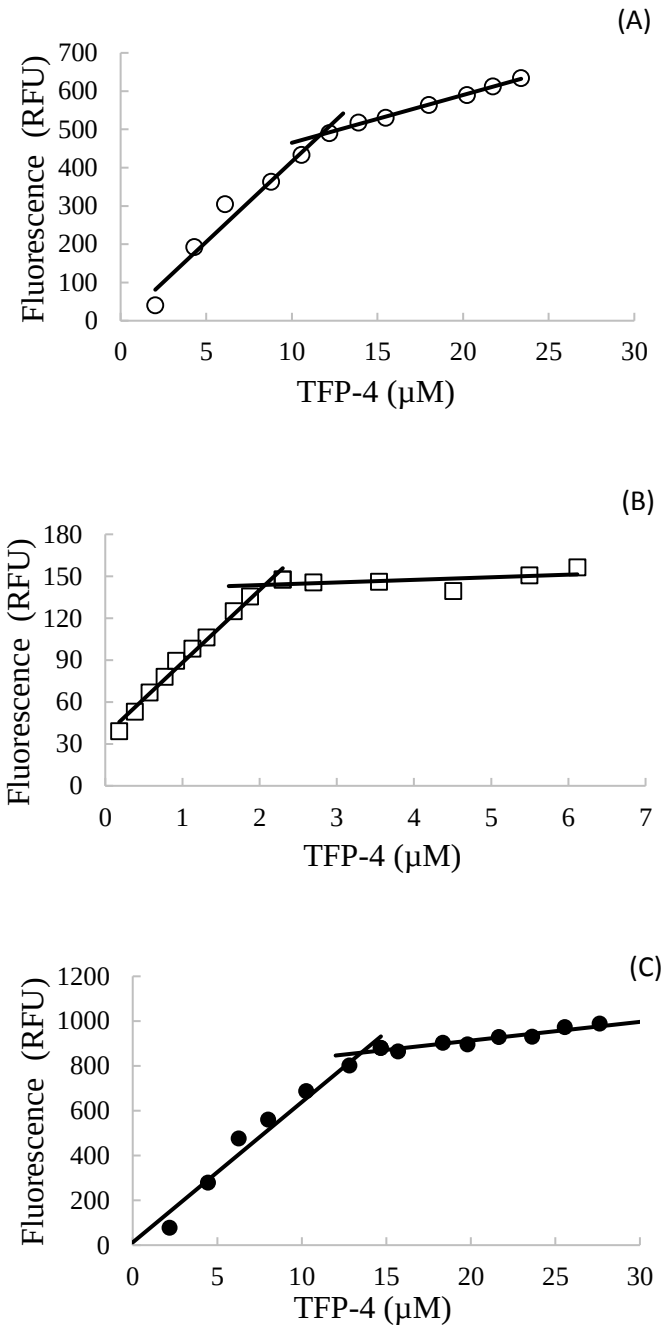

Figure 2.1: Fluorescence intensities of *D. desulfuricans* ND132 reacted with Thiol Fluorescent Probe IV (TFP-4). (A) Spheroplast lysate (open circles); (B) Cell wall fragments (open squares); (C) ND132 whole cells (closed circles). Each data point represents an individual experiment conducted in the same day.

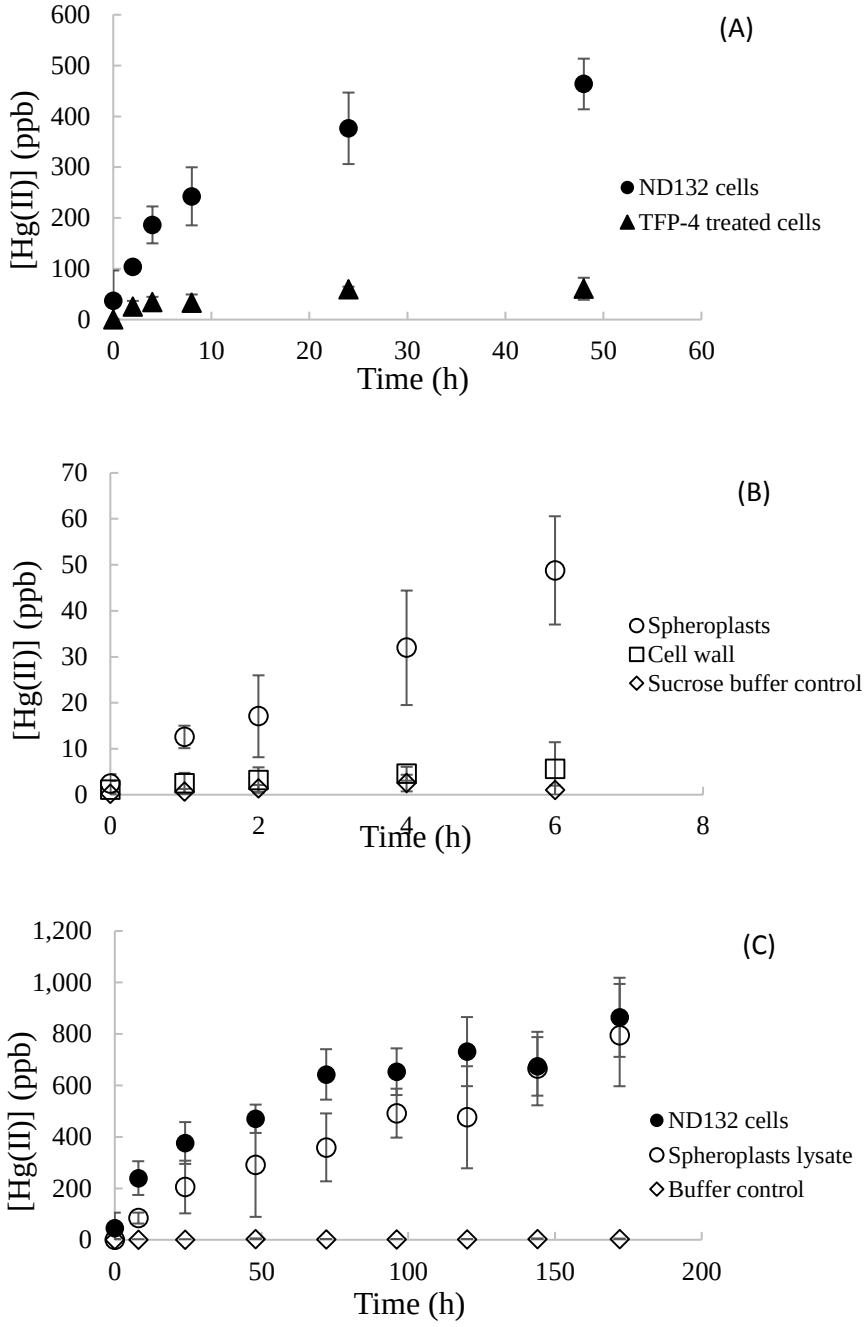

Figure 2.2: Oxidation of Hg(0) to Hg(II) by *D. desulfuricans* ND132. (A) Production of Hg(II) by whole cells (closed circles) and TFP-4 treated whole cells (closed triangle) in MOPS buffer. (B) Hg(II) formed by spheroplasts (open circles) and cell walls (open squares) in sucrose buffer. (C) Formation of Hg(II) by whole cells (closed circles) and spheroplasts lysate suspensions (open circles).

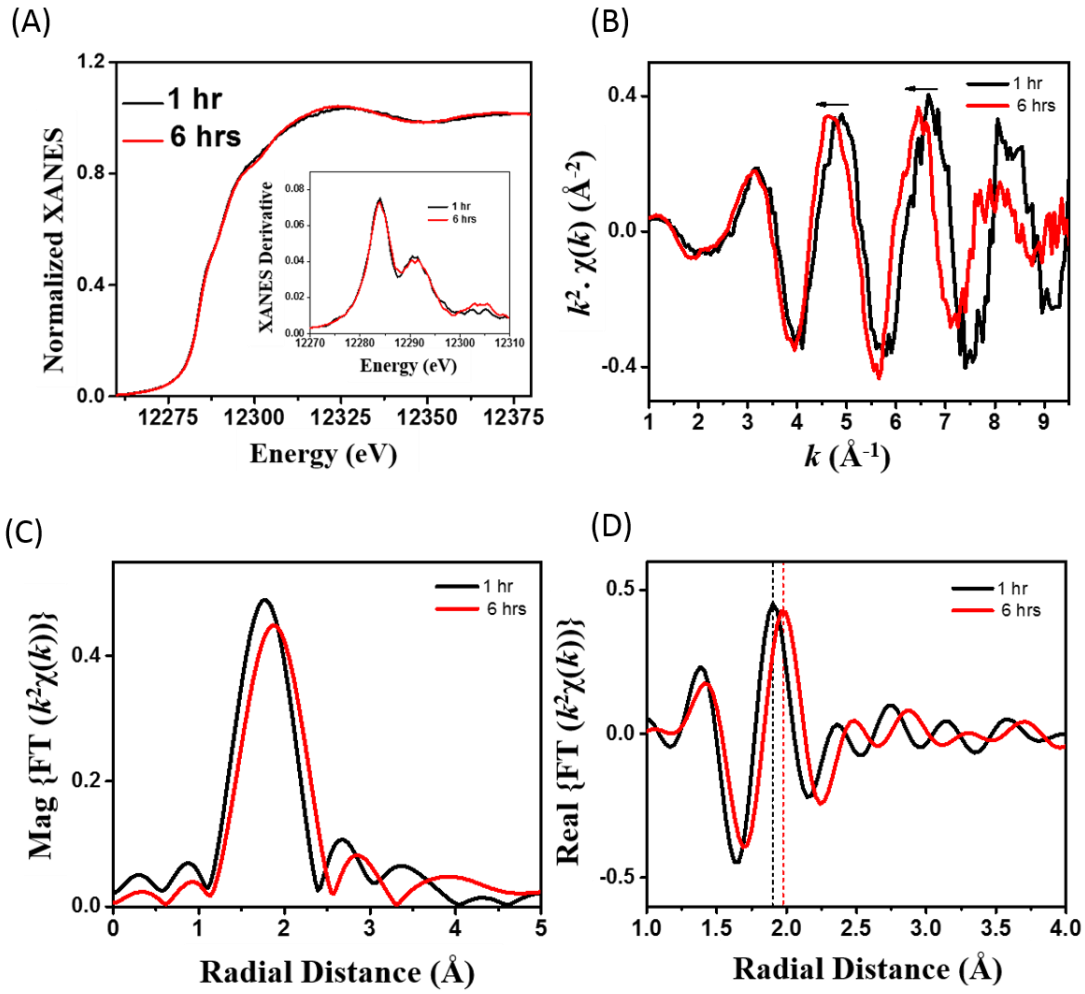

Figure 2.3: Structure characterization of Hg(0)-reacted *D. desulfuricans* ND132 spheroplasts by X-ray absorption spectroscopy (XAS) analysis at the Hg LIII-edge. (A) XANES spectra of spheroplasts samples collected at 1 h (black curve) and 6 h (red curve). The inset shows the first derivatives of the XANES spectra. (B) The k^2-weighted EXAFS spectra in k-space collected on the 1 h and 6 h spheroplasts samples. (C) Magnitude of the Fourier-transformed EXAFS spectra in R-space of 1 h and 6 h spheroplasts samples. (D) Real part of Fourier-transformed EXAFS spectra.

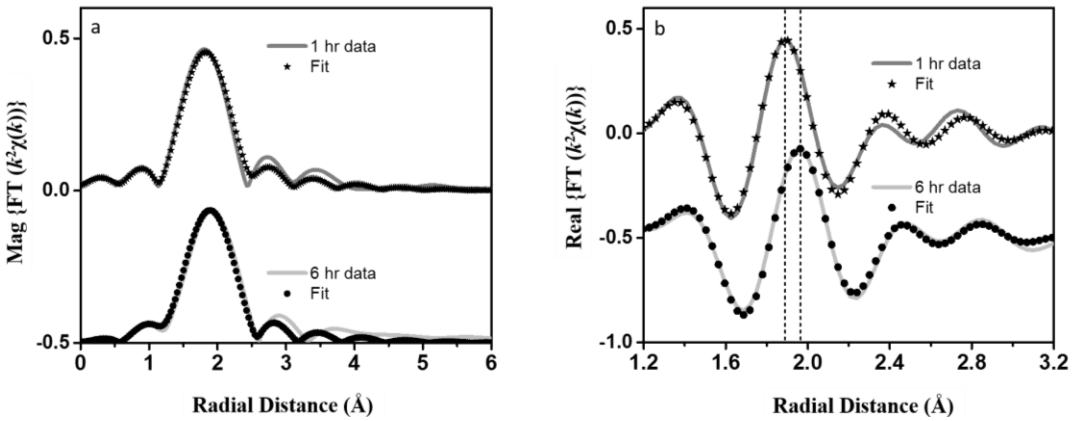

Figure 2.4: EXAFS data and fit for the (a) magnitude and (b) real part of the Fourier-transformed EXAFS spectra in R-space of 1 h and 6 h spheroplasts samples.

Table 2.1: Best fit values for EXAFS analysis of spheroplast samples.

Sample	**path**	**CN**	**R (Å)**	**$\sigma^2*10^{-3}(Å^{-1})$**	**ΔE (eV)**
ND132; 1 hr	Hg-S	1.36 ± 0.24	2.35 ± 0.01	2.5 ± 1.5	-1.46 ± 1.1
ND132; 6 hrs	Hg-S	2.48 ± 0.43	2.43 ± 0.01	8.1 ± 2.3	-1.46 ± 1.1

Note: CN, R and σ^2 represent coordination number, distance, and variance, respectively.

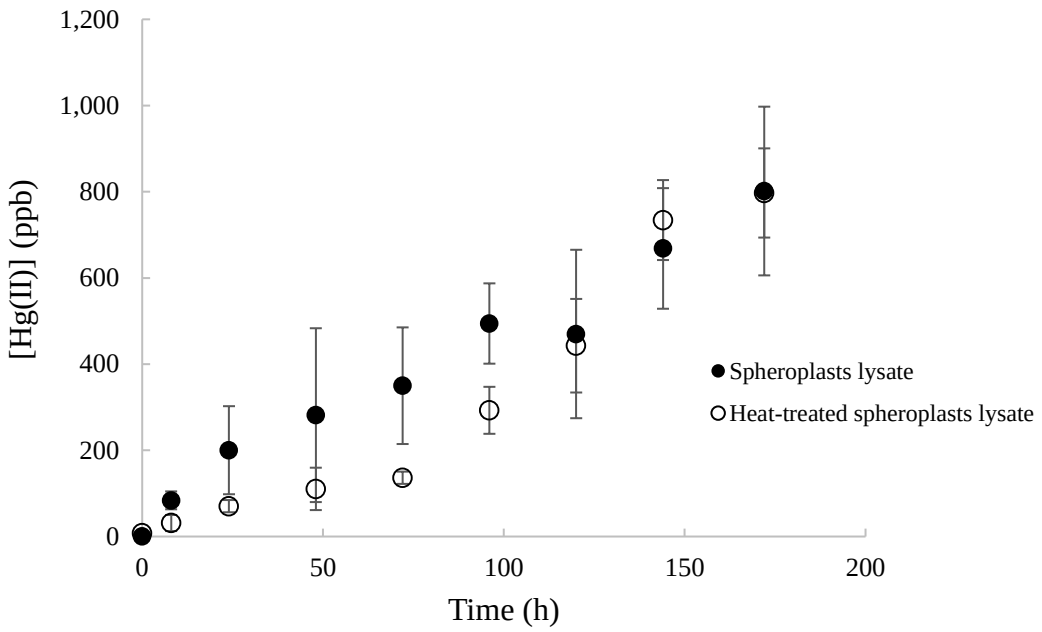

Supplement Figure S2.1: Oxidation of Hg(0) to Hg(II) by *D. desulfuricans* ND132 spheroplasts lysate (closed circles) and heat-treated spheroplasts lysate (open circles). Experiments were conducted with an initial cell concentration of 8×10^8 cells/mL. Spheroplasts lysate was treated in 80 °C water bath for 10 min. Points and error bars represent the means and standard deviations of triplicate experiments.

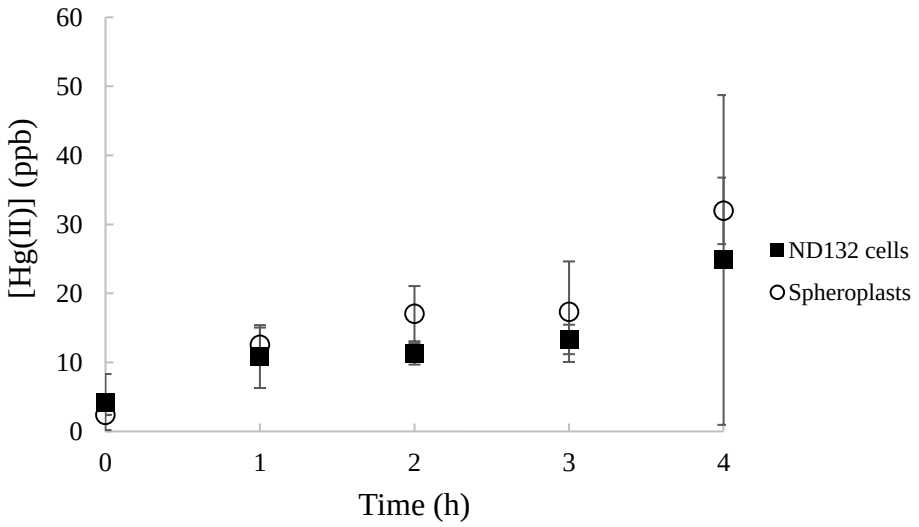

Supplement Figure S2.2: Oxidation of Hg(0) to Hg(II) by *D. desulfuricans* ND132 whole cells (closed squares) and spheroplasts (open circles) in sucrose buffer. Experiments were conducted with an initial cell concentration of 8×10^8 cells/mL. Points and error bars represent the means and standard deviations of triplicate experiments.

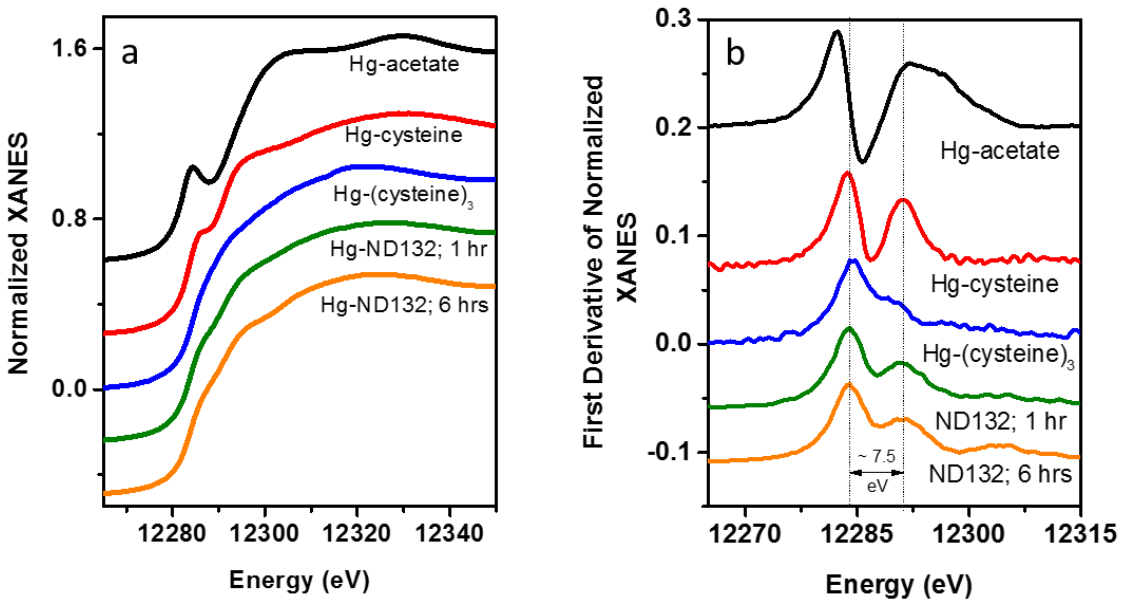

Supplement Figure S2.3: Structure characterizations on Hg(0)-reacted *D. desulfuricans* ND132 spheroplasts by X-ray absorption spectroscopy (XAS) analysis at the Hg L_{III}-edge. (a) Normalized XANES and (b) first derivative of XANES spectra of spheroplasts samples collected at 1 h and 6 h with Hg-acetate, Hg-cysteine, and Hg-$(cysteine)_3$ standards.

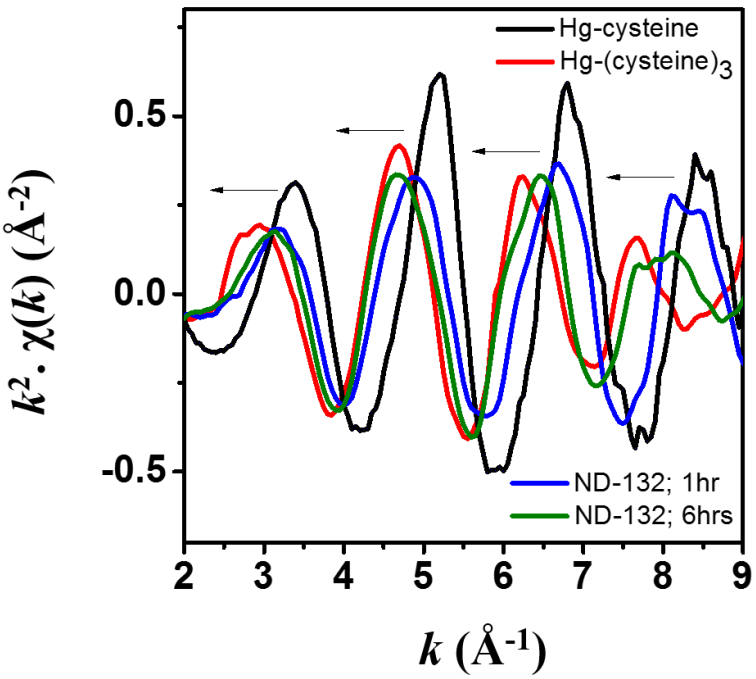

Supplement Figure S2.4: The k^2-weighted EXAFS spectra in k-space collected on the 1 h and 6 h spheroplasts samples with Hg-cysteine and Hg-$(cysteine)_3$ standards.

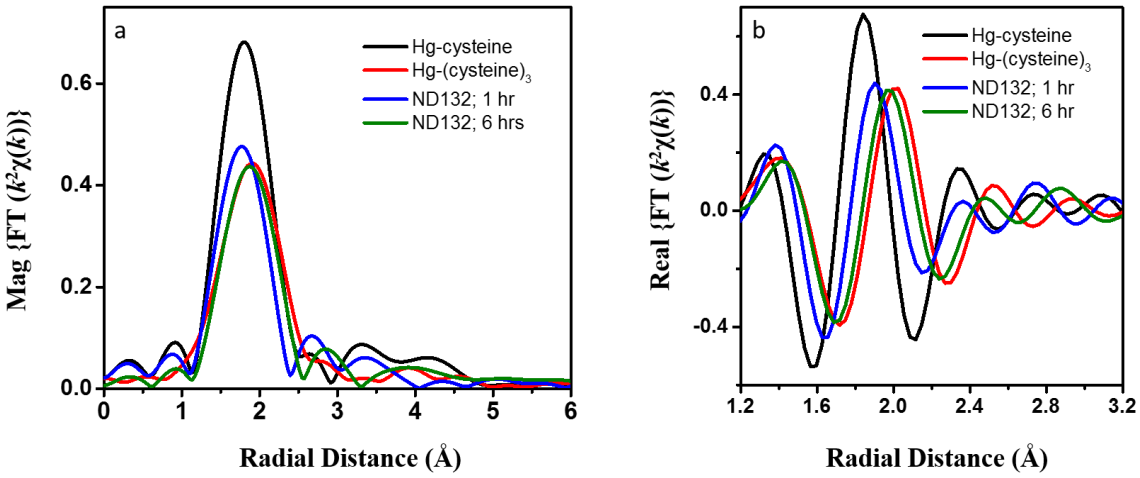

Supplement Figure S2.5: (a) Magnitude and (b) real part of the Fourier-transformed EXAFS spectra in R-space of 1 h and 6 h spheroplasts samples with Hg-cysteine and Hg-(cysteine)$_3$ standards.

Chapter 3 Adsorption of methylmercury onto *Geobacter bemidjiensis* Bem

Published in ES&T 52(20), 11564-11572.

Abstract:

The anaerobic bacterium *Geobacter bemidjiensis* Bem has the unique ability to both produce and degrade methylmercury (MeHg). While the adsorption of MeHg onto bacterial surfaces can affect the release of MeHg into aquatic environments as well as the uptake of MeHg for demethylation, the binding of MeHg to the bacterial envelope remains poorly understood. In this study, we quantified the adsorption of MeHg onto *G. bemidjiensis* and applied X-ray absorption spectroscopy (XAS) to elucidate the mechanism of MeHg binding. The results showed MeHg adsorption onto *G. bemidjiensis* cell surfaces was rapid and occurred via complexation to sulfhydryl functional groups. Titration experiments yielded cell surface sulfhydryl concentrations of 3.8 ± 0.2 μmol/g (wet cells). A one-site adsorption model with MeHg binding onto sulfhydryl sites provided excellent fits to adsorption isotherms conducted at different cell densities. The log K binding constant of MeHg onto the sulfhydryl sites was determined to be 10.5 ± 0.4. These findings provide a quantitative framework to describe MeHg binding onto bacterial cell surfaces and elucidate the importance of bacterial cells as possible carriers of adsorbed MeHg in natural aquatic systems.

Introduction:

Anaerobic bacteria play a central role in the production and degradation of methylmercury (MeHg) in the environment (Compeau and Bartha, 1985; Marvin-DiPasquale et al., 2000; Pak and Bartha, 1998). In anoxic systems, net MeHg

accumulation has been shown to be controlled by the balance of Hg methylation and MeHg demethylation rates (Avramescu et al., 2011; Tjerngren et al., 2012), which are strongly influenced by microbe-mercury interactions. Adsorption of MeHg onto bacterial cells is an important process that occurs during both mercury methylation and demethylation (Gilmour et al., 2011; Graham et al., 2012; Lin et al., 2015; Lu et al., 2017; Lu et al., 2016). MeHg adsorption onto Hg-methylating bacteria can affect the release of MeHg into aquatic environments (Lin et al., 2015), while MeHg adsorption onto methylmercury degrading bacteria may limit the uptake of MeHg for enzymatic demethylation processes (Barkay et al., 2003; Lu et al., 2017; Lu et al., 2016; Ndu et al., 2016; Silva and Rodrigues, 2015). Currently, the adsorption affinity and binding mechanism of MeHg onto bacterial cells are poorly understood.

Previous studies have found that sulfhydryl functional groups on bacterial surfaces are reactive moieties involved in heavy metal binding (Mishra et al., 2010; Mishra et al., 2011; Mishra et al., 2017; Nell and Fein, 2017; Wang et al., 2016; Yu and Fein, 2015; Yu and Fein, 2017). Despite the low abundance of sulfhydryl sites relative to the total metal binding sites in bacterial membranes, metals such as Cd(II) preferentially bind to sulfhydryl functional groups under low metal loading conditions (Yu and Fein, 2015). At environmentally relevant metal:biomass ratios, sulfhydryl sites also dominate the adsorption of Zn(II) and Ni(II) (Nell and Fein, 2017). Recently, Yu and Fein (2017) (Yu and Fein, 2017) showed that the adsorption of Hg(II), Cd(II), and Au(III) onto the Gram positive bacterium *Bacillus subtilis* is strongly enhanced by the elevated concentration of sulfhydryl sites within the cell envelopes. To date, the role of sulfhydryl

functional groups in the adsorption of MeHg onto bacterial surface has not been characterized.

Geobacter bemidjiensis Bem is a subsurface bacterium (Holmes et al., 2007; Nevin et al., 2005) that has been reported to both produce and degrade methylmercury (Gilmour et al., 2013; Lu et al., 2016). This gram-negative anaerobe carries the mercury methylation genes *hgcAB* (Lu et al., 2016; Parks et al., 2013), which enables *G. bemidjiensis* to convert inorganic Hg(II) to MeHg. Additionally, in contrast to other *Geobacter* species, strain Bem also carries a homolog of the alkylmercury lyase gene *merB* (Lu et al., 2016), which confers the ability to demethylate MeHg. Both of these mercury methylation and demethylation pathways are intracellular reactions that require transport across the cell envelope to occur. In the case of mercury methylation, MeHg produced by the bacterium can bind onto cell surface ligands thus influencing the release of MeHg into the dissolved phase. For methylmercury degradation, adsorption of MeHg onto the cell envelop can affect MeHg uptake and transport into the cell. A quantitative understanding of MeHg adsorption on cell surface functional groups would thus improve our ability to model Hg transformations by *G. bemidjiensis* and the distribution of MeHg during methylation and demethylation.

In this study, we conducted bulk adsorption experiments and spectroscopic analyses to investigate MeHg adsorption onto *G. bemidjiensis* Bem. The objectives of this study were to (1) quantify the extent of MeHg adsorption onto *G. bemidjiensis* cells; (2) characterize the local coordination environment of methylmercury adsorbed onto *G. bemidjiensis* cells; and (3) develop a surface complexation model to describe the MeHg adsorption reaction. The results of this study provide new insights into the mechanism of

MeHg adsorption onto an environmentally relevant Hg methylating and MeHg-degrading bacterium.

Material and methods:

Bacterial Culture and Assay Conditions: Strain *Geobacter bemidjiensis* Bem (gifted from B. Gu, Oak Ridge National Lab) was cultured at 30 °C under a nitrogen (N_2) headspace in ATCC Medium 1957 containing 40 mM fumarate and 30 mM acetate at pH 6.8. Cells were harvested at late exponential phase in an anaerobic glovebox, centrifuged for 8 min at 7900 g, and washed three times in 0.5 mM deoxygenated hypotonic MOPS buffer adjusted to 7.0 ± 0.2 with NaOH. Cells were then re-suspended in the MOPS buffer to a desired cell density for the MeHg adsorption experiments. The nutrient medium, growth phase, and wash procedure were the same for all experiments to minimize variations in cell size and cell surface properties.

Methylmercury Adsorption Experiments: A methylmercury chloride stock solution (50 μM) was prepared by diluting a standard solution (1000 ppm; Alfa Aesar) with deoxygenated Ultrapure Water (18.2 MΩ·cm) and stored in an ultrahigh-purity N_2 atmosphere. The MeHg stock solution was analyzed for both total mercury (THg) and MeHg, and the purity was determined to be >99% MeHg before experimentation. Inside a glove box (Coy; 5:95 H_2:N_2 headspace), MeHg adsorption experiments were initiated by adding known amounts of MeHg to each foil-wrapped serum bottles containing 100 mL *G. bemidjiensis* washed cells suspension, capped with a Teflon-lined butyl rubber stopper and sealed with aluminum caps. The reactors were then shaken at 60 rpm at 30 °C. To examine the adsorption kinetics, individual reactors were sacrificed at specific time points for mercury analyses. Aliquots were taken for THg, total methylmercury

(TMeHg), cell associated Hg ($MeHg_{cell}$), aqueous Hg ($MeHg_{aq}$), and intracellular Hg ($MeHg_{in}$) measurements. $MeHg_{cell}$ samples were collected by filtering the cell suspensions through 0.2 µm Isopore^{TM} polycarbonate membrane filters. $MeHg_{aq}$ was determined by analyzing the filtrate of samples filtered through 0.2 µm PVDF syringe filters. $MeHg_{in}$ was determined by removing the adsorbed MeHg using a wash protocol modified from Schaefer et al. (2009) (Schaefer and Morel, 2009) that desorbs metal ions but does not affect intracellular metal pools (Tang and Morel, 2006). Briefly, the adsorbed MeHg was removed by rinsing filtered cell suspensions with 5 mL of an oxalic acid-EDTA-Cl buffer twice and then with 5 mL 100 mM cysteine for 5 min. The concentration of adsorbed Hg ($MeHg_{ads}$) was calculated as the difference between $MeHg_{cell}$ and $MeHg_{in.}$ Finally, TMeHg measurements were performed and compared with THg values to verify that methylmercury degradation did not occur during the experiment.

To determine MeHg binding constants, adsorption isotherm experiments were performed by adding 10-500 nM MeHg to individual batch reactors containing cell densities ranging from 3 g/L − 0.3 g/L (wet wt), which correspond to $3 \times 10^8 - 3 \times 10^7$ cells/mL. After 2 h of equilibration, samples were collected from each reactor and digested for THg, $MeHg_{cell}$, and $MeHg_{aq}$ analyses. MeHg adsorption experiments at 3 g/L cells were repeated using *G. bemidjiensis* cells treated with 200 µM of Thiol Fluorescent Probe IV (TFP-4) (EMD Millipore Corporation) to block cellular sulfhydryl sites (Campuzano et al., 2015; Yi et al., 2009). Cells were treated with TFP-4 in a glove box and shaken in the dark for 2 h then washed three times with MOPS buffer before the adsorption experiment. Adsorption isotherms were modeled using FITEQL 2.0 (Westall,

1982) to determine the equilibrium constant of MeHg binding onto *G. bemidjiensis* and TFP-4 treated cells (see Supporting Information). The Davies equation was used to calculate activity coefficients dissolved aqueous species.

Mercury Analysis: TMeHg samples were preserved in 0.1 M H_2SO_4 at 4 °C, distilled by a Tekran 2750 gas manifold and heating system (EPA method 1630) and analyzed using Tekran 2700 gas chromatography coupled to cold vapor atomic fluorescence spectroscopy (GC−CVAFS). All other samples were digested in bromine monochloride to a final concentration of 0.02 M at 60 °C for at least 48 h and then analyzed by either cold vapor atomic fluorescence spectrometry using a Brooks Rand MERX Total Mercury Analytical System (EPA Method 1631) or cold vapor atomic absorption using a Leeman Laboratories Hydra AA Mercury Analyzer (EPA Method 245.1).

Determination of Sulfhydryl Functional Groups on Cell Surface: The abundance of sulfhydryl sites on the cell surface of *G. bemidjiensis* was quantified by the fluorescence-based method of Joe-Wong et al. (2012) using qBBr (monobromo(trimethylammonio)bimane bromide) (Sigma-Aldrich) (Joe-Wong et al., 2012). The qBBr molecule is a positively charged compound that forms highly fluorescent thioether bonds with exposed sulfhydryl moieties on the cell surface whose fluorescence increases prominently upon conjugation (Kosower et al., 1979). The positive charge of the molecule makes it difficult to pass through the inner membrane, thus allowing qBBr to preferentially react with cell envelope sulfhydryl sites. In the titration experiment, qBBr was added at specific concentrations (0-45 µM) to *G. bemidjiensis* cell suspensions (3 g/L) and then allowed to react in the dark for 2 h in a

30^{o}C shaker. Triplicate batch experiments were performed. The fluorescence was then measured in 1-mL quartz cuvettes at an excitation wavelength of 400 nm and peak emission intensity of 465 nm with a Molecular Devices Plate Reader.

Potentiometric titrations of *G. bemidjiensis* cell suspensions were also performed to quantify the total surface site concentration (Yu et al., 2014). This acid-base titration method measures the concentration and pKa values of proton-active sites within bacterial cell envelopes. Titrations were conducted using an autotitrator assembly with 10 g/L (10^9 cells/mL) of cells suspended in 0.1 M NaCl. Aliquots of 1 M HCl were added to the cell suspensions to adjust the pH to 3.0, followed by titration with 1 M NaOH to raise the pH to 9.7. These base titrations were the portion of the dataset used in the titration modeling. Three titrations experiments were conducted for *G. bemidjiensis*. All of the titrations were performed under a N_2 gas headspace to exclude atmospheric CO_2. The titration data were modeled using FITEQL 2.0 to determine the sulfhydryl site concentration and acid dissociation constant (pKa) of the proton-active surface functional groups. The number of surface sites was systematically varied in the model to determine the number of discrete sites required to fit the experimental data. The goodness of fit of each tested model was evaluated by comparing the values of the residual function from the FITEQL 2.0 output.

X-ray Absorption Spectroscopy: *G. bemidjiensis* cells with adsorbed MeHg were analyzed using X-ray absorption spectroscopy. Cell suspensions (3 g/L) were reacted with 50 nM or 500 nM MeHg for 2 h, and a 5 mL aliquot was taken to determine the concentration of adsorbed MeHg. The remaining cell suspension was pelleted by centrifugation and freeze dried. After grinding the freeze dried cells to a fine powder in an anaerobic chamber, the samples were placed in Teflon sample holders, covered with

Kapton thin film, and sealed with Kapton tape. The samples were then placed in deoxygenated containers in slotted flexiglass sample holder sandwiched between Kapton tape separated by thin Kapton film and shipped to the Advanced Photon Source at Argonne National Laboratory for XAS analysis. Hg LIII-edge XAFS spectra were collected at beamline 13-ID-E, GeoSoilEnviroCARS, using a Si (111) monochromatic crystal with a 13-element germanium detector. Samples were run under a N_2 atmosphere at ambient temperature and pressure. Energy calibration was performed such that the first inflection points of Au foil and HgSn amalgam were assigned as 11 919 and 12 284 eV, respectively. The beam was focused to 200 μm × 200 μm. Quick scans (5 min/scan) were performed on MeHg samples collecting 3 scans each at over 20 separate spots for each sample to limit the beam-induced chemistry and obtain highly reproducible scans. The k-space for the XAFS scans was collected up to 12.0 $Å^{-1}$. Five raw spectra were merged before background subtraction was performed. Data were processed using ATHENA and ARTEMIS (Ravel and Newville, 2005). The k-space data range used for these analyses were 2.5 to 8.0 $Å^{-1}$, using a Hanning window function dk set to 1.0. S_0^2 of 0.9 was used during simultaneous fitting of 68 μg /g and 455 μg /g MeHg-cell samples at multiple k (k_1, k_2, and k_3) weighting. Statistically significant lower reduced chi-square was used for inclusion of another atom in shell-by-shell fitting approach. R-factor of 1.5% was obtained for a fit range of 1.1 to 3.0 Å in Fourier transformed R space. R-factor is a non-statistical measure of goodness of fit, where lower value suggests a good reproduction of data by the model. Usually an XAFS model with R-factor around 1% is considered good.

Results and Discussion:

MeHg Adsorption onto *G. bemidjiensis* Bem Cell Surfaces. Kinetics experiments showed that *G. bemidjiensis* rapidly sorbed MeHg, with approximately 80% of MeHg sorbing in 15 minutes (Fig. 3.1A). MeHg sorption was concurrent to the removal of MeHg from solution. To determine the intracellular versus surface-bound distribution of cell-associated MeHg, a 100 mM cysteine solution was used to desorb MeHg from the cell surface. Approximately 90-100% of the sorbed MeHg was extracted by reaction with cysteine (Fig.3.1B and Table S3.1), indicating the MeHg was surface-bound. Adsorption isotherms were then conducted at different cell densities to determine the affinity of MeHg adsorption onto *G. bemidjiensis* (Fig. 3.2). The data showed that the concentration of adsorbed MeHg increased linearly with the aqueous MeHg concentration, and the MeHg loading increased with decreasing cell density (Fig 3.2A-C). To test if sulfhydryl sites were involved in MeHg adsorption, a thiol-specific probe TFP-4 was used to block the sulfhydryl sites associated with the bacterial cells. The TFP-4 treated cells adsorbed markedly less MeHg (Fig. 3.2D) compared to untreated cells (Fig. 3.2A). The decrease in MeHg adsorption was attributed to MeHg binding to low affinity sites on the bacterial surface due to the loss of sulfhydryl complexation in the TFP-4 treated cells.

Quantification of Sulfhydryl Sites. The concentration of sulfhydryl sites on cell surface of *G. bemidjiensis* was determined by titrating cell suspensions with the fluorescent probe qBBr which binds specifically to sulfhydryl sites within the cell envelope. When reacted with the qBBr fluorophore, the fluorescence emission increased steeply and linearly with increasing qBBr concentration until the cell surface sulfhydryl

sites became saturated with qBBr (Fig. 3.3). Further additions of qBBr showed weak fluorescence emission with increasing qBBr concentration, as this excess qBBr remained unbound to sulfhydryl sites and hence did not strongly fluoresce. In replicate experiments, the best-fit lines of the two linear regions of the qBBr titration data exhibited inflection points at 3.7 μmol/g, 3.6 μmol/g, and 4.0 μmol/g (wet wt). The average value for the inflection point of the triplicate experiments was 3.8 ± 0.2 μmol/g (1 standard deviation), corresponding to the concentration of reactive sulfhydryl sites on the cell surface of *G. bemidjiensis*. This sulfhydryl site concentration was higher than the highest MeHg concentration used in the adsorption isotherms experiments. At the maximum MeHg loading, the MeHg:sulfhydryl molar ratio was approximately 0.15. Thus, the sulfhydryl sites were well below saturation over the entire MeHg concentration range studied.

We then conducted acid-base potentiometric titrations with *G. bemidjiensis* washed cell suspensions to quantify the total concentration of proton-active sites on the cell surface and the acidity constant of each surface site type (Fig S3.1). Replicate titrations yielded an average total site concentration of 253.0 ± 2.9 μmol/g (wet wt). The titration curves were modeled using FITEQL 2.0 to determine individual site concentrations according the reaction:

$$R\text{-}L_iH \rightleftharpoons R\text{-}L_i^- + H^+ \quad (1)$$

where [R-L_iH] and [R-L_i^-] represent the concentrations of the *i*th neutral and deprotonated organic acid functional group on the bacterial cell surface, respectively. The acidity constant of each surface site type was quantified with the corresponding mass action equation:

$$K_{a,i} = \frac{[R\text{-}L_i^-]\, a_{H^+}}{[R\text{-}L_iH]} \quad (2)$$

A four site model provided the best-fit to the titration data. The best-fit model yielded pKa values of 3.9 ± 0.4, 5.4 ± 0.3, 7.2 ± 0.2, and 9.6 ± 0.1 with corresponding site concentrations of 76.0 ± 7.6, 70.3 ± 11.1, 37.9 ± 4.0 and 68.8 ± 5.1 µmol/g, respectively (Table 3.1). Previously, Yu et al. (2014) showed that site 4 (pKa 9.2–9.4) of bacterial strains *Bacillus licheniformis*, *Bacillus subtilis*, *Bacillus cereus*, *Shewanella oneidensis* and *Pseudomonas fluorescens* contained sulfhydryl sites (Kosower et al., 1979). Furthermore, the pKa value of site 4 is similar to that of sulfhydryl functional groups of thiol molecules such as cysteine, glutathione and some proteins, with values ranging from 8.06 to 10.75 (Tajc et al., 2004). Therefore, we suggest that site 4 likely represents a mixture of site types, some of which are sulfhydryl functional groups, and all of which exhibiting similar pKa values.

XAS Analysis of Adsorbed MeHg. X-ray absorption spectroscopy was performed to examine the local bonding environment of the adsorbed MeHg. The first derivative of normalized X-ray absorption near edge structure (XANES) and the X-ray absorption fine structure (XAFS) spectra of *G. bemidjiensis* reacted with 50 nM and 500 nM MeHg are displayed in Figure 3.4A and B, respectively. The amount of MeHg adsorbed to those two samples were 68 µg /g and 455 µg /g (dry wt), respectively. Derivative of the XANES spectra of the two samples were nearly identical and both spectra exhibited two main peaks (Fig 3.4A). The energy difference between the two peaks was used to calculate the ΔE value. Because a larger ΔE corresponds to Hg-ligand complexes with ionic character and a smaller ΔE to complexes with more covalent character (Powers, 1982), we used this value to infer the local bonding environment of

MeHg. The derivative of the XANES spectra showed a ΔE value of 7.0 eV, which is similar to ΔE values of Hg-cysteine$_2$ (ΔE = 7.2 eV) (Colombo et al., 2013, 2014) and MeHg-cysteine (ΔE = 7.7 eV) (Rajan et al., 2008). The measured ΔE value is distinct from MeHgCl (ΔE = 9.0 eV) and MeHg-glutamic acid (ΔE = 8.8 eV) (Rajan et al., 2008), thus ruling out the formation of chloride and oxygen bonds on the cell surface.

The k^2-weighted χ(k) spectra of the 68 µg /g and 455 µg /g samples were nearly identical and no phase shift in the k^2 weighted χ(k) XAFS oscillations between the two samples was observed (Fig. 4B). This indicates that the stoichiometry of MeHg-cell complexes was the same at the two different MeHg loadings. Both 68 µg /g and 455 µg /g samples were best fit with 0.9 +/- 0.1 sulfur atom at ~2.34 angstrom and 0.9 +/ 0.1 carbon atom at ~2.03 angstrom, indicating that the Hg-C bond in MeHg remained intact when adsorbed on the bacterial surface and that MeHg was bonded exclusively to sulfhydryl sites of *G. bemidjiensis* (Fig 3.4C and 3.4D, Table 3.2). No changes in the Hg−S bond distance was observed suggesting that the MeHg−S complexes were the same in both samples (Fig 3.4C and 3.4D). Notably, the binding distance and the ratios of Hg atoms to C and S atoms are similar to MeHg-DOM bonding (Hintelmann et al., 1997; Karlsson and Skyllberg, 2003; Qian et al., 2002; Ravichandran, 2004; Skyllberg et al., 2005; Yoon et al., 2005).

MeHg Adsorption Constant. Because the XAFS data showed MeHg binding to the sulfhydryl functional groups with a 1:1 MeHg:site stoichiometry (Fig 3.4B, Table 3.2), the adsorption isotherms were used to determine a stability constant for the MeHg-sulfhydryl complex formed on the cell surface using the following reactions:

$$R\text{-}L_4^- + MeHg^+ \rightleftharpoons R\text{-}L_4\text{-}MeHg \qquad (3)$$

$$MeHgCl \rightleftharpoons MeHg^{+} + Cl^{-} \quad (4)$$

$$R\text{-}L_4H \rightleftharpoons R\text{-}L_4^{-} + H^{+} \quad (5)$$

where R-L_4-MeHg is the MeHg adsorbed onto the cell surface, and R-L_4^- is the sulfhydryl portion of site 4 with a pKa value of 9.5 and a sulfhydryl site concentration of 3.8 ± 0.2 µmol/g as determined by the acid-base titration and fluorescent titration experiments, respectively. The stability constant was quantified with the corresponding mass action equation:

$$K_{MeHg\text{-}L4} = \frac{[R\text{-}L_4\text{-}MeHg]}{[R\text{-}L_4^-]\, a_{MeHg^+}} \quad (6)$$

The MeHg binding constant was remarkably consistent for three adsorption data sets. At cell densities of 3 g/L, 0.6 g/L, and 0.3 g/L, the adsorption data yielded log $K_{MeHg\text{-}L4}$ values of 10.3, 10.6, and 10.5, respectively (Table 3.3). The model fits displayed in Figure 3.2 show good agreement with the experimental data. The one-site model for MeHg binding onto R-L_4^- provided excellent fits to all three adsorption isotherms with r^2 values greater than 0.95 (Table 3.3). No improvement in fit was obtained using a two-site model by including an additional site for MeHg binding. Because error in the log K binding constant arises from scatter in the adsorption data, we calculated the upper and lower limit for the one-site model by systematically varying the log K values to determine the envelope that encompasses 68% (1 standard deviation) of the experimental data points. The error analysis yielded log K values with uncertainties of 10.3 ± 0.1, 10.6 ± 0.3 and 10.5 ± 0.1 for the three cell densities. Propagation of error from uncertainties in the sulfhydryl site concentrations (3.8 ± 0.2 µmol/g) had a negligible effect on log K binding constants. Combining all data sets, the average log K value for the one-site model

was 10.5 ± 0.4. This binding constant is comparable to the log K value of Hg(II) complexation to sulfhydryl sites on *Geobacter sulfurreducens* PCA at circumneutral pH conditions (log K = 10.9 ± 0.3) (Dunham-Cheatham et al., 2014).

We then modeled the adsorption isotherm of the sulfhydryl-blocked cells (Fig. 3.2D). Because sulfhydryl sites represented only ~1.5% of the total surface sites, MeHg adsorbed to the vast number of low affinity sites on the cell surface when the high affinity sulfhydryl sites were blocked. To examine MeHg binding the low affinity sites, we first tested a one-site adsorption model with MeHg binding to site 1. The resulting log K value for MeHg binding was 3.8 with a corresponding r^2 value of 0.96 (Table 3.3). Since our data were not collected as a function of pH, the binding site for MeHg is not well-constrained. Therefore, we also considered MeHg binding to alternate cell surface sites (e.g., sites 2, 3 or 4). The resulting binding constants are shown in Table 3.3 and yielded equally good fits to the experimental data. Thus, with these data we were unable to conclusively identify the MeHg adsorption site on sulfhydryl-blocked cells. Nonetheless, the binding constants allowed us to compare the partitioning of MeHg to the low affinity adsorption sites relative to the sulfhydryl functional groups. We noted that the stability constants for the weak surface complexes (log K ranging between 3.8 to 6.4) were significantly lower than the R-L_4-MeHg complex (log K = 10.5). To compare the partitioning of MeHg, we constructed a two-site model where MeHg was adsorbed onto the sulfhydryl site and one of the weak sites. The two-site model showed that MeHg was overwhelmingly partitioned to the sulfhydryl site. No matter which weak site was selected, more than 99% of the MeHg was adsorbed to the sulfhydryl functional groups.

These modeling results offer an explanation as to why MeHg binds exclusively to sulfhydryl sites as observed in the XAFS experiments.

Environmental Implications: The rapid and extensive adsorption of MeHg onto *G. bemidjiensis* indicates that cell surfaces are reactive interfaces that can accumulate MeHg produced by Hg-methylating bacteria. The adsorption model presented in this study provides a quantitative framework to understand MeHg binding to the cell envelope of *Geobacter* species during MeHg production. Previous studies have shown that approximately 80% of the MeHg produced by *G. bemidjiensis* is adsorbed onto cell surfaces (Lu et al., 2016) and more than 90% of MeHg is bound to *G. sulfurreducens* PCA (Lin et al., 2015). Similar to our experiments, MeHg adsorption was kinetically fast, reaching equilibrium in less than 30 minutes. The amount of adsorbed MeHg measured in these previous experiments is in agreement with the distribution of MeHg predicted by our surface complexation model. Because MeHg binds strongly to cell surfaces during methylation, the fate of this adsorbed MeHg is expected to be tied to that of the bacterial cells. For example, if the Hg-methylating bacteria are mobile, then the adsorbed MeHg would be carried along with the particulate phase for environmental transport. MeHg is known to be partitioned onto particulate matter in aquatic environments (Cardona-Marek et al., 2007; Ortiz et al., 2015), where bacterial cells typically represent a significant fraction of the particulate phase (Böckelmann et al., 2000; Weiss et al., 1996). Conversely, if the bacterial cells are attached to sediment surfaces or form biofilms, then the adsorbed MeHg would have limited environmental mobility.

Our results suggest that the concentration of cellular sulfhydryl sites is an important factor that controls the extent to which bacterial cells can act as carriers of

adsorbed MeHg. The concentration of sulfhydryl sites on bacterial surfaces appears to vary between bacterial species. Whereas *G. bemidjiensis* has 3.8 ± 0.2 μmol/g of cell surface sulfhydryl sites, corresponding to 2.3×10^7 sites/cell, the closely related Hg-methylating bacterium *G. sulfurreducens* PCA has at least 10 times higher reactive sulfhydryl sites in its cell envelope (Mishra et al., 2017). In comparison, the non Hg-methylating bacteria *B. cereus, B. subtilis* and *S. oneidensis* have intermediate cell surface sulfhydryl site concentrations of 16.6, 22.5, and 33.1 μmol/g (Yu et al., 2014). Notably, these values are in the same order of magnitude as sulfhydryl site concentrations found in solid organic particles (~22 μmol/g) (Skyllberg, 2008), and hence bacteria are likely to be able to compete effectively with solid organic particles for available MeHg in aquatic systems.

The log K value for MeHg binding to sulfhydryl sites on *G. bemidjiensis* (log K = 10.5 ± 0.4) is comparable to MeHg binding constants to certain humic and fulvic acids (log K ranging from 10.7 to 14.96) (Amirbahman et al., 2002; Hintelmann et al., 1995), but is lower than other estimates for natural organic matter. Hintelmann et al. (1997) reported MeHg binding constant of log K ~ 13-14.5 for strong sites in humic substances (Hintelmann et al., 1997). Qian et al. (2002) and Karlsson and Skyllberg (2003) employed XANES to determine reduced sulfur binding sites in organic matter and reported conditional binding constants under acidic pH conditions of 16.3-16.7 and 15.6-17.1, respectively (Karlsson and Skyllberg, 2003; Qian et al., 2002). While these studies suggest that MeHg binding to bacterial surfaces may be weaker than thiol-containing organic carbon, they also highlight difficulties in comparing log K values between bacterial cells and dissolved organic matter. Direct comparisons are difficult because of

differences in experimental methodologies, solution compositions, and calculation models. For example, conditional binding constants are higher under acidic conditions compared to neutral pH values. Khwaja et al. (2010) (Khwaja et al., 2010) found that the conditional MeHg binding constant for thiol-sites in Suwannee River fulvic acid decreases from log K = 15.6 at pH 2.98 to log K = 12.3 at pH 7.62. They also found that decreasing the pKa of the thiol binding sites decreases the log K value.

Nonetheless, the high binding constants for MeHg complexation to dissolved organic matter indicates that the desorption of MeHg from the *G. bemidjiensis* cell surface is facilitated by the presence of strong ligands (e.g. cysteine in Fig. 3.1B). In natural systems, the release of MeHg from bacterial surfaces would be enhanced by reactions with low-molecular-weight thiol compounds and other high affinity aqueous ligands. These include interactions with small thiol-containing molecules which typically exhibit MeHg binding constants between log K ~ 16-17 (Reid and Rabenstein, 1981) as well as some humic and fulvic acids (Amirbahman et al., 2002; Hintelmann et al., 1997; Khwaja et al., 2010). Natural waters containing high concentrations of dissolved sulfide (Dyrssen et al., 1985) would also favor the desorption process. Interestingly, MeHg desorption from Hg-methylation bacteria may stimulate additional methylation to occur. Lin et al. (2015) (Lin et al., 2015) found that the amount of MeHg produced by *G. sulfurreducens* PCA increases when cysteine is added to desorb cell-bound MeHg. Thus, adsorption-desorption reactions may play an important but poorly understood role in affecting net methylmercury production by *Geobacter* species. Furthermore, other Hg-methylating bacteria, such as *D. desulfuricans* ND132, export MeHg from their cells in a chemical form that does not readily adsorb to cell surfaces (Colombo et al., 2013;

Gilmour et al., 2011). This raises the possibility that MeHg produced by certain Hg-methylators is complexed to a strong ligand that prevents binding to the bacterial cell envelope.

Finally, MeHg has been shown to demethylate when it is adsorbed to marine particles containing bacterial cells (Ortiz et al., 2015), suggesting an interplay between adsorption and MeHg degradation. In experiments with *G. bemidjiensis* Bem, Lu et al. (2016) observed that the concentration of adsorbed MeHg decreases during MeHg degradation (Lu et al., 2016). It is currently unknown if adsorbed MeHg is bioavailable and directly internalized by metabolically active cells for demethylation. Recently, Ndu et al. (2016) demonstrated that non-specific binding of MeHg to cellular ligands decreases the rates of MeHg degradation (Ndu et al., 2016), thus suggesting that adsorbed MeHg is unavailable for direct uptake. In this case, adsorbed MeHg must first desorb into the aqueous phase and then re-enter the cell via passive or active transport for demethylation. Identification of the cell surface molecules that harbor the high affinity MeHg binding sites and elucidation of the MeHg uptake pathway in *G. bemidjiensis* are needed to better understand the role of adsorption in the MeHg demethylation process.

References:

Amirbahman, A., Reid, A.L., Haines, T.A., Kahl, J.S. and Arnold, C. (2002) Association of methylmercury with dissolved humic acids. Environmental Science & Technology 36, 690-695.

Avramescu, M.-L., Yumvihoze, E., Hintelmann, H., Ridal, J., Fortin, D. and Lean, D.R. (2011) Biogeochemical factors influencing net mercury methylation in contaminated freshwater sediments from the St. Lawrence River in Cornwall, Ontario, Canada. Science of the Total Environment 409, 968-978.

Barkay, T., Miller, S.M. and Summers, A.O. (2003) Bacterial mercury resistance from atoms to ecosystems. FEMS Microbiology Reviews 27, 355-384.

Böckelmann, U., Manz, W., Neu, T.R. and Szewzyk, U. (2000) Characterization of the microbial community of lotic organic aggregates ('river snow') in the Elbe River of Germany by cultivation and molecular methods. FEMS microbiology ecology 33, 157-170.

Campuzano, I.D., San Miguel, T., Rowe, T., Onea, D., Cee, V.J., Arvedson, T. and McCarter, J.D. (2015) High-Throughput Mass Spectrometric Analysis of Covalent Protein-Inhibitor Adducts for the Discovery of Irreversible Inhibitors A Complete Workflow. Journal of biomolecular screening, 1087057115621288.

Cardona-Marek, T., Schaefer, J., Ellickson, K., Barkay, T. and Reinfelder, J.R. (2007) Mercury speciation, reactivity, and bioavailability in a highly contaminated estuary, Berry's Creek, New Jersey Meadowlands. Environmental science & technology 41, 8268-8274.

Colombo, M.J., Ha, J., Reinfelder, J.R., Barkay, T. and Yee, N. (2013) Anaerobic oxidation of Hg(0) and methylmercury formation by *Desulfovibrio desulfuricans* ND132. Geochimica et Cosmochimica Acta 112, 166-177.

Colombo, M.J., Ha, J., Reinfelder, J.R., Barkay, T. and Yee, N. (2014) Oxidation of Hg(0) to Hg(II) by diverse anaerobic bacteria. Chemical Geology 363, 334-340.

Compeau, G. and Bartha, R. (1985) Sulfate-reducing bacteria: principal methylators of mercury in anoxic estuarine sediment. Applied and environmental microbiology 50, 498-502.

Dunham-Cheatham, S., Farrell, B., Mishra, B., Myneni, S. and Fein, J.B. (2014) The effect of chloride on the adsorption of Hg onto three bacterial species. Chemical Geology 373, 106-114.

Dyrssen, D., Haraldsson, C., Westerlund, S. and Årén, K. (1985) Indication of thiols in Black Sea deep water. Marine Chemistry 17, 323-327.

Gilmour, C.C., Elias, D.A., Kucken, A.M., Brown, S.D., Palumbo, A.V., Schadt, C.W. and Wall, J.D. (2011) Sulfate-reducing bacterium *Desulfovibrio desulfuricans* ND132 as a model for understanding bacterial mercury methylation. Appl Environ Microbiol 77, 3938-3951.

Gilmour, C.C., Podar, M., Bullock, A.L., Graham, A.M., Brown, S.D., Somenahally, A.C., Johs, A., Hurt, R.A., Bailey, K.L. and Elias, D.A. (2013) Mercury Methylation by Novel Microorganisms from New Environments. Environmental Science & Technology 47, 11810-11820.

Graham, A.M., Bullock, A.L., Maizel, A.C., Elias, D.A. and Gilmour, C.C. (2012) Detailed assessment of the kinetics of Hg-cell association, Hg methylation, and methylmercury degradation in several *Desulfovibrio* species. Appl Environ Microbiol 78, 7337-7346.

Hintelmann, H., Welbourn, P. and Evans, R. (1995) Binding of methylmercury compounds by humic and fulvic acids. Water, Air, and Soil Pollution 80, 1031-1034.

Hintelmann, H., Welbourn, P.M. and Evans, R.D. (1997) Measurement of complexation of methylmercury (II) compounds by freshwater humic substances using equilibrium dialysis. Environmental science & technology 31, 489-495.

Holmes, D.E., O'neil, R.A., Vrionis, H.A., N'guessan, L.A., Ortiz-Bernad, I., Larrahondo, M.J., Adams, L.A., Ward, J.A., Nicoll, J.S. and Nevin, K.P. (2007) Subsurface clade of *Geobacteraceae* that predominates in a diversity of Fe (III)-reducing subsurface environments. The ISME journal 1, 663-677.

Joe-Wong, C., Shoenfelt, E., Hauser, E.J., Crompton, N. and Myneni, S.C. (2012) Estimation of reactive thiol concentrations in dissolved organic matter and bacterial cell membranes in aquatic systems. Environ Sci Technol 46, 9854-9861.

Karlsson, T. and Skyllberg, U. (2003) Bonding of ppb levels of methyl mercury to reduced sulfur groups in soil organic matter. Environmental science & technology 37, 4912-4918.

Khwaja, A.R., Bloom, P.R. and Brezonik, P.L. (2010) Binding strength of methylmercury to aquatic NOM. Environmental science & technology 44, 6151-6156.

Kosower, N.S., Kosower, E.M., Newton, G.L. and Ranney, H.M. (1979) Bimane fluorescent labels: labeling of normal human red cells under physiological conditions. Proceedings of the National Academy of Sciences 76, 3382-3386.

Lin, H., Lu, X., Liang, L. and Gu, B. (2015) Thiol-Facilitated Cell Export and Desorption of Methylmercury by Anaerobic Bacteria. Environmental Science & Technology Letters 2, 292-296.

Lu, X., Gu, W., Zhao, L., Haque, M.F.U., DiSpirito, A.A., Semrau, J.D. and Gu, B. (2017) Methylmercury uptake and degradation by methanotrophs. Science Advances 3, e1700041.

Lu, X., Liu, Y., Johs, A., Zhao, L., Wang, T., Yang, Z., Lin, H., Elias, D.A., Pierce, E.M., Liang, L., Barkay, T. and Gu, B. (2016) Anaerobic Mercury Methylation and Demethylation by *Geobacter bemidjiensis* Bem. Environ Sci Technol 50, 4366-4373.

Marvin-DiPasquale, M., Agee, J., McGowan, C., Oremland, R.S., Thomas, M., Krabbenhoft, D. and Gilmour, C.C. (2000) Methyl-mercury degradation pathways: a comparison among three mercury-impacted ecosystems. Environmental Science & Technology 34, 4908-4916.

Mishra, B., Boyanov, M., Bunker, B.A., Kelly, S.D., Kemner, K.M. and Fein, J.B. (2010) High- and low-affinity binding sites for Cd on the bacterial cell walls of *Bacillus subtilis* and *Shewanella oneidensis*. Geochimica et Cosmochimica Acta 74, 4219-4233.

Mishra, B., O'Loughlin, E.J., Boyanov, M.I. and Kemner, K.M. (2011) Binding of HgII to high-affinity sites on bacteria inhibits reduction to Hg0 by Mixed FeII/III phases. Environmental science & technology 45, 9597-9603.

Mishra, B., Shoenfelt, E., Yu, Q., Yee, N., Fein, J.B. and Myneni, S.C. (2017) Stoichiometry of mercury-thiol complexes on bacterial cell envelopes. Chemical Geology 464, 137-146.

Ndu, U., Barkay, T., Schartup, A.T., Mason, R.P. and Reinfelder, J.R. (2016) The effect of aqueous speciation and cellular ligand binding on the biotransformation and bioavailability of methylmercury in mercury-resistant bacteria. Biodegradation 27, 29-36.

Nell, R.M. and Fein, J.B. (2017) Influence of sulfhydryl sites on metal binding by bacteria. Geochimica et Cosmochimica Acta 199, 210-221.

Nevin, K.P., Holmes, D.E., Woodard, T.L., Hinlein, E.S., Ostendorf, D.W. and Lovley, D.R. (2005) *Geobacter bemidjiensis* sp. nov. and *Geobacter psychrophilus* sp. nov., two novel Fe(III)-reducing subsurface isolates. Int J Syst Evol Microbiol 55, 1667-1674.

Ortiz, V.L., Mason, R.P. and Ward, J.E. (2015) An examination of the factors influencing mercury and methylmercury particulate distributions, methylation and demethylation rates in laboratory-generated marine snow. Marine chemistry 177, 753-762.

Pak, K.-R. and Bartha, R. (1998) Mercury methylation and demethylation in anoxic lake sediments and by strictly anaerobic bacteria. Applied and Environmental Microbiology 64, 1013-1017.

Parks, J.M., Johs, A., Podar, M., Bridou, R., Hurt, R.A., Smith, S.D., Tomanicek, S.J., Qian, Y., Brown, S.D. and Brandt, C.C. (2013) The genetic basis for bacterial mercury methylation. Science 339, 1332-1335.

Powers, L. (1982) X-ray absorption spectroscopy application to biological molecules. Biochimica et Biophysica Acta (BBA)-Reviews on Bioenergetics 683, 1-38.

Qian, J., Skyllberg, U., Frech, W., Bleam, W.F., Bloom, P.R. and Petit, P.E. (2002) Bonding of methyl mercury to reduced sulfur groups in soil and stream organic matter as determined by X-ray absorption spectroscopy and binding affinity studies. Geochimica et cosmochimica acta 66, 3873-3885.

Rajan, M., Darrow, J., Hua, M., Barnett, B., Mendoza, M., Greenfield, B.K. and Andrews, J.C. (2008) Hg L_3 XANES study of mercury methylation in shredded Eichhornia crassipes. Environmental science & technology 42, 5568-5573.

Ravel, B. and Newville, M. (2005) ATHENA and ARTEMIS: interactive graphical data analysis using IFEFFIT. Physica Scripta 2005, 1007.

Ravichandran, M. (2004) Interactions between mercury and dissolved organic matter--a review. Chemosphere 55, 319-331.

Reid, R.S. and Rabenstein, D.L. (1981) Nuclear magnetic resonance studies of the solution chemistry of metal complexes. XVII. Formation constants for the complexation of methylmercury by sulfhydryl-containing amino acids and related molecules. Canadian Journal of Chemistry 59, 1505-1514.

Schaefer, J.K. and Morel, F.M. (2009) High methylation rates of mercury bound to cysteine by *Geobacter sulfurreducens*. Nature geoscience 2, 123.

Silva, P.J. and Rodrigues, V. (2015) Mechanistic pathways of mercury removal from the organomercurial lyase active site. PeerJ 3, e1127.

Skyllberg, U. (2008) Competition among thiols and inorganic sulfides and polysulfides for Hg and MeHg in wetland soils and sediments under suboxic conditions: Illumination of controversies and implications for MeHg net production. Journal of Geophysical Research: Biogeosciences 113.

Skyllberg, U., Qian, J. and Frech, W. (2005) Combined XANES and EXAFS study on the bonding of methyl mercury to thiol groups in soil and aquatic organic matter. Physica Scripta 2005, 894.

Tajc, S.G., Tolbert, B.S., Basavappa, R. and Miller, B.L. (2004) Direct determination of thiol p K a by isothermal titration microcalorimetry. Journal of the American Chemical Society 126, 10508-10509.

Tang, D. and Morel, F.M. (2006) Distinguishing between cellular and Fe-oxide-associated trace elements in phytoplankton. Marine Chemistry 98, 18-30.

Tjerngren, I., Karlsson, T., Björn, E. and Skyllberg, U. (2012) Potential Hg methylation and MeHg demethylation rates related to the nutrient status of different boreal wetlands. Biogeochemistry 108, 335-350.

Wang, Y., Schaefer, J.K., Mishra, B. and Yee, N. (2016) Intracellular Hg (0) oxidation in *Desulfovibrio desulfuricans* ND132. Environmental science & technology 50, 11049-11056.

Weiss, P., Schweitzer, B., Amann, R. and Simon, M. (1996) Identification in situ and dynamics of bacteria on limnetic organic aggregates (lake snow). Applied and environmental microbiology 62, 1998-2005.

Westall, J.C. (1982) FITEQL: A computer program for determination of chemical equilibrium constants from experimental data. Department of Chemistry Oregon State University.

Yi, L., Li, H., Sun, L., Liu, L., Zhang, C. and Xi, Z. (2009) A Highly Sensitive Fluorescence Probe for Fast Thiol-Quantification Assay of Glutathione Reductase. Angewandte Chemie International Edition 48, 4034-4037.

Yoon, S.-J., Diener, L.M., Bloom, P.R., Nater, E.A. and Bleam, W.F. (2005) X-ray absorption studies of CH_3Hg^+-binding sites in humic substances. Geochimica et Cosmochimica Acta 69, 1111-1121.

Yu, Q. and Fein, J.B. (2015) The effect of metal loading on Cd adsorption onto *Shewanella oneidensis* bacterial cell envelopes: The role of sulfhydryl sites. Geochimica et Cosmochimica Acta 167, 1-10.

Yu, Q. and Fein, J.B. (2017) Enhanced Removal of Dissolved Hg (II), Cd (II), and Au (III) from Water by *Bacillus subtilis* Bacterial Biomass Containing an Elevated Concentration of Sulfhydryl Sites. Environmental science & technology 51, 14360-14367.

Yu, Q., Szymanowski, J., Myneni, S.C. and Fein, J.B. (2014) Characterization of sulfhydryl sites within bacterial cell envelopes using selective site-blocking and potentiometric titrations. Chemical Geology 373, 50-58.

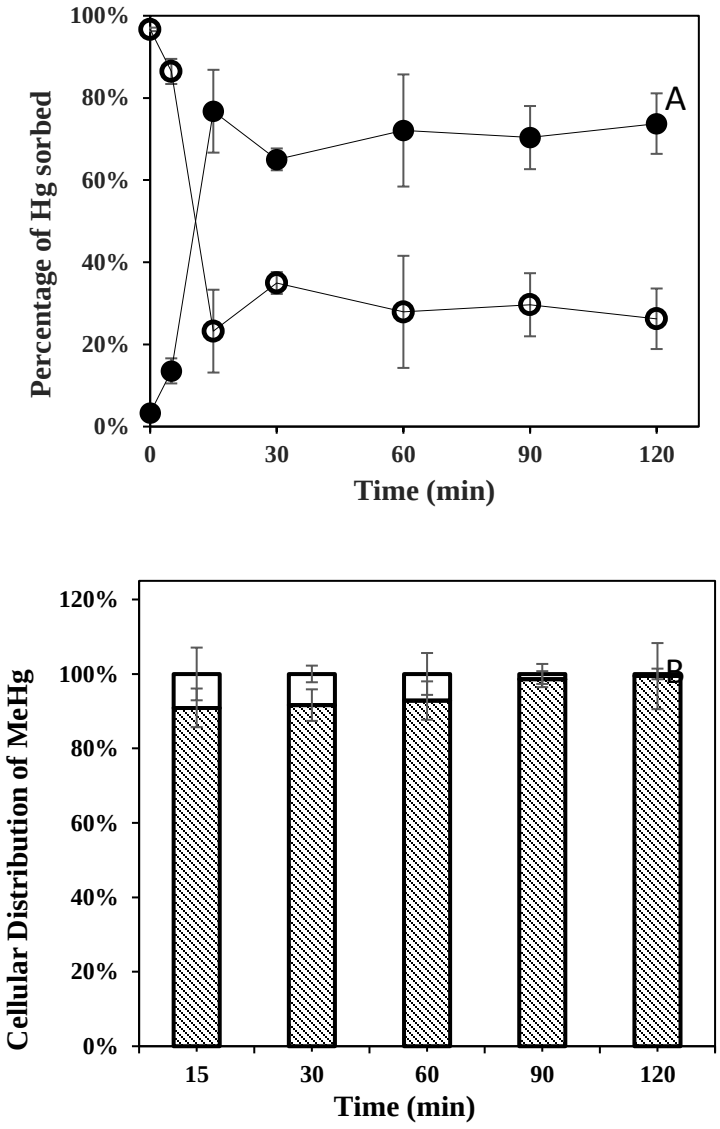

Figure 3.1. MeHg adsorption onto *Geobacter bemidjiensis* Bem. (A) MeHg adsorbed on *G. bemidjiensis* Bem (closed circles) and the aqueous concentration of MeHg remaining in solution (open circles); (B) Intracellular MeHg (solid white) and cell surface adsorbed MeHg (shaded pattern). Intracellular MeHg was assessed by difference in cysteine back extractions from cells. Experiments were conducted in MOPS buffer with cell density of 3 g/L (3×10^8 cells/mL) and a total MeHg concentration of 50 nM. Error bars represent 1σ values of triplicate experiments.

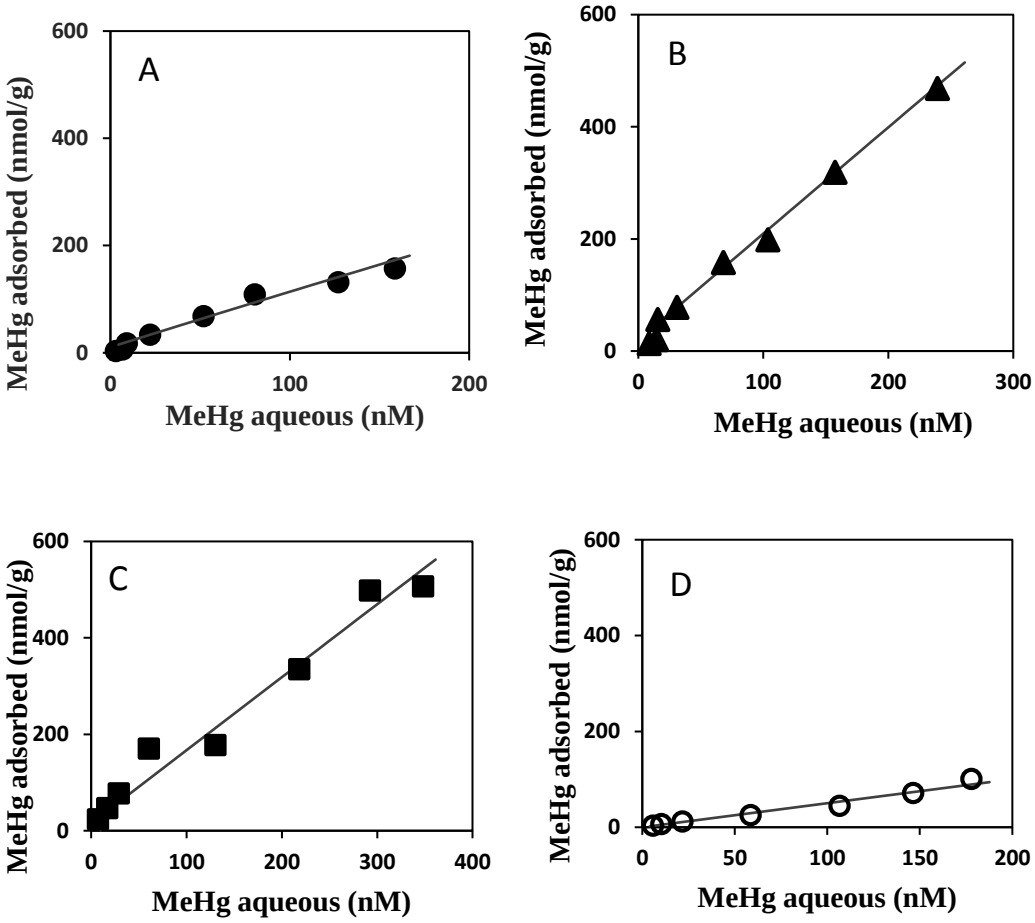

Figure 3.2. MeHg adsorption isotherms conducted at different cell densities: (A) 3 g/L, (B) 0.6 g/L, and (C) 0.3 g/L. (D) MeHg adsorption isotherm conducted with TFP-4 treated cells (3 g/L). The Y-axis represents the amount of MeHg adsorbed per gram of cells, and the X-axis represents the residual concentration of MeHg dissolved in the aqueous phase. The solid black lines represent the best fitting one-site adsorption model.

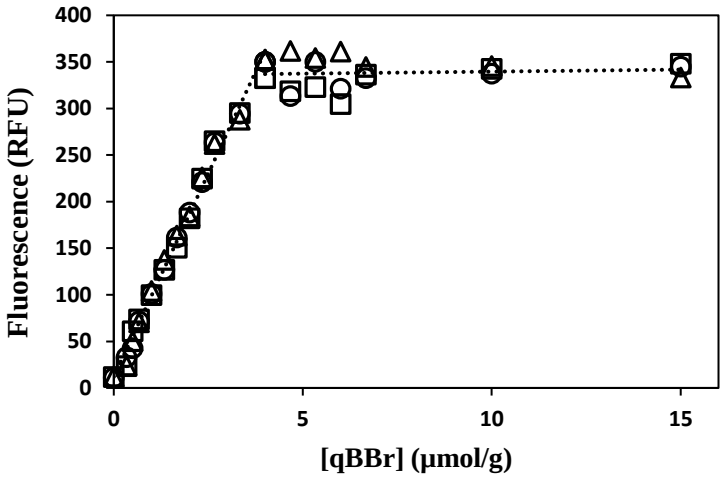

Figure 3.3. Fluorescence intensities of *G. bemidjiensis* reacted with varying qBBr concentrations. Experiments were conducted at a cell density of 3 g/L and each data point represents an individual batch experiment. Three sets of experiments were conducted represented by squares, circles, and triangles. The dashed line represents the best-fit line for the linear regions of the titration data.

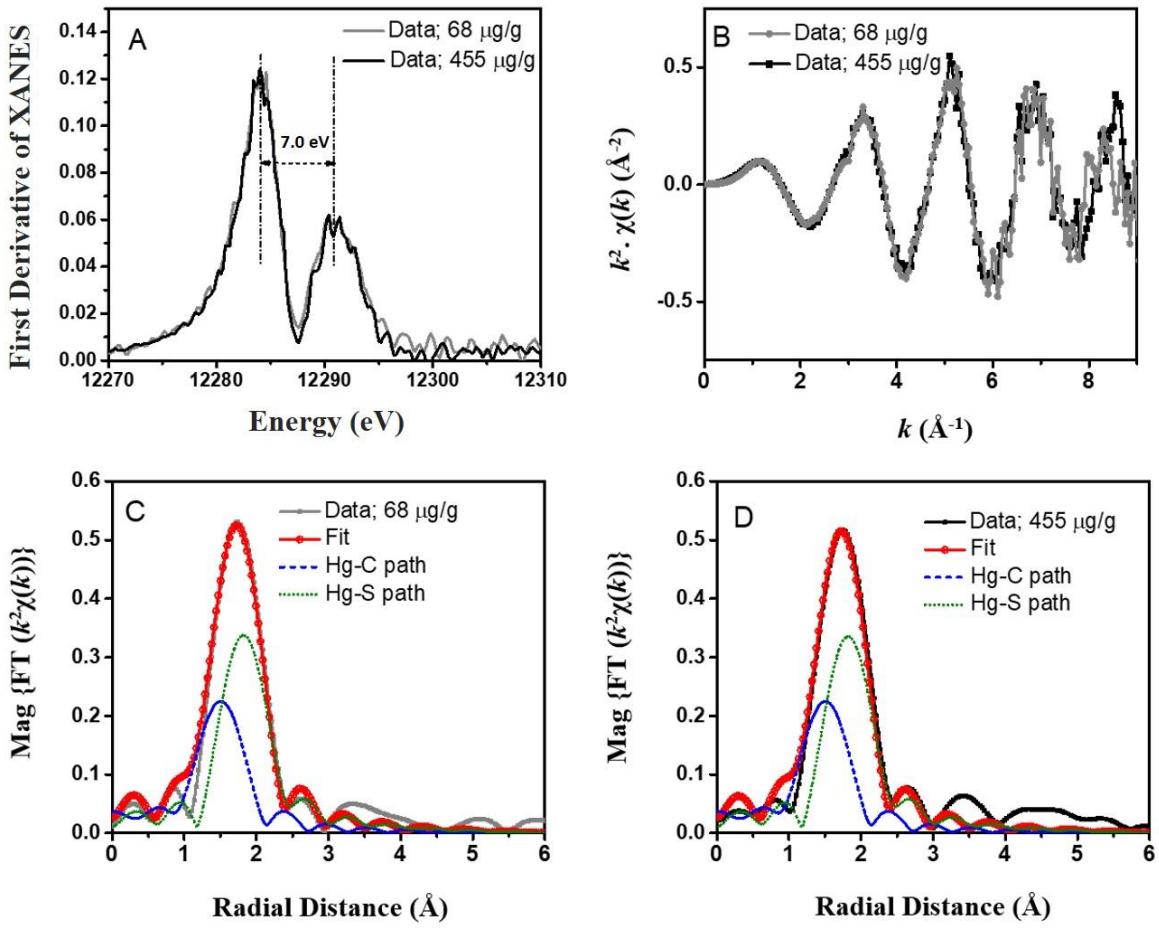

Figure 3.4. Structure characterization and fit of MeHg-reacted *G. bemidjiensis* by X-ray absorption spectroscopy analysis. (A) Derivative of normalized XANES; (B) The k^2-weighted EXAFS data of 68 µg/g and 455 µg/g MeHg adsorbed bacterial samples; (C) Magnitude of EXAFS Fourier-transformed data and along with Hg-C and Hg-S signal contributions for 68 µg/g samples; and (D) Magnitude of EXAFS Fourier-transformed data and along with Hg-C and Hg-S signal contributions for 455 µg/g sample.

Table 3.1. Surface site concentrations and acidity constants of *G. bemidjiensis*

	pKa_1	**Sites 1 (µmol/g)**	**pKa_2**	**Site 2 (µmol/g)**
G. bemidjiensis	3.9 ± 0.4	76.0 ± 7.6	5.4 ± 0.3	70.3 ± 11.1
	pKa_3	**Site 3 (µmol/g)**	**pKa_4**	**Site 4 (µmol/g)**
	7.2 ± 0.2	37.9 ± 4.0	9.6 ± 0.1	68.8 ± 5.1

Table 3.2. XAFS best fit values for simultaneous modeling of MeHg adsorbed onto *G. bemidjiensis*

	Path	N	R (Å)	$\sigma^2 \times 10^{-3}$ ($Å^2$)	ΔE (eV)	S_0^2
68 µg/g MeHg	Hg-C	0.9 ± 0.1	2.03 ± 0.01	3.3 ± 2.1	1.2 ± 1.4	0.9
	Hg-S	0.9 ± 0.1	2.34 ± 0.01	1.8 ± 1.1		
455 µg/g MeHg	Hg-C	0.9 ± 0.1	2.03 ± 0.01	3.3	1.2 ± 1.4	0.9
	Hg-S	0.9 ± 0.1	2.34 ± 0.01	1.8		

Table 3.3. Log K values for MeHg adsorption onto *G. bemidjiensis* Bem and thiol-blocked cells.

	Cell density[a]	**Surface site**	**Log K[b]**	**r^2**
Geobacter bemidjiensis	3 g/L	Site 4	10.3 ± 0.1	0.95
	0.6 g/L	Site 4	10.6 ± 0.3	0.98
	0.3 g/L	Site 4	10.5 ± 0.1	0.96
Thiol-blocked *Geobacter bemidjiensis*	3 g/L	Site 1	3.8 ± 0.1	0.96
	3 g/L	Site 2	3.8 ± 0.1	0.96
	3 g/L	Site 3	4.5 ± 0.1	0.96
	3 g/L	Site 4	6.4 ± 0.1	0.96

[a]wet wt.

[b]Log K adsorption constants with corresponding 1σ uncertainty.

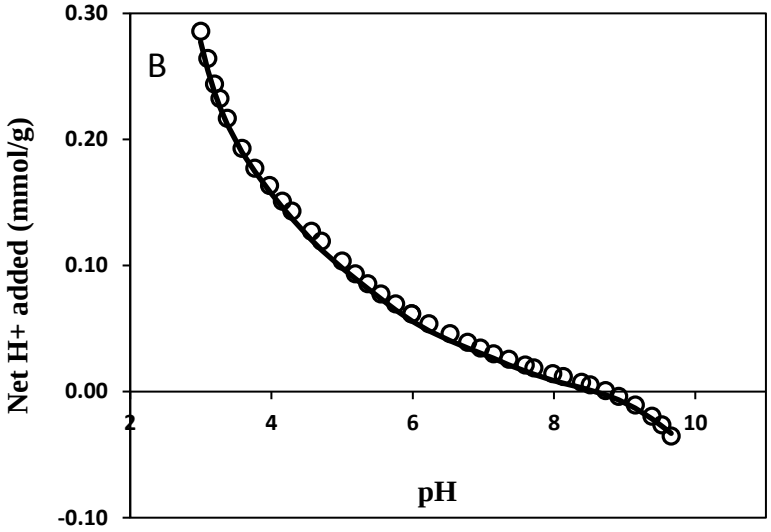

Supplement Figure S3.1. Representative acid-base titration curves of *G. bemidjiensis* cells to quantify the proton-active sites on the cell surface of *G. bemidjiensis*. The curve represents the best-fitting 4-site nonelectrostatic surface complexation model for *G. bemidjiensis.*

Chapter 4 Using mercury stable isotopes to investigate bacterial Hg(II) uptake

Abstract:

Methylmercury (MeHg) is neurotoxic and anaerobic microorganisms play an important role in MeHg production. However, little is known about the uptake of inorganic Hg [Hg(II)] into bacterial cells prior to methylation. Mercury stable isotopes provide a new tool to examine the cellular mechanisms by which anaerobic bacteria take up and convert Hg(II) to MeHg. In this study, we traced changes in Hg isotope ratios of cellular Hg(II) in *Geobacter sulfurreducens* and a mutant *hgcAB* to investigate the transport of Hg(II) into the cells and its associated isotope fractionation prior to methylation. Hg(II) in different cellular compartments was collected and analyzed for Hg concentration and δ^{202}Hg values. In 24 h, little Hg(II) was reduced to Hg(0) by wild-type *G. sulfurreducens*, while about 50% of Hg(II) was reduced by the mutant. Both strains accumulated Hg(II) intracellularly that was depleted in δ^{202}Hg relative to dissolved Hg(II) outside the cells in which δ^{202}Hg was enriched, perhaps reflecting isotope fractionation during Hg(II) uptake. Although previous results showed that δ^{202}Hg values of cumulative MeHg exceeded the initial δ^{202}Hg value of Hg(II) provided, intracellular Hg(II) was isotopic light, indicating that multiple pools of Hg(II) with widely divergent Hg isotopic compositions were generated by these cells, or that extracellular dissolved Hg(II) accumulated by a separate uptake pathway was utilized for methylation.

Introduction:

Methylmercury (MeHg) is neurotoxic and its bioaccumulation in food web poses risk to wildlife and human health (Clarkson, 1997). The production of MeHg is mediated by anaerobic microorganisms (Barkay and Wagner-Döbler, 2005) in various environments such as freshwater systems (Gilmour et al., 2013), wetlands (Schaefer et al., 2014), sediments (Compeau and Bartha, 1985; Fleming et al., 2006), and rice paddies (Gilmour et al., 2013). Molecular studies of environmental samples and pure culture experiments showed that several groups of anaerobic microorganisms were capable of converting Hg(II) to MeHg. The conversion of MeHg from Hg(II) requires a mercury methylase *hgcA* and an associated ferredoxin *hgcB* gene (Parks et al., 2013). To date, mercury methylation has been identified in anaerobic microorganisms encoding *hgcAB*, including sulfate reducing bacteria (SRB), iron reducing bacteria (IRB), methanogens and firmicutes (Fleming et al., 2006; Gilmour et al., 2011; Gilmour et al., 2013; Schaefer and Morel, 2009; Yu et al., 2013). Despite having the *hgcAB* gene, these different groups of microorganisms show different extents and rates of methylation indicating that physiological controls and uptake processes play important roles in the production of MeHg.

Microbial Hg(II) methylation is an intracellular process (Gilmour et al., 2011; Schaefer and Morel, 2009) and the transport of Hg(II) from extracellular environment to cytoplasm is a key step for methylation. Mercury methylation rates increased when Hg(II) was introduced to bacterial cells as a Hg-thiol complex (Schaefer and Morel, 2009), possibly because dissolved thiols prevented the complexation of Hg(II) to bacterial cells and enhanced the bioavailability for uptake. However, Hg(II) uptake by

IRB *Geobacter sulfurreducens* PCA was dependent on the characteristics of the thiols in the external medium (Schaefer et al., 2011), while the SRB *Desulfovibrio desulfuricans* ND132 did not have this limitation and showed an affinity for a variety of thiols during uptake. Recent studies indicated that Hg(II) enters bacterial cells through active uptake (Schaefer et al., 2011; Szczuka et al., 2015). Uptake of Hg(II) by *G. sulfurreducens* PCA and *D. desulfuricans* ND132 required energy (Schaefer et al., 2011) and may be a result of accidental uptake by metal transporter(s) (Schaefer et al., 2014). Interestingly, *Shewanella oneidensis*, an IRB strain incapable of methylation, undergoes a similar Hg uptake processes to *G. sulfurreducens* PCA (Szczuka et al., 2015), indicating a possible common uptake mechanism in phylogenetically distant proteobacteria.

Mercury stable isotopes have been used to track mercury sources, bioaccumulation and examine a variety of mercury transformations (Blum et al., 2014) over the past decade. The seven stable isotopes of Hg can undergo kinetic and equilibrium fractionation that is recorded as both mass dependent fractionation (MDF), represented by δ^{202}Hg, and mass independent fractionation (MIF), denoted as Δ^{xxx}Hg. These isotopic tracers have been used to examine "dark" cellular transformations by anaerobic bacteria including Hg reduction, demethylation, and methylation (Janssen et al., 2016; Kritee et al., 2009; Kritee et al., 2008; Kritee et al., 2007; Perrot et al., 2015). Reduction of Hg(II) by *mer*-mediated and non-specific co-metabolic pathways caused significant kinetic MDF producing an isotopically light product pool of Hg(0) (Kritee et al., 2007; Kritee et al., 2008). Similar trends in MDF were also observed in demethylation of MeHg via Hg resistance pathway (Kritee et al., 2009) as well as in Hg(II) methylation (Perrot et al., 2015).

A recent examination of fractionation during Hg(II) methylation by Janssen et al. (2016) observed that the δ^{202}Hg value of cumulative MeHg produced by *G. sulfurreducens* PCA and *D. desulfuricans* ND132 exceeded that of the Hg(II) to which they were exposed. These results suggest that an isotopically heavier pool of Hg(II) was also utilized for methylation in addition to the initial Hg(II) provided to the organisms (Janssen et al., 2016), which could be associated with the transport and compartmentalization of Hg(II). The steps leading to the differentiation of isotope pools is unknown, but the discrimination among Hg stable isotopes provides a unique tool to probe how Hg accumulates in specific cellular pools.

In this study, we performed Hg(II) uptake experiments on *Geobacter* pure strains and traced the changes in Hg(II) isotope ratios during the cellular Hg(II) partitioning processes prior to methylation. The objectives of this study are to: (1) characterize the concentration of subcellular pools of inorganic Hg(II) in pure cultures and (2) use Hg isotope fractionation to examine the subcellular pools of inorganic Hg(II) in mercury methylating bacteria and its non-methylating mutant. This study enables us to understand the transport and accumulation of Hg(II) in cellular pools that are available for methylation.

Materials and Methods:

Microorganisms and Culture Conditions: Strain *G. sulfurreducens* PCA and a mutant *hgcAB* were cultured in modified ATCC Medium 1957 with 40 mM fumarate as

an electron acceptor and 10 mM acetate as an electron donor at pH 6.8. The media was purged under ultrapure N_2 gas and autoclaved. Both strains were incubated at 30 °C.

Generation of *hgcAB* mutant: A mutant of *G. sulfurreducens* lacking the mercury methylation genes *hgcAB* was generated as a non-methylating control for isotope experiments. Electrocompetent cells were generated by harvesting *G. sulfurreducens* PCA at OD_{660} 0.15. Cells were washed 2 times with electroporation buffer containing 1 mM HEPES, 1 mM $MgCl_2$, and 175 mM sucrose at pH 7, washes were performed at a temperature of 4 °C and under anaerobic conditions. Washed cells were gently resuspended in electroporation buffer with DMSO (final concentration 10%), aliquoted in Eppendorf tubes (50 uL each) and stored at -80°C. Primers for *hgcAB* (Mutate GSU1440-1441) deletion were designed as previously described (Parks et al, 2013) and the pTL8 plasmid Kanamycin cassette, upstream region of GSU1440 and downstream region of GSU 1441 were amplified using PCR. The three PCR products were then purified using gel extraction and the concentration of each fragment were measured. Cross-over PCR was conducted by adding each fragment at a 1:1:1 molar ratio, and the products were sequenced to verify the successful generation of the recombinant. Electroporation was performed to introduce the cross-over product to the electrocompetent cells. The cells were transferred to *Geobacter* growth medium with 200 µg/mL kanamycin. Isolation of the *hgcAB* mutant was performed by transferring the cells grown in the growth media to agar plates with 200 µg/mL kanamycin and incubated in an anaerobic chamber. After multiple transformations, a single colony was picked and resuspended into anaerobic growth medium with 200 µg/mL kanamycin. The final mutant strain was examined using gel electrophoresis. Hg(II) methylation experiments

were performed on the mutant and no methylation was observed (Figure S4.1), confirming the deletion of the *hgcAB* genes.

Hg(II) uptake experiments: Hg(II) uptake experiments were conducted with washed cells under fermentative conditions. The assay buffer for *G. sulfurreducens* PCA and the *hgcAB* mutant consisted of 10 mM MOPS amended with 1 mM acetate and fumarate. Bacterial cells were harvested at late exponential phase, centrifuged at 7000 RPM for 7 min, and washed 3 time using assay buffer. Washed cells were then resuspended in assay buffer at a final OD_{660} ~ 0.1. Hg(II) stock solution was prepared by mixing 10 µM cysteine with 50 nM mercuric nitrate (NIST 3133) and equilibrating for 2 h. Hg(II) stock solution was then spiked into cell suspension making the final concentration of cysteine 10 µM and Hg(II) 50 nM. Cells were incubated with Hg(II) at 30 °C for 5 min to 24 h. At each time point, Hg(0) was collected to test if Hg(II) reduction occurred. The headspace of the reactor was purged with ultrapure N_2 gas for 5 times the volume of headspace at a flow rate 40 mL/min into a gold trap. The Hg(0) existed in the headspace was trapped onto the gold trap. Subsamples were then taken out for THg, cell-associated Hg, intracellular Hg, and dissolved Hg measurements. MeHg was also collected for strain *G. sulfurreducens* PCA. Briefly, to collect cell-associated Hg, 5 mL sample was taken out and filtered through a 0.2 µm polycarbonate filter and rinsed twice with assay buffer before collection. Intracellular Hg was collected by filtering 5 mL sample through a 0.2 µm polycarbonate filter, rinsed twice with rinse buffer, and then fully saturated (filter completely covered) with Oxaloacetate-EDTA-Cl buffer for 5 min. The same process was then repeated on the filter twice more using a fresh glutathione (3 mM)-ascorbic acid (1 mM) solution before a final wash with rinse

buffer prior to collection. Dissolved Hg was collected by filtering a 5 mL sample through a 0.2 µm PVDF syringe filter. All the samples were preserved in 0.02 M bromine monochloride (BrCl) and digested in a 60 °C oven for 48 h before Hg concentration and isotope analyses. The remaining *G. sulfurreducens* PCA assay in the reactor was saved for MeHg analysis and was stored at -20 °C until analysis.

Abiotic control experiment: The potential influence of Hg(II) adsorption/desorption on Hg isotope fractionation in cells was examined in an abiotic experiment with a thiol resin (QuadraSil- Mercaptopropyl 1.0-1.5 mmol g^{-1} loading). To examine the fractionation of Hg(II)-cysteine when binding to sulfhydryl sites, the QuadraSil resin was used to represent thiols on the cell surface. Experiments were conducted with a series of resin amount varying from 0.5 mg to 200 mg in a pre-equilibrated solution of 100 mM cysteine and 1 ppm $Hg(NO_3)_2$ (NIST 3133) under anoxic conditions. After reacting for 24 h, Hg(II) remaining in the solution was collected by filtering the mixture through a 0.2 µm syringe filter and digested in 10% (v/v) BrCl for 48 h.

Mercury analysis: The gold trap loaded with Hg(0) was desorbed using a rapid pre-concentration method which entailed a 40 min desorption time divided into 6 temperature intervals. The Hg(0) was purged off the gold trap using ultra high purity argon and collected into a 2 mL 40% $3HNO_3$:1BrCl oxidant (Janssen et al., 2019). For total mercury analysis, the samples digested by BrCl aliquots were neutralized with hydroxylamine hydrochloride prior to tin (II) reduction coupled to gold amalgamation and cold vapor atomic fluorescence spectrometry (CVAFS) using a Brooks Rand MERX -T (EPA Method 1631). For MeHg analysis, samples were distilled using a mixed reagent

of 400 uL 50% H_2SO_4, 400 uL 1 M $CuSO_4$ and 200 uL 20% KCl (EPA method 1630). The distillates were then derivatized using sodium tetraethylborate and analyzed by gas chromatography coupled to CVAFS on an automated Tekran 2700.

Mercury isotope analysis: Preparation of MeHg isotope samples were performed by distillation and resin pre-concentration (AG1-X4). The resin was pretreated to allow the neutral MeHgCl species to pass through the column while the charge inorganic species was bound to the resin matrix. Percent recoveries of the resin elution were >90% when compared to MeHg concentrations loaded onto the column. Additionally, the same process was performed on MeHgCl standard solution (Brooks Rand) to ensure no fractionation occurred during the separation process.

Mercury isotope measurements of all the samples were analyzed on a Neptune Plus MC-ICP-MS using a cold vapor introduction system. Briefly, samples in the BrCl matrix were diluted with MilliQ water to a concentration of 1 ng/mL and the BrCl content 5%. Hydroxylamine was added to reduce excess oxidants when necessary. Bracketing standard NIST 3133 and a secondary standard UM Almaden (NIST RM 8610) were also prepared with matrix and concertation matched to the samples. Samples and standards were then reduced in line with 3% tin (II) chloride in 10% HCl introduced into a custom gas liquid separator. Gaseous Hg was released from solution using a counter flow of Ar gas which was introduced to the plasma. A 40 ng mL^{-1} solution of thallium was also simultaneously introduced to the gas liquid separator for mass bias correction. The MC-ICP-MS was optimized for sensitivity (1V per 1 ng mL^{-1}) and stability (Janssen et al., 2019; Yin et al., 2016). Mass dependent fractionation (MDF) is expressed in terms of δ^{202}Hg which is calculated as:

$$\delta^{202}\text{Hg}\ (‰) = \left[\frac{\left(\frac{^{202}Hg}{^{198}Hg}\right)sample}{\left(\frac{^{202}Hg}{^{198}Hg}\right)standard} - 1\right] \times 1000 \qquad \text{Eq. 1}$$

Accuracy and precision of isotope measurements were assessed with the UM Almaden standard which are in agreement with the literature values (Janssen et al., 2019).

Results:

Hg uptake in *G. sulfurreducens* PCA and *hgcAB* mutant: *G. sulfurreducens* PCA cultures (wild type and mutant) exposed to Hg(II)-cysteine displayed partition of Hg(II) in cell suspension across 24 hours (Fig 4.1). The accumulation of Hg by wild type and mutant cultures of *G. sulfurreducens* PCA exposed to Hg(II)-cysteine was very rapid, with cellular Hg(II) (intracellular plus adsorbed) reaching quasi-steady state within 1 to 3 h (Fig 4.1). After 24 h, 60% and 90% of total cellular Hg(II) accumulated in the intracellular pools of the wild type and *hgcAB* mutant strains, respectively. While the amount of Hg(II) remaining in the dissolved phase was relatively unchanged in incubations of wild type cells, this pool declined over time in incubations with mutant cells. Adsorbed Hg(II) was higher in the wild type than mutant cells, and declined over time in the mutant.

Hg(II) reduction in *G. sulfurreducens* PCA and *hgcAB* mutant: In addition to cellular uptake of Hg(II), cultures of *Geobacter spp.* have also demonstrated the ability to reduce inorganic Hg(II). While minimal Hg(II) was reduced by the wild type, about 50% Hg(II) was reduced by *hgcAB* mutant in 24 h (Fig 4.1B). Hg(0) produced was trapped for

both strains. In the mutant, a kinetic isotope fractionation of Hg(0) was observed. The δ^{202}Hg values of trapped Hg(0) were initially lower than with the reactant Hg(II) by about -0.7‰ and increased to 1.3‰ after 24 h (Fig 4.2).

Mercury isotope fractionation during Hg(II) uptake in *Geobacter*: In the wild type strain, δ^{202}Hg values of both cell-associated Hg(II) [intracellular plus adsorbed Hg(II)] and intracellular Hg(II) [Hg(II) in the periplasm and cytosol] were depleted in comparison to Hg(II) in the dissolved phase (Fig 4.3A), reflecting isotope fractionation during Hg(II) uptake. Although some variation in δ^{202}Hg values was observed (e.g. the intracellular 3 h point and the dissolved 9 h point), these were relatively small and may not represent a real change of isotopic signatures considering analytical uncertainty (1SD = 0.05‰) (Fig 4.3A). After 24 h, the difference in δ^{202}Hg values between dissolved and intracellular Hg was 0.2‰ (Fig 4.3A), representing the isotopic change during Hg(II) uptake. δ^{202}Hg values of MeHg were -0.68‰ and -0.48‰ at 3 h and 6 h, respectively (Table S4.1).

In the *hgcAB* mutant, intracellular Hg(II) was initially (at 1 h) enriched in ^{202}Hg relative to dissolved Hg(II), but the δ^{202}Hg value of intracellular Hg(II) decreased from +0.1‰ to -0.1‰ over the next 8 hours of the incubation (Fig 4.3B). During the next 15 h, both intracellular and total cell associated Hg(II) became gradually enriched in ^{202}Hg. The δ^{202}Hg value of dissolved Hg(II) steadily increased during the incubation likely the result of the removal of isotopically light Hg associated with cellular accumulation and Hg(II) reduction. The δ^{202}Hg trends for cell-associated Hg(II) and intracellular Hg(II) were similar, with the latter remaining isotopically lighter (Fig 4.3B). Notably, similar to the wild type, the difference in δ^{202}Hg values between dissolved and intracellular Hg(II)

was also about 0.2‰ (Fig 4.3B). No mass independent fractionation was observed in either strain during Hg(II) uptake (Table S4.2, Table S4.3).

Mercury isotope fractionation during sorption of Hg(II) to sulfhydryl-functionalized beads: Abiotic Hg(II)-thiol sorption experiments were performed with a thiol resin incubated with a Hg(II)-cysteine solution to mimic thiol interactions on the cellular surface and examine the influence of Hg(II) adsorption/desorption processes on Hg isotope fractionation. The percentage of adsorbed Hg(II) increased with the concentration of resin and reached 50% at 200 mg/L of thiol resin (Fig 4.4A). After equilibration for 24 h, δ^{202}Hg values of Hg(II) in solution were around 0‰ regardless of resin concentrations (Fig 4.4B), indicating no equilibrium fractionation between aqueous cysteine-complexed Hg(II) and thiol resin sorbed Hg(II) over the range (1 to 50%) of sorption examined. These results demonstrate that if the thiols on the resin are similar to cell surface thiols, fractionation between dissolved and cell surface adsorbed Hg(II) was unlikely in our experiments with *Geobacter*. However, although the calculated δ^{202}Hg values of Hg(II) accumulated in the outer membrane of wild type cells was around 0‰, δ^{202}Hg values of Hg(II) in the outer membrane of the mutant increased to about +1‰ (Fig S4.2), indicating the membrane associated fractionation.

Discussion:

Hg(II) reduction plays an important role controlling bioavailable Hg(II) in the environment. While the wild type reduced very little Hg(II), the *hgcAB* mutant reduced 50% of the Hg(II) to which it was exposed (Fig 4.1) and resulted in mercury isotope fractionation with lighter isotopes preferentially reduced (Fig 4.2). The reduction reaction

contributed to the difference of Hg(II) isotope signatures between the two strains and led to enrichment of ^{202}Hg in dissolved and cell-associated Hg(II) pools in *hgcAB* mutant compared to wild-type *G. sulfurreducens* PCA cells (Fig 4.3). Presumably, *hgcAB* mutant cells reduced more Hg(II) because deletion of the *hgcAB* gene pair lead to physiological changes in the cells, as evidenced by changes in the cell's proteome and carbon metabolic pathways (Qian et al., 2016). The abundances of 281 proteins, including membrane proteins associated with electron transport such as c-type cytochromes, *PilA-C* and *OmpB*, were higher in *hgcAB* mutant than wild type cells. The respiratory electron-transport chain in the bacterial cell wall was proposed as the site of Hg(II) reduction (Kritee et al., 2008; Wiatrowski et al., 2006). Increased levels of electron transport in the *hgcAB* mutant may explain the higher rates of Hg(II) reduction by mutant than wild type cells (Fig 4). Electron transfer to Hg(II) by electron-transport proteins possibly leads to mercury isotope fractionation (Kritee et al., 2008). When reduction occurred in mutant *Geobacter* cells, the Hg(II) pool available for uptake initially became heavier (1 to 3 h) after the depletion of lighter Hg(II) isotopes. However, δ^{202}Hg values of cellular Hg(II) decreased with time. With minimal reduction in the wild type, heavier isotopes were still favored for uptake initially, but decreased with time. The subsequent decrease in δ^{202}Hg values of cellular Hg(II) was caused by either fractionation during Hg(II) uptake or the exudation of cellular Hg(II) into the dissolved phase.

Although the results of previous research show that thiol-bound Hg was enriched in light Hg isotopes relative to aqueous $HgCl_2$ and $Hg(OH)_2$ (Wiederhold et al., 2010), no equilibrium fractionation was observed when aqueous Hg-cysteine complexes were equilibrated with thiol resin (Fig 4.4B). This indicates that the exchange of Hg(II)

between Hg(II)-cysteine and cell surfaces may not have contributed to the isotopic composition of Hg(II) in the outer membrane or intracellular pools of *Geobacter*. However, the calculated δ^{202}Hg values of outer membrane were isotopically heavy in the mutant (Fig S4.2), indicating that this relative small pool of cellular Hg (~10%) accumulated the residual ^{202}Hg-enriched Hg(II) after cell-surface Hg reduction. Other processes such as unknown Hg(II) uptake processes in the outer membrane or formation of Hg(II)-sulfide compounds caused by biodegradation of excess cysteine (Thomas et al., 2019) may have also lead to the observed Hg isotope fractionation of outer membrane Hg(II). Cellular transport of Hg(II) may play an important role determining the bioavailable Hg(II) pools for methylation. Despite the difference of Hg(II) pools generated by Hg(II) reduction, cellular Hg(II) in both wild type and mutant cells showed decreasing δ^{202}Hg values during the first 9 h of our experiments (Fig 4.3) when most of the MeHg in the incubations with wild-type cells was produced (Figure S4.1). In contrast, MeHg showed an enrichment of ^{202}Hg over time with δ^{202}Hg values exceeding that of the initial Hg(II) provided (Fig S4.3) (Janssen et al., 2016). Although the fractionation caused by Hg(II) transport through outer and inner membranes is unknown, the opposite stable Hg isotope trends of intracellular Hg(II) and produced MeHg indicate that either multiple cellular pools of Hg(II) with widely divergent Hg isotopic compositions were generated by the bacteria, or that extracellular dissolved Hg(II) accumulated by a separate uptake pathway was used for methylation.

We propose the possible Hg(II) uptake steps are (Fig 4.5): (1) Hg(II) in the aqueous phase redistributes on the cell outer membrane by ligand exchange. This step does not likely lead to any significant mercury isotope fractionation. In parallel, Hg(II) is

then transported through the outer membrane into periplasm, perhaps as the Hg(II)-cysteine complex, which may cause Hg isotope fractionation. (2) In the periplasm, Hg(II) can either be taken up by unknown membrane transporter(s) or as Hg-cysteine complexes directly without metal exchange (Schaefer et al., 2014) through the inner membrane into the cytosol. The transportation is a rate-limiting step since the rate of Hg(II) taken up by spheroplasts (cells with only inner membrane) of *G. sulfurreducens* PCA is higher than whole cells (Schaefer et al, 2014). Dynamic processes such as exchange of intracellular Hg(II) and Hg(II) in the outer membrane may lead to fractionation. (3) Hg(II) dissociates from the transporter(s) and forms Hg(II)-thiol complexes with different thiols ($Hg\text{-}SR_1$ and $Hg\text{-}SR_2$) in the cytosol. The variation of Hg(II) affinities to different thiols may result in fractionation. Isotopically heavier pools of Hg(II) ($Hg\text{-}SR_1$) are more bioavailable to interact with *hgcAB* for MeHg production, while isotopic lighter pools ($Hg\text{-}SR_2$) are less bioavailable and accumulate intracellularly. Steps (2) and (3) together cause a shift in isotopic composition of Hg(II), leading to different pools of Hg(II) for methylation and resulting in the production of isotopically heavier MeHg as observed by Janssen et al (Janssen et al., 2016). Our results indicate that Hg(II) uptake processes are complicated. More research is still needed to understand the dynamics of Hg(II) uptake prior to Hg(II) methylation.

References:

Barkay, T. and Wagner-Döbler, I. (2005) Microbial transformations of mercury: potentials, challenges, and achievements in controlling mercury toxicity in the environment. Advances in applied microbiology 57, 1-52.

Blum, J.D., Sherman, L.S. and Johnson, M.W. (2014) Mercury isotopes in earth and environmental sciences. Annual Review of Earth and Planetary Sciences 42, 249-269.

Clarkson, T.W. (1997) The toxicology of mercury. Critical reviews in clinical laboratory sciences 34, 369-403.

Compeau, G.C. and Bartha, R. (1985) Sulfate-Reducing Bacteria: Principal Methylators of Mercury in Anoxic Estuarine Sediment. Applied and Environmental Microbiology 50, 498.

Fleming, E.J., Mack, E.E., Green, P.G. and Nelson, D.C. (2006) Mercury Methylation from Unexpected Sources: Molybdate-Inhibited Freshwater Sediments and an Iron-Reducing Bacterium. Applied and Environmental Microbiology 72, 457.

Gilmour, C.C., Elias, D.A., Kucken, A.M., Brown, S.D., Palumbo, A.V., Schadt, C.W. and Wall, J.D. (2011) Sulfate-reducing bacterium *Desulfovibrio desulfuricans* ND132 as a model for understanding bacterial mercury methylation. Appl. Environ. Microbiol. 77, 3938-3951.

Gilmour, C.C., Podar, M., Bullock, A.L., Graham, A.M., Brown, S.D., Somenahally, A.C., Johs, A., Hurt, R.A., Bailey, K.L. and Elias, D.A. (2013) Mercury Methylation by Novel Microorganisms from New Environments. Environmental Science & Technology 47, 11810-11820.

Janssen, S.E., Lepak, R.F., Tate, M.T., Ogorek, J.M., DeWild, J.F., Babiarz, C.L., Hurley, J.P. and Krabbenhoft, D.P. (2019) Rapid pre-concentration of mercury in solids and water for isotopic analysis. Analytica chimica acta 1054, 95-103.

Janssen, S.E., Schaefer, J.K., Barkay, T. and Reinfelder, J.R. (2016) Fractionation of mercury stable isotopes during microbial methylmercury production by iron-and sulfate-reducing bacteria. Environmental science & technology 50, 8077-8083.

Kritee, K., Barkay, T. and Blum, J.D. (2009) Mass dependent stable isotope fractionation of mercury during mer mediated microbial degradation of monomethylmercury. Geochimica et Cosmochimica Acta 73, 1285-1296.

Kritee, K., Blum, J.D. and Barkay, T. (2008) Mercury stable isotope fractionation during reduction of Hg (II) by different microbial pathways. Environmental science & technology 42, 9171-9177.

Kritee, K., Blum, J.D., Johnson, M.W., Bergquist, B.A. and Barkay, T. (2007) Mercury stable isotope fractionation during reduction of Hg (II) to Hg (0) by mercury resistant microorganisms. Environmental science & technology 41, 1889-1895.

Parks, J.M., Johs, A., Podar, M., Bridou, R., Hurt, R.A., Smith, S.D., Tomanicek, S.J., Qian, Y., Brown, S.D., Brandt, C.C., Palumbo, A.V., Smith, J.C., Wall, J.D., Elias, D.A. and Liang, L. (2013) The Genetic Basis for Bacterial Mercury Methylation. Science 339, 1332.

Perrot, V., Bridou, R., Pedrero, Z., Guyoneaud, R., Monperrus, M. and Amouroux, D. (2015) Identical Hg Isotope Mass Dependent Fractionation Signature during Methylation by Sulfate-Reducing Bacteria in Sulfate and Sulfate-Free Environment. Environmental Science & Technology 49, 1365-1373.

Qian, C., Johs, A., Chen, H., Mann, B.F., Lu, X., Abraham, P.E., Hettich, R.L. and Gu, B. (2016) Global proteome response to deletion of genes related to mercury methylation and dissimilatory metal reduction reveals changes in respiratory metabolism in Geobacter sulfurreducens PCA. Journal of proteome research 15, 3540-3549.

Schaefer, J., Kronberg, R.M., Morel, F. and Skyllberg, U. (2014) Detection of a key Hg methylation gene, hgcA, in wetland soils. Environmental microbiology reports 6, 441-447.

Schaefer, J.K. and Morel, F.M. (2009) High methylation rates of mercury bound to cysteine by Geobacter sulfurreducens. Nature geoscience 2, 123.

Schaefer, J.K., Rocks, S.S., Zheng, W., Liang, L., Gu, B. and Morel, F.M. (2011) Active transport, substrate specificity, and methylation of Hg (II) in anaerobic bacteria. Proceedings of the National Academy of Sciences 108, 8714-8719.

Szczuka, A., Morel, F.M. and Schaefer, J.K. (2015) Effect of thiols, zinc, and redox conditions on Hg uptake in *Shewanella oneidensis*. Environmental science & technology 49, 7432-7438.

Thomas, S.A., Catty, P., Hazemann, J.-L., Michaud-Soret, I. and Gaillard, J.-F. (2019) The role of cysteine and sulfide in the interplay between microbial Hg(II) uptake and sulfur metabolism. Metallomics 11, 1219-1229.

Wiatrowski, H.A., Ward, P.M. and Barkay, T. (2006) Novel reduction of mercury (II) by mercury-sensitive dissimilatory metal reducing bacteria. Environmental science & technology 40, 6690-6696.

Wiederhold, J.G., Cramer, C.J., Daniel, K., Infante, I., Bourdon, B. and Kretzschmar, R. (2010) Equilibrium mercury isotope fractionation between dissolved Hg (II) species and thiol-bound Hg. Environmental science & technology 44, 4191-4197.

Yin, R., Krabbenhoft, D.P., Bergquist, B.A., Zheng, W., Lepak, R.F. and Hurley, J.P. (2016) Effects of mercury and thallium concentrations on high precision determination of mercury isotopic composition by Neptune Plus multiple collector inductively coupled plasma mass spectrometry. Journal of Analytical Atomic Spectrometry 31, 2060-2068.

Yu, R.-Q., Reinfelder, J.R., Hines, M.E. and Barkay, T. (2013) Mercury Methylation by the Methanogen *Methanospirillum hungatei*. Applied and Environmental Microbiology 79, 6325.

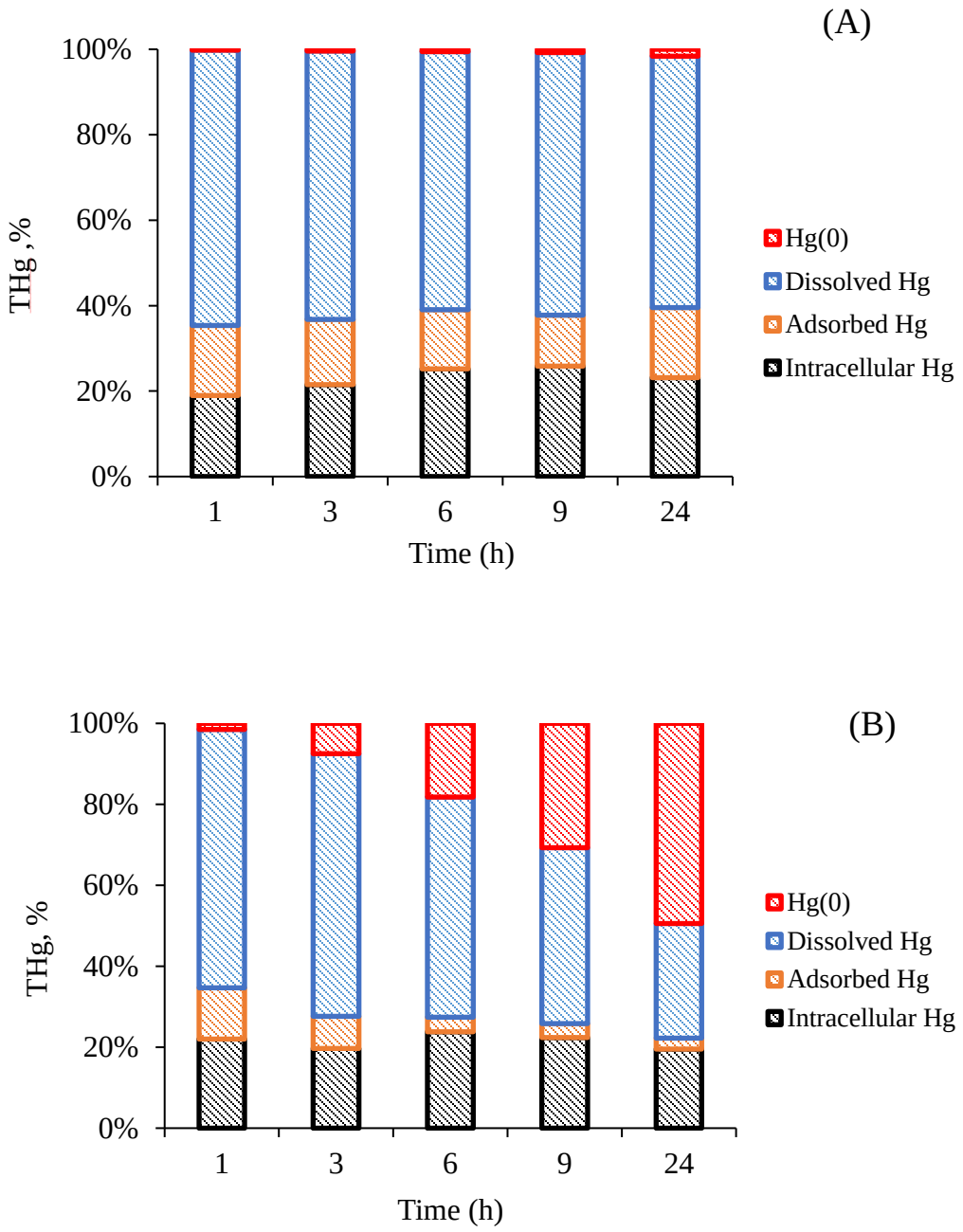

Figure 4.1: Total mercury mass balance of (A) *G. sulfurreducens* PCA wild type and (B) *hgcAB* mutant. Black bars, orange bars, blue bars and red bars represent the percentage of intracellular, adsorbed, dissolved mercury and Hg(0), respectively.

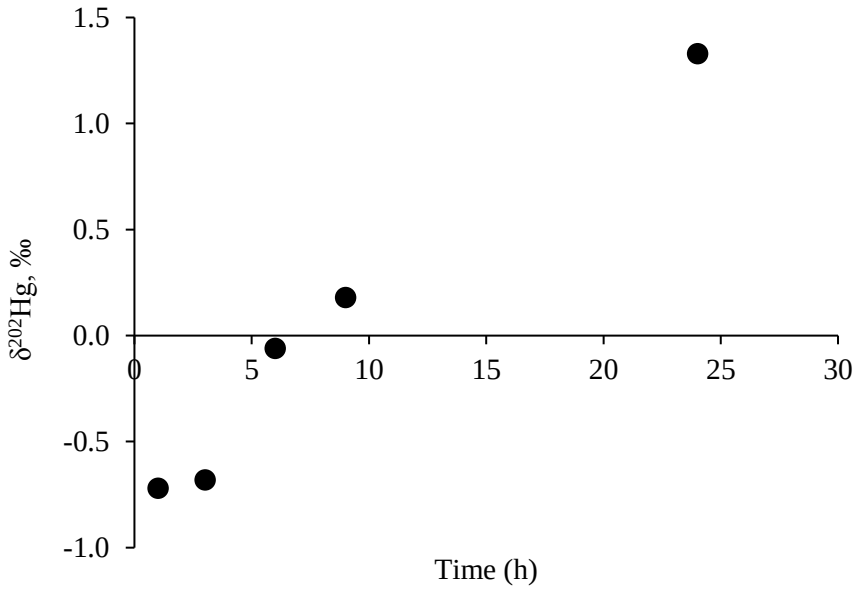

Figure 4.2: Mass-dependent fractionation of ^{202}Hg in Hg(0) produced by *hgcAB* mutant during Hg(II) reduction reactions. Hg(0) was collected using gold traps from the same reactor.

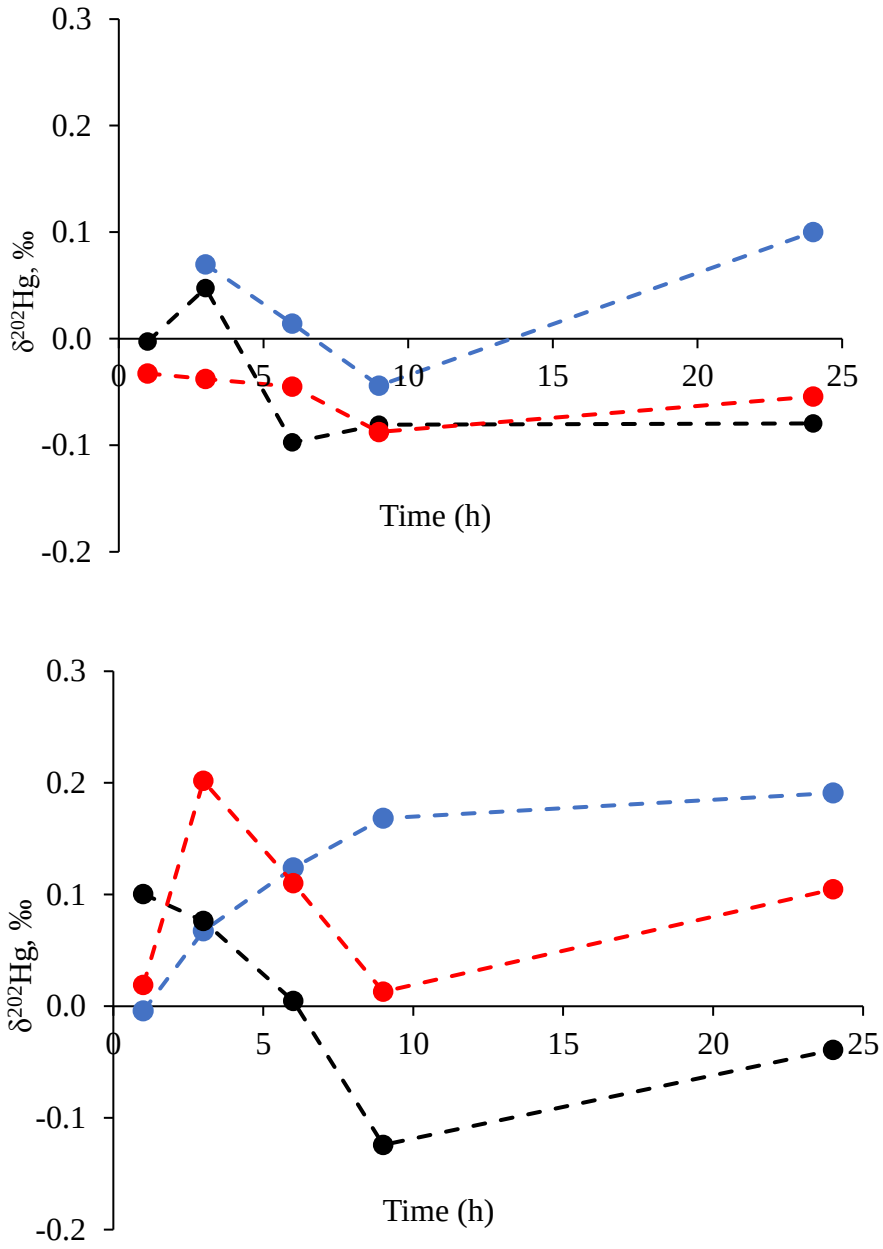

Figure 4.3: δ^{202}Hg values in different cell compartments of (A) *G. sulfurreducens* PCA wild type and (B) *hgcAB* mutant. Black, blue and red dots represent the isotope composition of intracellular, dissolved and cell-associated mercury, respectively.

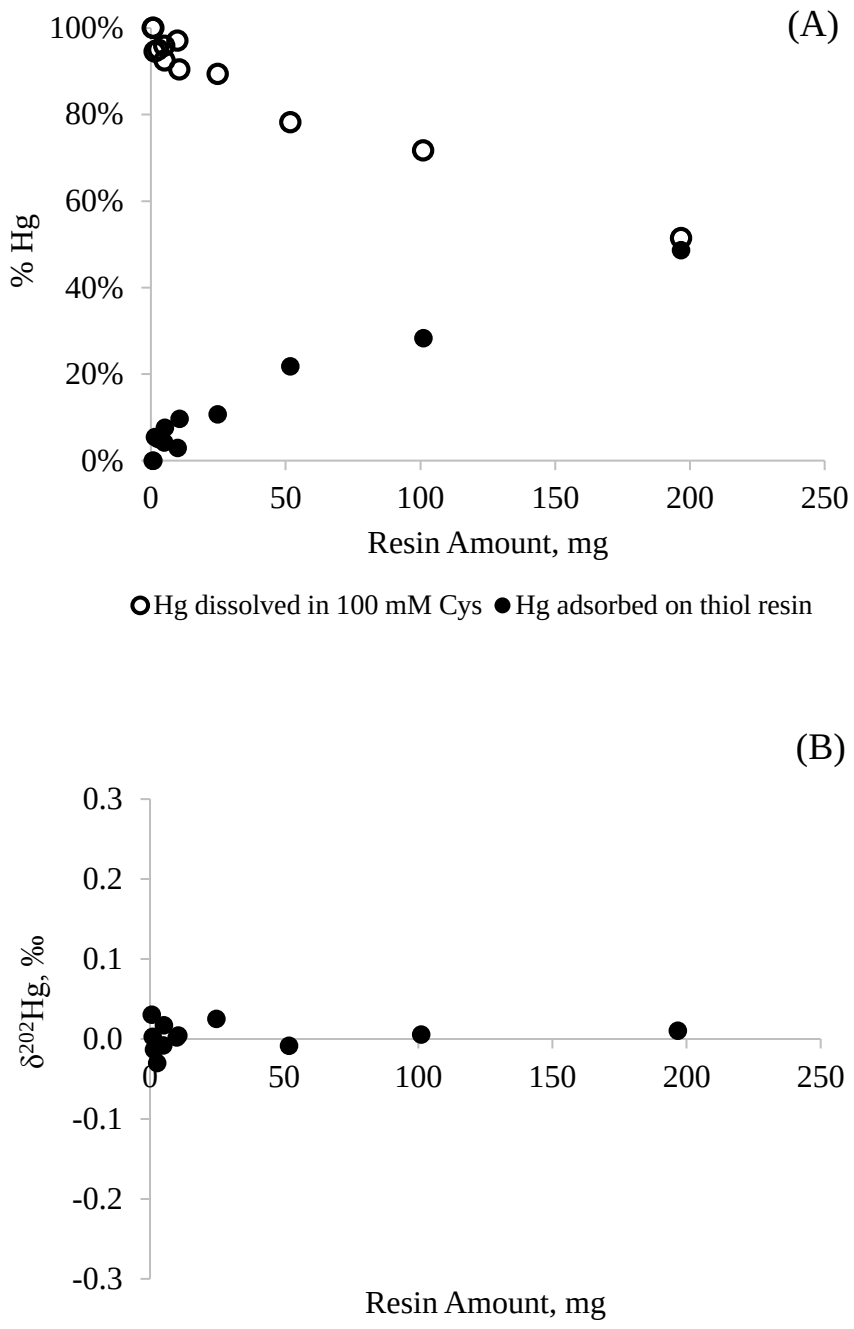

Figure 4.4: Hg(II) equilibrium between 100 mM cysteine solution and different amounts of thiol resin. (A) Percentage of Hg(II) adsorbed on the thiol resin (black dots) and remained in the solution (black circle). (B) Hg(II) isotope fractionation in dissolved phase after equilibration between cysteine solution and the thiol resin.

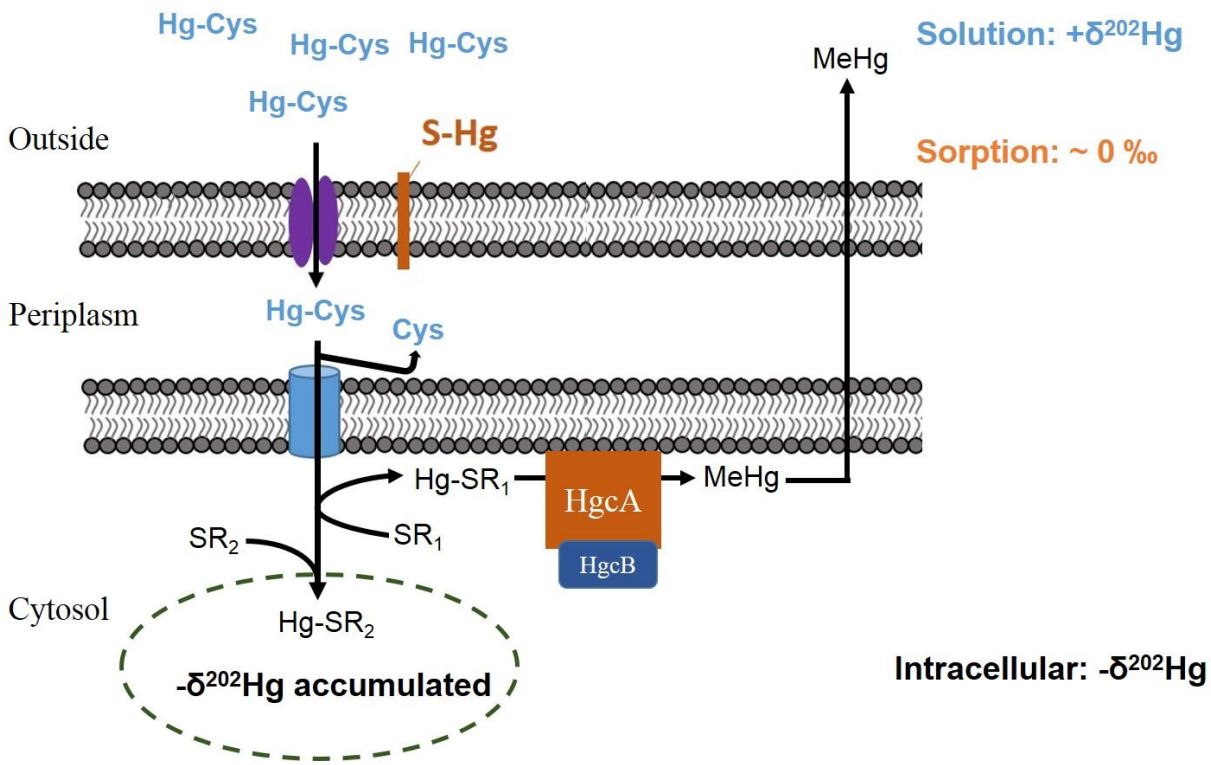

Figure 4.5: Conceptual model of Hg(II) uptake processes in Hg-methylation bacteria.

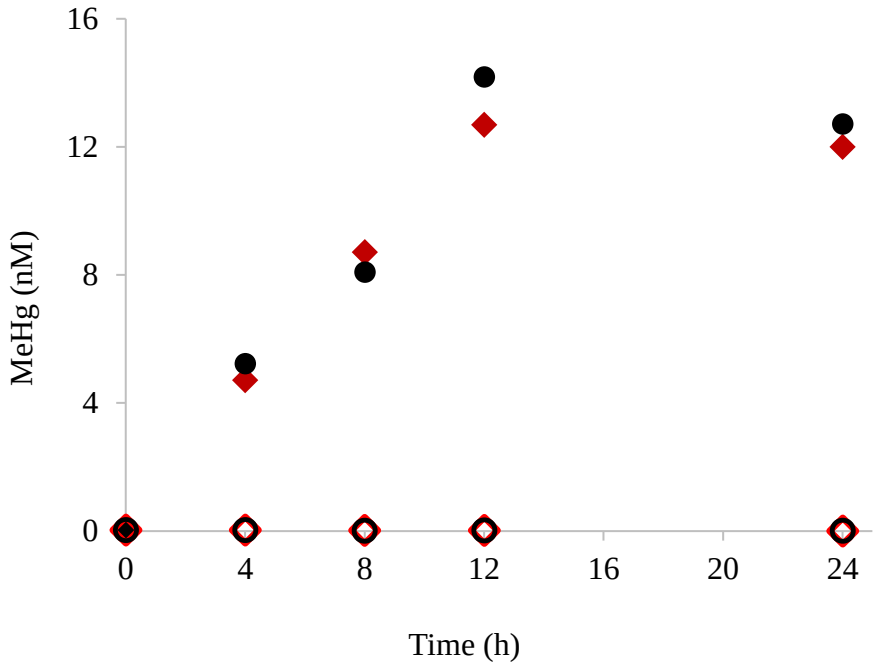

Supplement Figure S4.1: Hg(II) methylation by *G. sulfurreducens* PCA wild type and hgcAB mutant. Filled circles and diamonds represent replicate experiments of Hg(II) methylation by *G. sulfurreducens* PCA wild type. Unfilled circles and diamonds represent replicate experiments of Hg(II) methylation by *hgcAB* mutant. Initial Hg(II) added was 25 nM mercuric nitrate equilibrated with 10 µM cysteine.

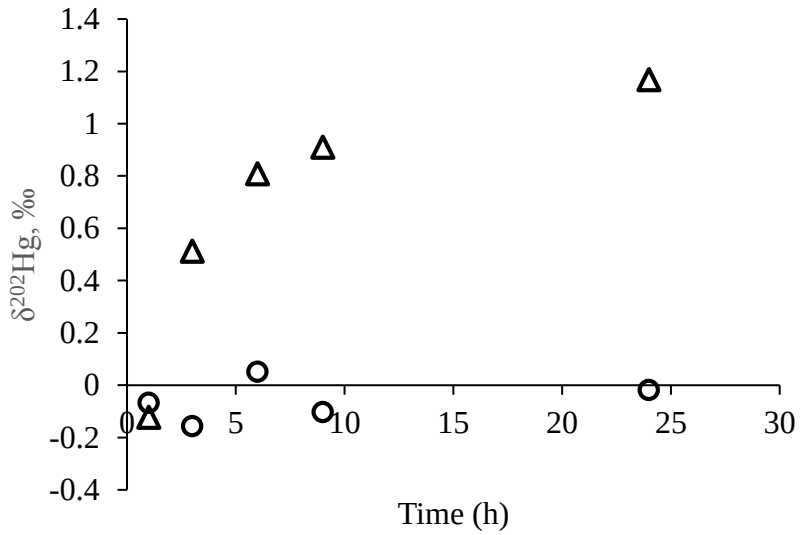

Supplement Figure S4.2: Calculated δ^{202}Hg values in the outer membrane of *G. sulfurreducens* PCA wild type (circles) and the mutant (triangles).

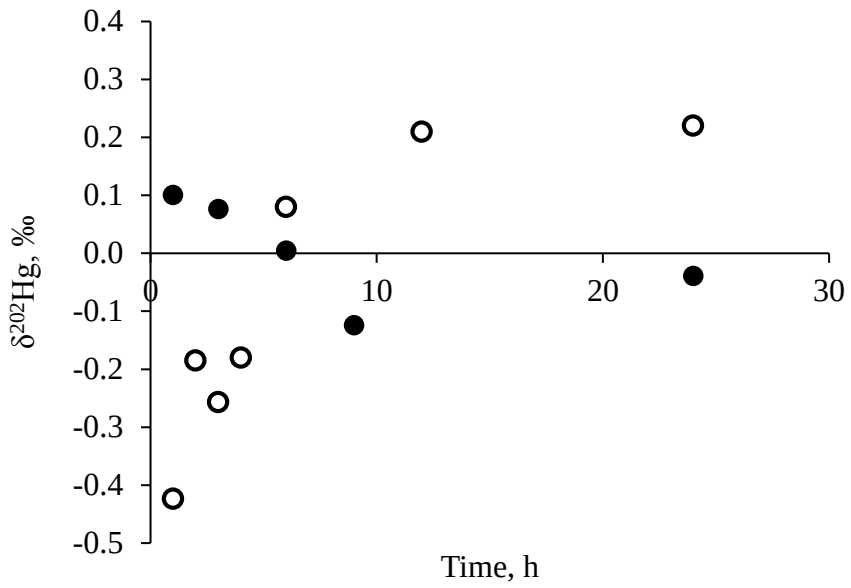

Supplement Figure S4.3: Trends of δ^{202}Hg in intracellular Hg(II) of *hgcAB* mutant (black dots) compared to MeHg produced by *G. sulfurreducens* PCA wild type (black circles). MeHg data was obtained from Table S2 of paper "Fractionation of mercury stable isotopes during microbial methylmercury production by iron- and sulfate-reducing bacteria".

Supplement Table S4.1 MeHg produced by *G. sulfurreducens* PCA

Time (h)	MeHg (nM)	δ^{202}Hg (‰)
1	0.10	Too low to measure
3	2.59	-0.68
6	4.39	-0.48

Supplement Table S4.2: The δ^{202}Hg values of Hg(II) in cell compartments of *G. sulfurreducens* PCA wild type. Samples were collected from the same reactor.

Time	Substance	Reps	Conc (nM)	δ199 Avg	δ200 Avg	δ201 Avg	δ202 Avg	δ204 Avg	Δ199 Avg	Δ200 Avg	Δ201 Avg	Δ204 Avg
1 h	Cell associated	1	18.95	-0.05	-0.07	0.00	-0.02	0.01	-0.04	-0.06	0.01	0.04
1 h	Cell associated	2	16.17	-0.03	-0.02	-0.06	-0.05	-0.02	-0.02	0.01	-0.02	0.06
3 h	Cell associated	1	18.23	-0.01	-0.01	-0.03	-0.04	0.00	0.00	0.01	0.00	0.06
3 h	Cell associated	2	16.57	-0.02	-0.02	-0.01	-0.04	0.01	-0.01	0.00	0.02	0.06
6 h	Cell associated	1	18.01	-0.03	0.00	-0.01	-0.04	-0.05	-0.01	0.02	0.02	0.02
6 h	Cell associated	2	15.73	/	/	/	/	/	/	/	/	/
9 h	Cell associated	1	16.88	-0.04	-0.03	-0.05	-0.07	-0.06	-0.03	0.01	0.00	0.04
9 h	Cell associated	2	16.86	-0.03	-0.05	-0.05	-0.10	-0.12	0.00	0.00	0.03	0.03
24 h	Cell associated	1	15.60	0.00	0.01	-0.05	-0.03	-0.04	0.01	0.03	-0.02	0.01
24 h	Cell associated	2	16.11	-0.04	-0.03	-0.03	-0.08	-0.07	-0.02	0.01	0.03	0.05
Time	Substance	Reps	Conc (nM)	δ199 Avg	δ200 Avg	δ201 Avg	δ202 Avg	δ204 Avg	Δ199 Avg	Δ200 Avg	Δ201 Avg	Δ204 Avg
1 h	Dissolved	1	32.03	/	/	/	/	/	/	/	/	/

3 h	Dissolved	1	29.73	0.04	0.02	0.06	0.07	0.12	0.02	-0.02	0.01	0.01
6 h	Dissolved	1	26.09	0.01	0.02	0.04	0.01	0.15	0.00	0.01	0.03	0.13
9 h	Dissolved	1	27.42	-0.02	-0.02	0.00	-0.04	0.03	-0.01	0.00	0.03	0.09
24 h	Dissolved	1	23.57	0.04	0.05	0.03	0.10	0.19	0.02	0.00	-0.05	0.04

Time	Substance	Reps	Conc (nM)	δ199 Avg	δ200 Avg	δ201 Avg	δ202 Avg	δ204 Avg	Δ199 Avg	Δ200 Avg	Δ201 Avg	Δ204 Avg
1 h	Intracellular	1	9.81	0.00	0.01	0.00	0.00	-0.01	0.00	0.01	0.01	-0.01
1 h	Intracellular	2	9.01	-0.04	0.02	0.03	0.00	0.01	-0.04	0.02	0.03	0.01
3 h	Intracellular	1	13.80	0.01	0.02	-0.03	0.05	0.06	-0.01	0.00	-0.07	-0.01
3 h	Intracellular	2	6.53	/	/	/	/	/	/	/	/	/
6 h	Intracellular	1	10.90	/	/	/	/	/	/	/	/	/
6 h	Intracellular	2	10.87	-0.05	-0.06	-0.10	-0.10	-0.14	-0.02	-0.01	-0.02	0.01
9 h	Intracellular	1	11.62	0.01	-0.01	0.00	-0.02	-0.08	0.01	0.01	0.02	-0.05
9 h	Intracellular	2	11.49	-0.04	-0.09	-0.14	-0.14	-0.23	-0.01	-0.02	-0.04	-0.02
24 h	Intracellular	1	9.62	-0.02	-0.05	-0.08	-0.11	-0.14	0.01	0.00	0.00	0.02
24 h	Intracellular	2	8.92	0.03	-0.02	-0.05	-0.05	-0.08	0.04	0.01	-0.01	-0.01

Time	Substance	Reps	Conc (nM)	δ199 Avg	δ200 Avg	δ201 Avg	δ202 Avg	δ204 Avg	Δ199 Avg	Δ200 Avg	Δ201 Avg	Δ204 Avg
1 h	Hg(0)	1	0.09									
3 h	Hg(0)	1	0.17									
6 h	Hg(0)	1	0.24			Concentration too low to measure isotopes						
9 h	Hg(0)	1	0.35									
24 h	Hg(0)	1	0.63									

Supplement Table S4.3: The δ^{202}Hg values of Hg(II) in cell compartments of *hgcAB* mutant. Samples were collected from the same reactor.

Time	Substance	Reps	Conc (nM)	δ199 Avg	δ200 Avg	δ201 Avg	δ202 Avg	δ204 Avg	Δ199 Avg	Δ200 Avg	Δ201 Avg	Δ204 Avg
1 h	Cell associated	1	18.81	0.00	0.00	0.03	0.02	0.05	-0.01	0.00	0.02	0.03
1 h	Cell associated	2	17.25									
3 h	Cell associated	1	14.20	-0.04	0.06	0.09	0.13	0.31	-0.07	0.00	-0.01	0.11
3 h	Cell associated	2	13.12	0.03	0.12	0.18	0.27	0.42	-0.04	-0.01	-0.02	0.02
6 h	Cell associated	1	12.90	-0.03	0.02	0.03	0.07	0.12	-0.05	-0.02	-0.03	0.01
6 h	Cell associated	2	12.09	0.02	0.10	0.09	0.15	0.24	-0.01	0.02	-0.02	0.02
9 h	Cell associated	1	12.72	-0.02	0.01	-0.03	0.00	-0.03	-0.02	0.01	-0.03	-0.03
9 h	Cell associated	2	12.92	0.01	0.04	0.03	0.03	0.01	0.00	0.03	0.01	-0.02
24 h	Cell associated	1	13.02	0.01	0.04	0.03	0.06	0.10	-0.01	0.01	-0.02	0.00
24 h	Cell associated	2	11.64	0.00	0.05	0.03	0.15	0.19	-0.04	-0.02	-0.08	-0.03
Time	Substance	Reps	Conc (nM)	δ199 Avg	δ200 Avg	δ201 Avg	δ202 Avg	δ204 Avg	Δ199 Avg	Δ200 Avg	Δ201 Avg	Δ204 Avg
1 h	Dissolved	1	33.15	0.03	0.06	-0.02	0.00	0.00	0.03	0.06	-0.02	0.00

3 h	Dissolved	1	32.06	0.04	0.06	0.04	0.07	0.04	0.03	0.03	-0.01	-0.06
6 h	Dissolved	1	24.75	0.05	0.07	0.13	0.12	0.21	0.02	0.01	0.04	0.03
9 h	Dissolved	1	21.57	-0.02	0.07	0.10	0.17	0.28	-0.06	-0.01	-0.02	0.02
24 h	Dissolved	1	15.74	0.00	0.08	0.11	0.19	0.28	-0.05	-0.02	-0.03	0.00

Time	Substance	Reps	Conc (nM)	δ199 Avg	δ200 Avg	δ201 Avg	δ202 Avg	δ204 Avg	Δ199 Avg	Δ200 Avg	Δ201 Avg	Δ204 Avg
1 h	Intracellular	1	11.37	0.00	0.06	0.07	0.09	0.19	-0.02	0.01	0.00	0.06
1 h	Intracellular	2	11.53	0.04	0.10	0.08	0.11	0.22	0.01	0.04	0.00	0.05
3 h	Intracellular	1	9.61	-0.01	0.05	0.03	0.12	0.17	-0.04	-0.01	-0.06	0.00
3 h	Intracellular	2	9.86	-0.03	0.03	-0.01	0.04	0.10	-0.04	0.01	-0.03	0.05
6 h	Intracellular	1	12.42	-0.08	0.01	-0.03	0.01	-0.02	-0.08	0.01	-0.04	-0.04
6 h	Intracellular	2	9.30	0.01	0.02	-0.03	0.00	0.02	0.01	0.02	-0.03	0.03
9 h	Intracellular	1	12.12	-0.06	-0.07	-0.07	-0.12	-0.17	-0.03	-0.01	0.02	0.01
9 h	Intracellular	2	10.12	-0.09	-0.09	-0.13	-0.13	-0.14	-0.05	-0.02	-0.03	0.05
24 h	Intracellular	1	11.25	-0.08	-0.03	-0.07	-0.04	-0.04	-0.07	-0.01	-0.04	0.02
24 h	Intracellular	2	10.47	-0.04	0.01	-0.07	-0.04	-0.11	-0.03	0.02	-0.04	-0.05

Time	Substance	Reps	Conc (nM)	δ199 Avg	δ200 Avg	δ201 Avg	δ202 Avg	δ204 Avg	Δ199 Avg	Δ200 Avg	Δ201 Avg	Δ204 Avg
1h	Hg(0)	1	0.76	-0.08	-0.32	-0.51	-0.72	-1.06	0.10	0.04	0.03	0.02
3 h	Hg(0)	1	3.69	-0.14	-0.35	-0.47	-0.68	-0.98	0.03	-0.01	0.04	0.03
6 h	Hg(0)	1	8.29	0.08	-0.05	-0.04	-0.06	-0.23	0.10	-0.02	0.01	-0.13
9 h	Hg(0)	1	15.27	0.23	0.12	0.17	0.18	0.21	0.18	0.03	0.03	-0.05
24 h	Hg(0)	1	27.45	0.48	0.71	1.07	1.33	2.04	0.14	0.04	0.07	0.04

Chapter 5 Conversion of elemental mercury to methylmercury in sediments by microbial communities

Abstract:

Pure cultures of anaerobic bacteria have been shown to transform elemental mercury [Hg(0)] to neurotoxic methylmercury [MeHg]. However, little is known about the microbial communities in sediments that mediate the biological transformation of Hg(0). In this study, we collected sediments from the San Jacinto River estuary (Texas, USA) and examined the formation of MeHg in incubations of sediment collected from the San Jacinto River estuary (Texas, USA) when liquid Hg(0) was provided as a mercury source. Our results show that MeHg production was greatly reduced by the addition of the methanogen inhibitor 2-bromoethanesulfonate (BES) while the addition of molybdate, an inhibitor of sulfate reducing bacteria, did not significantly diminish mercury methylation. The archaeal form of the mercury methylation gene *hgcA* was detected in these sediments in DNA extracts. RNA extraction and 16S rRNA sequencing showed that a member of the *Methanosarcinaceae* family of methanogens was active. Our results suggest that methanogenic archaea play an important role in the production of MeHg in estuarial sediments contaminated with Hg(0).

Introduction:

Elemental mercury [Hg(0)] is a major environmental contaminant (Lechler et al., 2000; Lechler et al., 1997; Pestana and Formoso, 2003; Pestana et al., 2000) and its discharge from industrial plants (Biester and Scholz, 1997; Boszke et al., 2008; Brooks and Southworth, 2011; Miller et al., 2013) and gold mining areas (Alpers et al., 2005;

Pestana and Formoso, 2003) can be an important source of mercury to aquatic ecosystems. When released into the environment, Hg(0) may undergo biological transformations that lead to the formation of neurotoxic methylmercury (MeHg). Laboratory experiments have demonstrated that anaerobic bacteria can mediate the conversion of Hg(0) to MeHg (Colombo et al., 2013; Hu et al., 2013). In both the sulfate-reducing Hg methylating bacterium *Desulfovibrio desulfuricans* ND132 (Wang et al., 2016), and the iron-reducing bacterium *Geobacter sulfurreducens* PCA (Hu et al., 2013), the uptake of Hg(0) and its oxidation to Hg(II) precedes methylation. Although pure cultures of bacteria have been shown to mediate anaerobic Hg(0) oxidation and methylation, the importance of these processes in the environment and the diversity of microorganisms that are able to carry them out are poorly understood.

The unique physical and chemical properties of Hg(0) affects its environmental interactions with sediments and microorganisms. While Hg(II) adsorbs and strongly partitions onto sediment surfaces (Hintelmann and Harris, 2004; Turner et al., 2001), dissolved gaseous Hg(0) can be transported in groundwater and migrate away from buried wastes (Walvoord et al., 2008). Hg(II) also strongly binds to organic matter (Ravichandran, 2004; Skyllberg, 2012) and sulfides (Skyllberg, 2012), which can hinder the cellular uptake of mercury for methylation (Chiasson-Gould et al., 2014; Jonsson et al., 2012). In contrast, dissolved Hg(0) is highly mobile and can diffuse into pore spaces and microenvironments that are not accessible to Hg(II). Furthermore, because of its neutral charge, Hg(0) readily crosses cell membranes (Colombo et al., 2013; Wang et al., 2016).

In this study, we investigated the production of MeHg in estuarine sediments incubated with Hg(0). The objective was to determine the native microorganisms involved in conversion of Hg(0) to MeHg. Sediment samples from the San Jacinto River estuary were collected and incubated with a liquid Hg(0) permeation source to supply reactors with aqueous Hg(0). Experiments with chemical inhibitors and molecular analyses were performed to characterize the microbial communities involved in methylmercury formation. The results indicate that in these estuarial sediments, methanogenic archaea play an important role in the conversion of Hg(0) to MeHg.

Methods:

Field Sampling: Sediment samples were collected on November 10, 2017 from the San Jacinto River at a site (location: 29°46'53.5"N, 95°06'04.8"W) in Channelview, Texas (USA), approximately 3 km east of the City of Houston. They were therefore collected a little over 10 weeks after the record rainfall and major flooding in the Houston metro area associated with Hurricane Harvey in August, 2017. The salinity and pH of water at the sampling site were 8 PSU and 7.04, respectively. Triplicate sediment samples spaced 50 to 100 cm apart were collected using an acid-cleaned plastic scoop and transferred to 500 mL acid-cleaned glass jars. Sediment-filled jars were placed in plastic bags and immediately stored on ice. Subsamples of sediment were freeze dried and analyzed for the concentration of total Hg (53.3 ± 10.1 ng/g) and MeHg (0.2 ± 0.1 ng/g) prior to the Hg(0) transformation experiments.

Hg(0) transformation experiments: Laboratory experiments were conducted using suspensions of the sediments to examine the production of MeHg when Hg(0) was

provided as a mercury source. Sediment samples were divided into 10 g subsamples and placed into aluminum foil-wrapped serum bottles. Artificial brackish water consisting of 7.5 g/L NaCl, 2.75 g/L $MgCl_2$-$6H_2O$, 0.375 g/L $CaCl_2$-$2H_2O$, 0.38 g/L KCl, 0.14 g/L Na_2SO_4 and 2.1g/L MOPS with pH adjusted to 7 was added to the sediments at a sediment:water ratio of 2:1 (w/w). Sediments were either untreated (control) or treated with sodium molybdate (2 mM), 2-bromoethanesulfonate (BES) (15 mM), or autoclaved (twice, 45 min/time). Sodium molybdate and BES were used to inhibit the activity of sulfate-reducing bacteria and methanogens, respectively, and autoclaving was performed to kill all microorganisms. Each treatment was performed in triplicate. The sediment slurries were then purged with ultrapure nitrogen gas (N_2) to remove oxygen. A silicone permeation tube containing a small (~30 μL) droplet of Hg(0) was added to each serum bottle which was then capped with a Teflon stopper and an aluminum seal. The headspace of each bottle was then purged again with ultrapure N_2 for 30 min. The sediment slurries were then incubated for seven days at room temperature. After the incubation, each bottle was purged with ultrapure N_2 and an aliquot of sediment slurries from two randomly selected bottles of the three replicates for each treatment was immediately sampled for DNA and RNA extraction. The remaining sediment was preserved by freeze-drying for non-purgeable mercury (NP-Hg) and MeHg analyses. Additional control incubations were conducted with no addition of Hg(0) to determine the background levels of MeHg production.

Mercury Analyses: Aliquots of sediments were freeze dried and digested in HCl and HNO_3 (4:1) for 24 hours and then diluted with 30 mL water prior to analysis. The concentrations of total Hg (THg) in sediment subsamples and non-purgeable Hg (NP-Hg)

in sediment slurry samples were measured by cold vapor atomic fluorescence spectroscopy (CVAFS). Using the NIST Standard Reference Material 1944 (New York/New Jersey Waterway Sediment), a recovery of 104% of the certified value (3.4 ± 0.5 µg/g) was obtained. To analyze MeHg, an aliquot of sediment was distilled using a Tekran 2750 gas manifold and heating unit with the addition of cupric sulfate (1 M) to mitigate interferences from remnant sulfide in the samples (EPA method 1630). The distillates were then measured using a Tekran 2700 Automated Methylmercury Analysis System. MeHg recovery was tested by spiking 10 µL of 10 ng/g MeHgCl solution (Brooks Rand) into the sediments, and the recovery was 109% ± 10%. Student's t test was used to examine the significance of differences among treatments.

Microbial Analyses: Both RNA and DNA were extracted from sediment using Qiagen RNeasy Powersoil Total RNA kit and RNeasy Powersoil DNA Elution kit following manufacturers' protocol. RNA products were DNase treated using Turbo DNase Kit (Thermo Fisher) and cDNA was synthesized using Superscript III First-strand cDNA Kit (Thermo Fisher) according to manufacturers' protocols. Detection of the archaeal *hgcA* gene, was performed using primers described by Schaefer et al (Schaefer et al., 2014). To validate the presence of methanogenic archaea in slurry incubations, *mcrA*, the gene encoding for methyl co-enzyme M in methanogens was detected using a previously described protocol (Steinberg and Regan, 2008).

Results and Discussion:

The addition of Hg(0) to sediment slurries resulted in the production of MeHg and NP-Hg. Approximately 50 ng/g MeHg was formed in the sediments after 7 days of

incubation when Hg(0) was provided as a Hg source (Fig. 5.1). The production of MeHg was abolished in autoclaved samples. MeHg formation was detected in sediment treated with sodium molybdate but was significantly diminished by the addition of BES ($P < 0.05$). In sediments with no addition of Hg(0), methylmercury production was not observed and MeHg concentrations remained at background levels (Fig 5.1). NP-Hg was formed under all experimental conditions (Fig. S5.1).

To further investigate the involvement of methanogens in MeHg production, the archaeal *hgcA* and *mcrA* genes, and active microbial communities were examined. The archaeal *hgcA* gene was detected in the control, BES-treated, and molybdate-treated samples (Fig. 5.2A). The analyses showed that *mcrA* genes and transcripts were present in the control experiments and sodium molybdate treated sediments, but were not detected in any of the BES treated samples (Fig. 5.2B). The diminishment of *mcrA* transcripts may indicate the death of methanogens after being treated with BES for 7 days. BES treatment inhibits the terminal step of methane formation by methyl-Coenzyme M reductase (Liu et al., 2011) which weakens the energy production, likely leading to cell death of methanogens.

The inhibition of MeHg production in estuarine sediments by BES suggest that methanogens were involved in the formation of MeHg. The involvement of methanogenic communities in MeHg production is consistent with previous studies that have identified numerous archaeal species as carriers of the *hgcAB* genes for Hg methylation (Gilmour et al., 2018; Gilmour et al., 2013; Podar et al., 2015; Yu et al., 2013). Notably, some methanogen species are capable of producing MeHg at rates and yields that are comparable to the well-known Hg-methylating sulfate-reducing and iron-

reducing bacteria (Gilmour et al., 2018; Yu et al., 2013). Methanogenic communities have also been identified as important Hg methylators in diverse habitats including freshwater environments (Avramescu et al., 2011; Bravo et al., 2018; Christensen et al., 2018; Gilmour et al., 2013), thawing Arctic soils (Podar et al., 2015), wetland soils (Schaefer et al., 2014), lake periphyton (Hamelin et al., 2011) and rice paddies (Gilmour et al., 2013). Methanogens family such as *Methanosarcinaceae* may exist in the sediments and contribute to MeHg production. The occurrence of *Methanosarcinaceae* in the PCB-contaminated sediments of the San Jacinto River we sampled (REF to PCB contamination of the San Jacinto) with a relatively high salinity (8 g/kg) is consistent with the metabolic diversity of these microorganisms. *Methanosarcinaceae* are known to occur in a variety of anaerobic environments, such as sediments from freshwater, high salinity, and wetland ecosystems, and organic waste treatment systems (Kendall and Boone, 2006). Their ability to obtain energy from a diversity of substrates including methylated amines, acetate, dimethyl sulfide, methanol, H_2/CO_2, methanethiol, and carbon monoxide (Balch et al., 1979; Rosenberg et al., 2014), and their tolerance of high salinity and ability to dehalogenate certain halogenated organic compounds (Rosenberg et al., 2014) illustrates how members of this family have adapted to diverse anaerobic environments. Interestingly, *Methanosarcinaceae* have also been found in forest soils where MeHg was biologically produced (Xu et al., 2019). Many of the *hgcAB*-carrying strains in the class *Methanomicrobia* belong to the *Methanosarcinaceae* family (Gilmour et al., 2018). Currently, 36 genomes have been sequenced in the *Methanosarcinaceae* family, 7 of which carry the *hgcA* gene. In addition, pure cultures of the strains *Methanomethylovorans hollandica* and *Methanolobus tindarius*, which belong to the

Methanosarcinaceae family, have been demonstrated experimentally to produce MeHg (Gilmour et al., 2013).

The conversion of Hg to MeHg by methanogens can be catalyzed by direct uptake of dissolved Hg(0), or alternatively, by importing abiotically oxidized Hg(II). In bacteria, Hg(0) can passively diffuse across the cell membrane. Once inside, Hg(0) is oxidized by reaction with cellular thiols and the oxidized mercury subsequently undergoes methylation (Colombo et al., 2014; Wang et al., 2016). Methanogens also contain cellular thiols such as cysteine containing molecules (e.g. coenzyme A) which may likewise participate in cytosolic Hg(0) oxidation. The concentration of free CoA thiol ranges from 0.40-1.54 µmol/g (dry weight) in thermophilic archaea (Hummel et al., 2005), however, the total intracellular thiol content of methanogens has not been examined. Coenzyme M (CoM; 2-mercaptoethanesulfonic acid) and coenzyme B (CoB; 7-mercaptoheptanoylthreonine phosphate), which play important roles in methane production, are also known to occur in methanogens (Fahey, 2001; Noll et al., 1986; Taylor and Wolfe, 1974). Glutathione, on the other hand, a thiol found in many bacteria, is not produced by archaea (Fahey, 2001). Although it is reasonable that the passive diffusion and intracellular oxidation of Hg(0) precedes Hg(II) methylation in methanogens as in Hg-methylating bacteria, it is possible that extracellular Hg(0) is abiotically oxidized to Hg(II) prior to uptake. Under anoxic conditions, organic matter and thiols can chemically oxidize Hg(0) to Hg(II) (Zheng et al., 2011; Zheng et al., 2013). If this oxidized Hg is bioavailable, then methanogens can potentially import it into their cells where it may be methylated. The mechanism(s) by which Hg enters methanogen cells remain poorly understood and require further study.

While the BES treatment suggests the involvement of methanogens in MeHg production, we note that other microbial groups may have also contributed formation of MeHg in the sediment incubations. The addition of sodium molybdate to the sediments did not abolish Hg methylation activity, however, one of the replicates (bottle C) showed MeHg inhibition comparable to the BES treated samples (Fig. 5.1). This suggest possible mercury methylation by sulfate-reducing bacteria. The sediments contained sufficient amounts of sulfate (6.4 mM) (Table S5.1) to support the activity of sulfate-reducing bacteria, and species belong to sulfate-reducing bacteria are known to methylate mercury (Ekstrom et al., 2003). These bacterial families may have contributed to MeHg production and affected mercury methylation by methanogens indirectly via syntrophic interactions.

The results of this study highlight the importance of methanogenic archaea in the production of MeHg when high sulfate estuarial sediments are contaminated with Hg(0). Methanogens are known to grow in high sulfate sediments under sulfate reducing conditions (Ferry and Lessner, 2008; Oremland and Taylor, 1978; Sela-Adler et al., 2017) and our data indicate that they play a key role in conversion of Hg(0) to MeHg. An important question for future investigation is the bioavailability of Hg(0) to different microbial groups. It is currently unknown if methanogens preferentially uptake Hg(0) compared to sulfate-reducing bacteria. For example, sulfidization of proximal organic matter and the cell surface sulfhydryl groups of sulfate reducing bacteria might oxidize and bind Hg(0), thereby limiting its entry into the cell. The distribution and concentration of thiols is a key control in this process, and detailed comparisons between archaeal

methanogens and sulfate-reducing bacteria, and the associated effects on Hg(0) bioavailability merit further study.

References:

Alpers, C.N., Hunerlach, M.P., May, J.T. and Hothem, R.L. (2005) Mercury contamination from historical gold mining in California.

Amir, A., McDonald, D., Navas-Molina, J.A., Kopylova, E., Morton, J.T., Xu, Z.Z., Kightley, E.P., Thompson, L.R., Hyde, E.R. and Gonzalez, A. (2017) Deblur rapidly resolves single-nucleotide community sequence patterns. MSystems 2, e00191-00116.

Avramescu, M.-L., Yumvihoze, E., Hintelmann, H., Ridal, J., Fortin, D. and Lean, D.R. (2011) Biogeochemical factors influencing net mercury methylation in contaminated freshwater sediments from the St. Lawrence River in Cornwall, Ontario, Canada. Science of the Total Environment 409, 968-978.

Balch, W., Fox, G., Magrum, L., Woese, C. and Wolfe, R. (1979) Methanogens: reevaluation of a unique biological group. Microbiological reviews 43, 260.

Biester, H. and Scholz, C. (1997) Determination of Mercury Binding Forms in Contaminated Soils: Mercury Pyrolysis versus Sequential Extractions. Environmental Science & Technology 31, 233-239.

Bokulich, N.A., Kaehler, B.D., Rideout, J.R., Dillon, M., Bolyen, E., Knight, R., Huttley, G.A. and Caporaso, J.G. (2018) Optimizing taxonomic classification of marker-gene amplicon sequences with QIIME 2's q2-feature-classifier plugin. Microbiome 6, 90.

Boszke, L., Kowalski, A., Astel, A., Barański, A., Gworek, B. and Siepak, J. (2008) Mercury mobility and bioavailability in soil from contaminated area. Environmental Geology 55, 1075-1087.

Bravo, A.G., Zopfi, J., Buck, M., Xu, J., Bertilsson, S., Schaefer, J.K., Poté, J. and Cosio, C. (2018) *Geobacteraceae* are important members of mercury-methylating microbial communities of sediments impacted by waste water releases. The ISME journal 12, 802.

Brooks, S.C. and Southworth, G.R. (2011) History of mercury use and environmental contamination at the Oak Ridge Y-12 Plant. Environmental pollution 159, 219-228.

Chiasson-Gould, S.A., Blais, J.M. and Poulain, A.J. (2014) Dissolved organic matter kinetically controls mercury bioavailability to bacteria. Environmental science & technology 48, 3153-3161.

Christensen, G.A., Somenahally, A.C., Moberly, J.G., Miller, C.M., King, A.J., Gilmour, C.C., Brown, S.D., Podar, M., Brandt, C.C. and Brooks, S.C. (2018) Carbon amendments alter microbial community structure and net mercury methylation potential in sediments. Appl. Environ. Microbiol. 84, e01049-01017.

Colombo, M.J., Ha, J., Reinfelder, J.R., Barkay, T. and Yee, N. (2013) Anaerobic oxidation of Hg (0) and methylmercury formation by *Desulfovibrio desulfuricans* ND132. Geochimica et Cosmochimica Acta 112, 166-177.

Colombo, M.J., Ha, J., Reinfelder, J.R., Barkay, T. and Yee, N. (2014) Oxidation of Hg (0) to Hg (II) by diverse anaerobic bacteria. Chemical Geology 363, 334-340.

Ekstrom, E.B., Morel, F.M. and Benoit, J.M. (2003) Mercury methylation independent of the acetyl-coenzyme A pathway in sulfate-reducing bacteria. Appl. Environ. Microbiol. 69, 5414-5422.

Fahey, R.C. (2001) Novel thiols of prokaryotes. Annual Reviews in Microbiology 55, 333-356.

Ferry, J.G. and Lessner, D.J. (2008) Methanogenesis in marine sediments. Annals of the New York Academy of Sciences 1125, 147-157.

Gilmour, C.C., Bullock, A.L., McBurney, A., Podar, M. and Elias, D.A. (2018) Robust mercury methylation across diverse methanogenic archaea. MBio 9(2), e02403-02417.

Gilmour, C.C., Podar, M., Bullock, A.L., Graham, A.M., Brown, S.D., Somenahally, A.C., Johs, A., Hurt, R.A., Bailey, K.L. and Elias, D.A. (2013) Mercury Methylation by Novel

Microorganisms from New Environments. Environmental Science & Technology 47, 11810-11820.

Hamelin, S., Amyot, M., Barkay, T., Wang, Y. and Planas, D. (2011) Methanogens: principal methylators of mercury in lake periphyton. Environmental science & technology 45, 7693-7700.

Hintelmann, H. and Harris, R. (2004) Application of multiple stable mercury isotopes to determine the adsorption and desorption dynamics of Hg(II) and MeHg to sediments. Marine Chemistry 90, 165-173.

Hu, H., Lin, H., Zheng, W., Tomanicek, S.J., Johs, A., Feng, X., Elias, D.A., Liang, L. and Gu, B. (2013) Oxidation and methylation of dissolved elemental mercury by anaerobic bacteria. Nature Geoscience 6, 751.

Hummel, C.S., Lancaster, K.M. and Crane III, E.J. (2005) Determination of coenzyme A levels in Pyrococcus furiosus and other Archaea: implications for a general role for coenzyme A in thermophiles. FEMS microbiology letters 252, 229-234.

Jonsson, S., Skyllberg, U., Nilsson, M.B., Westlund, P.-O., Shchukarev, A., Lundberg, E. and Björn, E. (2012) Mercury methylation rates for geochemically relevant Hg(II) species in sediments. Environmental science & technology 46, 11653-11659.

Kendall, M.M. and Boone, D.R. (2006) The order methanosarcinales. The Prokaryotes: Volume 3: Archaea. Bacteria: *Firmicutes,* Actinomycetes, 244-256.

Kerin, E.J., Gilmour, C.C., Roden, E., Suzuki, M., Coates, J. and Mason, R. (2006) Mercury methylation by dissimilatory iron-reducing bacteria. Appl. Environ. Microbiol. 72, 7919-7921.

King, J.K., Kostka, J.E., Frischer, M.E. and Saunders, F.M. (2000) Sulfate-reducing bacteria methylate mercury at variable rates in pure culture and in marine sediments. Appl. Environ. Microbiol. 66, 2430-2437.

Lechler, P., Miller, J., Lacerda, L., Vinson, D., Bonzongo, J.-C., Lyons, W. and Warwick, J. (2000) Elevated mercury concentrations in soils, sediments, water, and fish of the Madeira River basin, Brazilian Amazon: a function of natural enrichments? Science of the Total Environment 260, 87-96.

Lechler, P.J., Miller, J.R., Hsu, L.-C. and Desilets, M.O. (1997) Mercury mobility at the Carson River Superfund Site, west-central Nevada, USA: Interpretation of mercury speciation data in mill tailings, soils, and sediments. Journal of Geochemical Exploration 58, 259-267.

Miller, C.L., Watson, D.B., Lester, B.P., Lowe, K.A., Pierce, E.M. and Liang, L. (2013) Characterization of soils from an industrial complex contaminated with elemental mercury. Environmental Research 125, 20-29.

Noll, K.M., Rinehart, K.L., Tanner, R.S. and Wolfe, R.S. (1986) Structure of component B (7-mercaptoheptanoylthreonine phosphate) of the methylcoenzyme M methylreductase system of Methanobacterium thermoautotrophicum. Proceedings of the National Academy of Sciences 83, 4238.

Oremland, R.S. and Taylor, B.F. (1978) Sulfate reduction and methanogenesis in marine sediments. Geochimica et cosmochimica acta 42, 209-214.

Pestana, M.H.D. and Formoso, M.L.L. (2003) Mercury contamination in Lavras do Sul, south Brazil: a legacy from past and recent gold mining. Science of The Total Environment 307, 125-140.

Pestana, M.H.D., Lechler, P., Formoso, M.L.L. and Miller, J. (2000) Mercury in sediments from gold and copper exploitation areas in the Camaquã River Basin, Southern Brazil. Journal of South American Earth Sciences 13, 537-547.

Podar, M., Gilmour, C.C., Brandt, C.C., Soren, A., Brown, S.D., Crable, B.R., Palumbo, A.V., Somenahally, A.C. and Elias, D.A. (2015) Global prevalence and distribution of genes and microorganisms involved in mercury methylation. Science Advances 1, e1500675.

Ravichandran, M. (2004) Interactions between mercury and dissolved organic matter—a review. Chemosphere 55, 319-331.

Rognes, T., Flouri, T., Nichols, B., Quince, C. and Mahé, F. (2016) VSEARCH: a versatile open source tool for metagenomics. PeerJ 4, e2584.

Rosenberg, E., DeLong, E.F., Lory, S., Stackebrandt, E. and Thompson, F. (2014) The prokaryotes: other major lineages of Bacteria and the Archaea. Springer.

Schaefer, J., Kronberg, R.M., Morel, F. and Skyllberg, U. (2014) Detection of a key Hg methylation gene, hgcA, in wetland soils. Environmental microbiology reports 6, 441-447.

Sela-Adler, M., Ronen, Z., Herut, B., Antler, G., Vigderovich, H., Eckert, W. and Sivan, O. (2017) Co-existence of methanogenesis and sulfate reduction with common substrates in sulfate-rich estuarine sediments. Frontiers in microbiology 8, 766.

Skyllberg, U. (2012) Chemical speciation of mercury in soil and sediment. Environmental chemistry and toxicology of mercury, 219-258.

Steinberg, L.M. and Regan, J.M. (2008) Phylogenetic comparison of the methanogenic communities from an acidic, oligotrophic fen and an anaerobic digester treating municipal wastewater sludge. Appl. Environ. Microbiol. 74, 6663-6671.

Taylor, C.D. and Wolfe, R.S. (1974) Structure and methylation of coenzyme M (HSCH2CH2SO3). Journal of Biological Chemistry 249, 4879-4885.

Turner, A., Millward, G.E. and Le Roux, S.M. (2001) Sediment− water partitioning of inorganic mercury in estuaries. Environmental science & technology 35, 4648-4654.

Walvoord, M.A., Andraski, B.J., Krabbenhoft, D.P. and Striegl, R.G. (2008) Transport of elemental mercury in the unsaturated zone from a waste disposal site in an arid region. Applied Geochemistry 23, 572-583.

Wang, Y., Schaefer, J.K., Mishra, B. and Yee, N. (2016) Intracellular Hg (0) oxidation in *Desulfovibrio desulfuricans* ND132. Environmental science & technology 50, 11049-11056.

Xu, J., Buck, M., Eklöf, K., Ahmed, O.O., Schaefer, J.K., Bishop, K., Skyllberg, U., Björn, E., Bertilsson, S. and Bravo, A.G. (2019) Mercury methylating microbial communities of boreal forest soils. Scientific reports 9, 518.

Yu, R.-Q., Reinfelder, J.R., Hines, M.E. and Barkay, T. (2013) Mercury methylation by the methanogen *Methanospirillum hungatei*. Appl. Environ. Microbiol. 79, 6325-6330.

Zheng, W., Liang, L. and Gu, B. (2011) Mercury reduction and oxidation by reduced natural organic matter in anoxic environments. Environmental science & technology 46, 292-299.

Zheng, W., Lin, H., Mann, B.F., Liang, L. and Gu, B. (2013) Oxidation of Dissolved Elemental Mercury by Thiol Compounds under Anoxic Conditions. Environmental Science & Technology 47, 12827-12834.

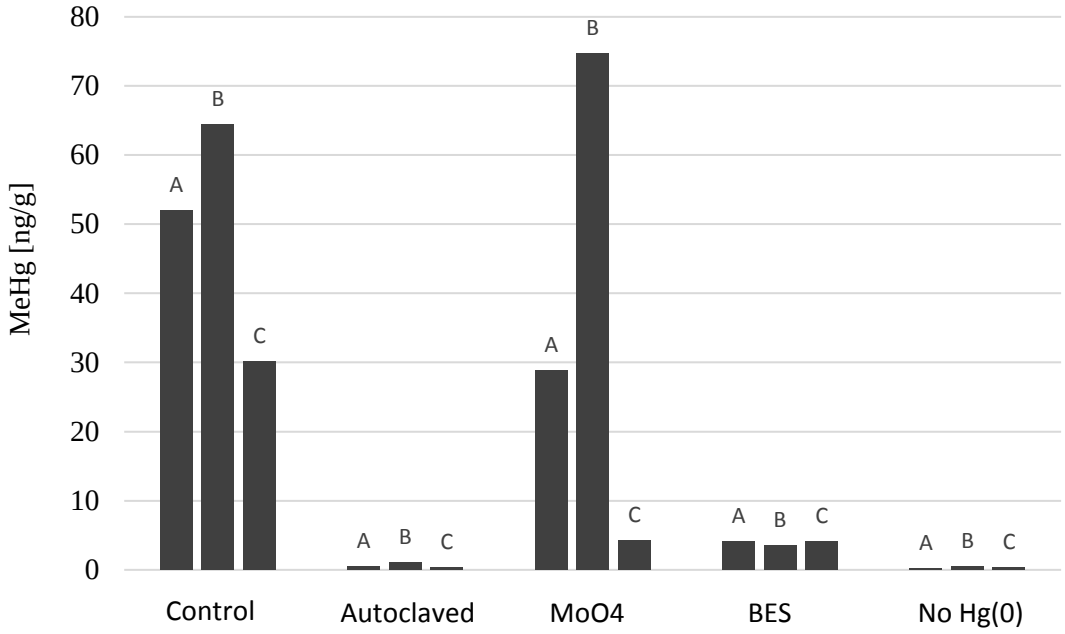

Figure 5.1: Formation of MeHg in the sediments after 7 days when Hg(0) was provided as a Hg source. Concentration of MeHg was normalized by the mass of freeze-dried sediment. A, B and C represent the number of triplicate bottles for each incubation condition. Each bar represents an individual sediment incubation experiment.

(A)

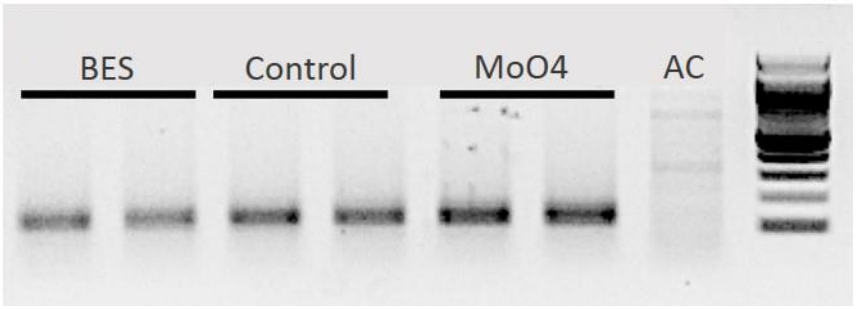

(B)

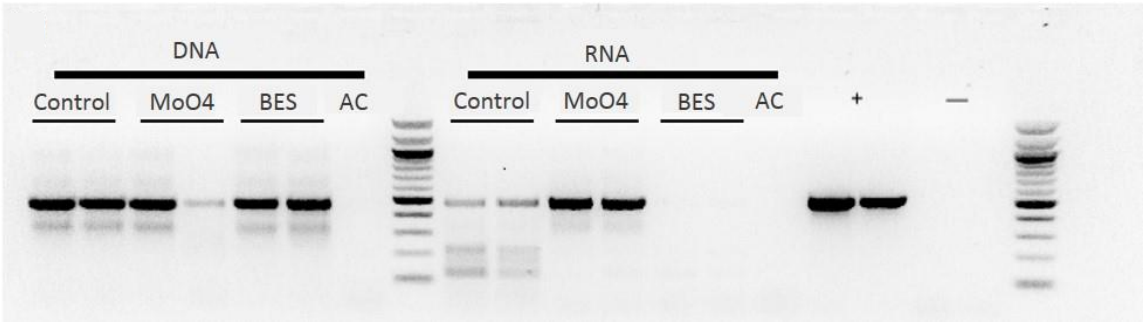

Figure 5.2: (A) Presence of archaeal *hgcA* genes in sediment DNA. Archaeal *hgcA* was detected in the sediment (no treatment control, bottle A and B), BES (bottle A and C) and $NaMoO_4$ (bottle A and B) treatments. Autoclaved treatment (abbreviated AC, bottle A and B) had no detectable archaeal *hgcA*. (B) *mcrA* in DNA and RNA extracts. Control (bottle A and B) and sodium molybdate (bottle A and B) incubations show presence of *mcrA* genes and transcripts. *mcrA* transcripts were not detected in BES treated sediments (Bottle A and C).

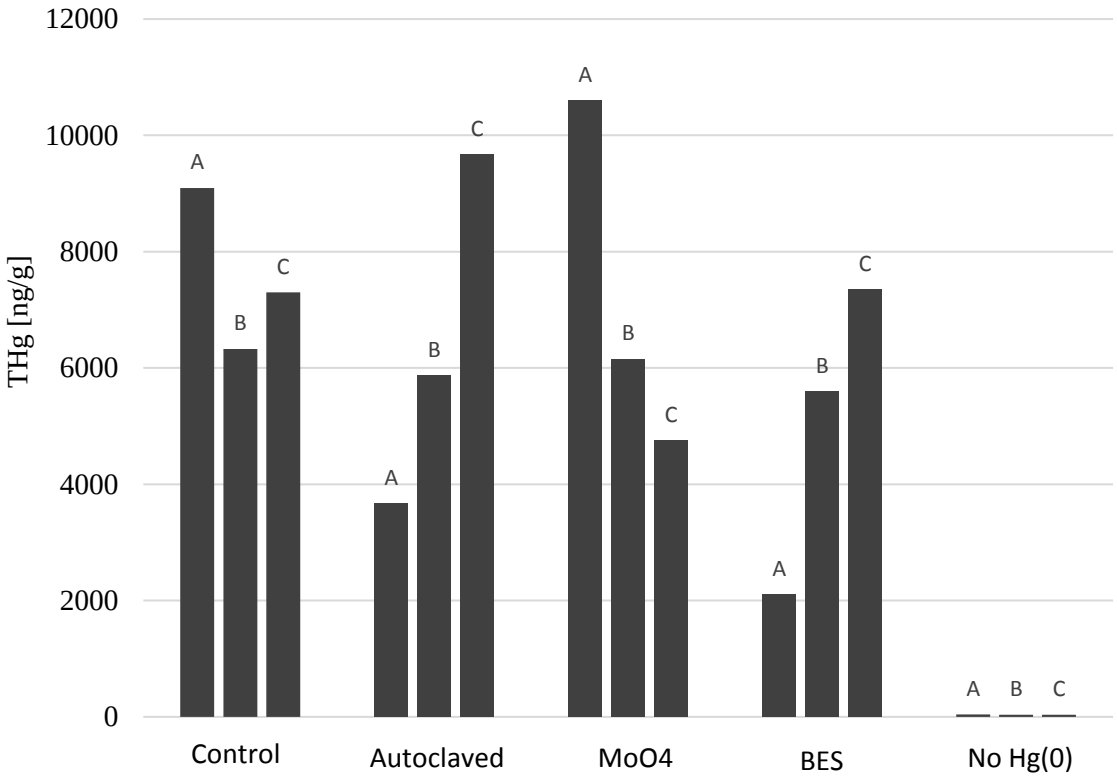

Supplement Figure S5.1: Formation of Non-purgeable Hg (NP-Hg) in the sediments after 7 days when Hg(0) was provided as the dominant Hg source. The concentration of NP-Hg was normalized to the mass of freeze-dried sediment. A, B and C represent the number of triplicate bottles for each incubation condition. Each bar represents an individual sediment incubation experiment.

Supplement Table S5.1 Information of sampling sites

Site number	Location	THg (ng/g dry mass)	Temperature (°C)	pH	Salinity (g/Kg)	Description
Site 1	29.389081, -94.882005	15.1 ± 2.1	18.9	7.70	21	Coarse sand
Site 2	29.6495676, -95.01140	17.8 ± 0.9	21.2	7.49	19	Fine Sand
Site 3	29.760407, -95.082353	15.5 ± 3.5	23.4	7.32	15	Sticky mud
Site 4	29.781528, -95.101339	53.3 ± 10.1	21.4	7.04	8	Sticky mud, warning sign of PCB contamination Sulfate: 6.4 mM
Site 5	29.798637, -95.080968	6.5 ± 0.8	20.1	7.50	3	Smooth fine particles
Site 6	29.824596, -95.082124	28.3 ± 5.2	19.6	6.54	1	Sticky mud

Chapter 6 Conclusion

This thesis dissertation focused on understanding transformation steps mediated by anaerobic microorganisms that influence the fate and transport of mercury, including the oxidation of Hg(0), adsorption of MeHg, Hg(II) uptake prior to methylation, and the production of MeHg by microbial communities when Hg(0) was provided as the dominant Hg source. Both lab work and field work were performed to elucidate the important role of anaerobic bacteria in the transformation of mercury. The application of thiol measurement methods, X-ray absorption spectroscopy, mercury stable isotopes and molecular level microbial analysis provided approaches to study the interaction of anaerobic bacteria and mercury, and to add important pathways in the big picture of global mercury cycling.

The first objective of this study was to understand the mechanism of Hg(0) oxidation by sulfate-reducing bacteria *D. desulfuricans* ND132. The experiments were conducted as an extension of the previous discovery that strain *D. desulfuricans* ND132 was able to oxidize Hg(0) and produce MeHg when Hg(0) was provided as the sole mercury source. To localize where Hg(0) oxidation occurs, Hg(0) oxidation experiments were performed on spheroplasts and cell walls of the bacterial cells. More Hg(0) was oxidized by spheroplasts, indicating that Hg(0) is majorly an intracellular process. Thiol measurement and X-ray absorption spectroscopy analyses demonstrated that Hg(0) is oxidized by cellular thiols and the oxidized Hg(II) binds to cellular thiol functional groups. The intracellular thiol concentration is higher than that of cell walls of *D. desulfuricans* ND132, which further explains the observation that more Hg(0) was oxidized intracellularly. This chapter proposed the possible pathway of Hg(0) oxidation

by *D. desulfuricans* ND132 in which Hg(0) diffuses into the bacterial cells and then oxidized by intracellular thiols prior to methylation.

The second objective of this study was to examine the adsorption of MeHg which may control its the production and degradation. This chapter was based off of a previous observation that a strain of iron-reducing bacterium *Geobacter bemidjiensis* Bem has the ability to both produce and degrade MeHg. However, the adsorption of MeHg which can affect the uptake and release of MeHg was poorly studied. By performing MeHg adsorption kinetic experiments and X-ray absorption spectroscopy, we found rapid MeHg adsorption on *G. bemidjiensis* via complexation to thiols. The log K binding constant was modeled based on data collected from thiol measurement and MeHg adsorption isotherm experiments and the value was determined as 10.5 ± 0.4. This study provides an important parameter that could be used in models which are designed to estimate the fate and transport of mercury in the environment.

Although iron-reducing bacteria was known to play an important role in methylating mercury, the process which Hg(II) was taken up by the bacterial cells was poorly understood. The objective of this work to determine the partition of Hg(II) when provided to *G. sulfurreducens* PCA cells prior to methylation. Mercury stable isotopes was used as tools for tracing the transport of Hg(II) and the fractionation associated with the uptake provides insight on the Hg(II) pools that are bioavailable for methylation. Our results showed Hg(II) reduction by *G. sulfurreducens* PCA leads to fractionation and a heavier Hg(II) pool remained after Hg(0) was produced. The heavier Hg(II) pool was taken up initially but depleted in ^{202}Hg with time. The shift of isotopic composition in different compartment of bacterial cells demonstrated isotope fractionation during Hg(II)

uptake processes. Hg(II) accumulated intracellularly was isotopic light while the MeHg produced was found isotopic heavy, indicating multiple Hg(II) pools were generated during the uptake processes.

The last objective of this work was to understand the methylation of mercury by the microbial communities in the sediments when new Hg(0) contaminant was released to the environment. Shortly after Hurricane Harvey, Hg(0) beads were found spread in the residential area and may have been transported into the sediments by the flood. We collected the sediment from the San Jacinto River estuary and performed Hg(0) transformation experiments after inhibiting the activity of certain microbial communities in the sediment. The results showed rapid generation of NP-Hg and MeHg after seven days. Methanogens were found to play an important role in the transformation of mercury. Our findings indicated that methanogens were largely overlooked in the sediments with high sulfate content.

Suggestions for Future Research

This research demonstrated the role of microorganisms in some steps of mercury transformations. However, the cycling of mercury included lots of complicated processes that need to be further explored.

Although Hg(0) transformation have been studied using sulfate-reducing and iron-reducing bacteria (Colombo et al., 2013; Hu et al., 2013), little is known on Hg(0) transformation by archaea. The rate and extent of Hg(0) oxidation and methylation by pure archaea strains should also be established to further understand the importance of archaea in MeHg production. Archaeal cellular sites that are available for mercury

complexation should also be examined to better elucidate the mechanisms of mercury transformations by archaea.

Hg(II) uptake is an important step prior to methylation. Multiple pathways have been demonstrated for Hg(II) uptake (An et al., 2019; Benoit et al., 2001; Schaefer et al., 2014). However, factors such as pH, concentration of ligands that complexes with mercury and existence of compounds that affects the activity of microorganism may influence the transport of Hg(II) into the cells. It is important to use one microorganism as a model to test if Hg(II) uptake pathways are influenced by environmental factors.

In Chapter 4, mercury stable isotope was used as a tool to understand the Hg(II) uptake process. However, the fractionation of Hg(II) when being taken up in the periplasm and cytosol was not teased apart. Hg(II) uptake experiments can be repeated using spheroplasts to understand the fractionation of Hg(II) during the transportation via transporters on the inner membrane. With this information, a more systematic model indicating the change of intracellular bioavailable Hg(II) pool for methylation could be established.

Finally, it is known that mercury has a high affinity towards sulfur compounds (Skyllberg, 2008). As an element in the same group as sulfur, selenium also binds mercury and affects the toxicity of mercury (Cuvin-Aralar and Furness, 1991). It would be interesting to test if the existence of selenium influences the transformation of mercury mediated by microorganisms by altering the activity of the cells or changing the bioavailability of mercury.

This dissertation extended our understanding of mercury transformation by anaerobic microorganisms. More research aiming to better understand the mechanisms

leading to MeHg production, broader species of microorganisms evolved in mercury transformation and biogeochemical controls on mercury cycling are still needed to be conducted.

References:

An, J., Zhang, L., Lu, X., Pelletier, D.A., Pierce, E.M., Johs, A., Parks, J.M. and Gu, B. (2019) Mercury Uptake by *Desulfovibrio desulfuricans* ND132: Passive or Active? Environmental science & technology.

Benoit, J.M., Gilmour, C.C. and Mason, R.P. (2001) Aspects of Bioavailability of Mercury for Methylation in Pure Cultures of *Desulfobulbus propionicus* (1pr3). Applied and Environmental Microbiology 67, 51.

Colombo, M.J., Ha, J., Reinfelder, J.R., Barkay, T. and Yee, N. (2013) Anaerobic oxidation of Hg(0) and methylmercury formation by *Desulfovibrio desulfuricans* ND132. Geochimica et Cosmochimica Acta 112, 166-177.

Cuvin-Aralar, M.L.A. and Furness, R.W. (1991) Mercury and selenium interaction: a review. Ecotoxicology and environmental safety 21, 348-364.

Hu, H., Lin, H., Zheng, W., Tomanicek, S.J., Johs, A., Feng, X., Elias, D.A., Liang, L. and Gu, B. (2013) Oxidation and methylation of dissolved elemental mercury by anaerobic bacteria. Nature Geoscience 6, 751.

Schaefer, J.K., Szczuka, A. and Morel, F.o.M. (2014) Effect of divalent metals on Hg (II) uptake and methylation by bacteria. Environmental science & technology 48, 3007-3013.

Skyllberg, U. (2008) Competition among thiols and inorganic sulfides and polysulfides for Hg and MeHg in wetland soils and sediments under suboxic conditions: Illumination of controversies and implications for MeHg net production. Journal of Geophysical Research: Biogeosciences 113.